In presenting the dissertation as a partial fulfillment of the requirements for an advanced degree from the Georgia Institute of Technology, I agree that the Library of the Institute shall make it available for inspection and circulation in accordance with its regulations governing materials of this type. I agree that permission to copy from, or to publish from, this dissertation may be granted by the professor under whose direction it was written, or, in his absence, by the Dean of the Graduate Division when such copying or publication is solely for scholarly purposes and does not involve potential financial gain. It is understood that any copying from, or publication of, this dissertation which involves potential financial gain will not be allowed without written permission.

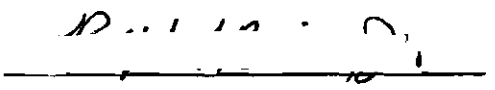

7/25/68

AN INVESTIGATION OF THE KNUDSEN LIMITING LAW OF THERMAL TRANSPIRATION

A THESIS

Presented to

The Faculty of the Division of Graduate

Studies and Research

by

Ralph Lendon Buice, Jr.

In Partial Fulfillment

of the Requirements for the Degree

Doctor of Philosophy

in the School of Chemistry

Georgia Institute of Technology

June, 1972

AN INVESTIGATION OF THE KNUDSEN LIMITING LAW

OF THERMAL TRANSPIRATION

Approved:

Chairman

Date approved by Chairman: June 5, 1972

ACKNOWLEDGMENTS

I am grateful to Dr. G. A. Miller for the suggestion of this problem, and for his guidance, direction, and patience during the course of this research.

I am also grateful to the other members of the reading committee, Dr. R. A. Pierotti and Dr. T. F. Moran, for the careful reading and critical evaluation of this manuscript. The efforts of the reading committee aided significantly in making this a better dissertation.

I am indebted to Dr. W. M. Spicer for allowing me to hold a teaching assistantship during most of my graduate education.

I would also like to thank Mrs. Betty Sims for the careful editing and typing of this manuscript.

Finally, a very special appreciation is due my parents whose understanding and encouragement throughout my education have made this degree possible. I dedicate my dissertation to them.

TABLE OF CONTENTS

LIST OF TABLES

LIST OF ILLUSTRATIONS

SUMMARY

A number of experiments by various workers have shown considerable deviations from the Knudsen limiting law of thermal transpiration. Molecular beam experiments indicate that, for a number of practical technical surfaces, a measurable fraction of gas molecules in the incident beam is reflected specularly rather than according to the cosine law of diffuse reflection. A Monte Carlo computer model, in which the faster moving molecule has the greater chance of being specularly reflected, was devised to study the deviations from the limiting law. Clausing transmission probabilities were calculated for capillary tubes of different L/D ratios under isothermal as well as temperature gradient conditions.

According to the computer model, the transmission probability, Q, was found to be relatively insensitive to a temperature gradient across a capillary. In addition, the model indicated that the value of the transmission probability depended primarily upon the temperature of the entrance reservoir. It was found that, according to the Monte Carlo calculations, as the degree of specular reflection increased, the forward and reverse transmission probabilities diverged. When, on the average, 8 per cent of the molecules were scattered specularly in the model, the forward and reverse transmission probabilities differed by about 12 per cent. The results seemed to indicate that specular reflection might account for the observed deviations from the limiting law.

Isothermal flow experiments at several temperatures were made for a number of light gases (hydrogen, deuterium, helium, argon) to measure experimentally the effect of temperature on the transmission probability. A long tube with an L/D ratio of about 280 was used in the experiments. Such experiments, which covered temperatures ranging from 77°K. to 353°K., indicated that the values of the transmission probability were temperature dependent over a much wider range than had been previously reported. It was shown experimentally that deviations from the Knudsen limiting law on the order of 1 to 5 per cent could be accounted for because of the temperature dependence of the transmission probability. The results indicated that flow experiments provide an experimental means of measuring Clausing transmission probabilities with an average error of about 0.15 per cent.

The experimentally measured transmission probabilities were found to correlate well with the Lennard-Jones force constants for each gas as previously indicated by Lund and Berman.

The experimental measurements also indicated that the transmission probabilities were characteristic of the gas.

The experimental values of the transmission probabilities were found to be about 15 per cent lower than the theoretical values calculated from the variational solution of De Marcus. Deviations of up to 30 per cent have been reported in the literature with the deviations becoming larger as the L/D ratio of the capillary increases.

The indications are that backscattering plays an important role in this disagreement and that a full theoretical treatment of the problem must include some degree of backscattering.

CHAPTER I

INTRODUCTION

Under conditions where the molecular mean free path of a gas is small compared to typical container dimensions, the properties of the gas depend essentially upon the frequency and nature of the intermolecular collisions. Early investigations of such properties were carried out largely by means of the study of the flow of gases in cylindrical tubes. If the velocity of transport, u, is not so great that the flow becomes turbulent, the motion of the gas will be similar to the laminar flow of a liquid and will be governed by the viscosity.

Present (1) derives an equation for the motion of the gas in the following way. Consider a short cylinder of fluid of radius, r, and of length, dx. In steady flow, the pressure difference, dp, between the ends of the cylinder produces a force that is balanced by the viscous drag over the curved surface. The viscous shearing stress is $\eta \frac{du}{dr}$, where $\frac{du}{dr} < 0$, and η is a proportionality constant called the coefficient of viscosity. The viscous drag on the curved surface is given by

$$2\pi r dx \eta \frac{du}{dr} \qquad (1)$$

so that the condition for steady flow is governed by the equation

$$2\pi r dx\eta \frac{du}{dr} + \pi r^2 dp = 0. \tag{2}$$

If this equation is rearranged,

$$\frac{du}{dr} = -\left(\frac{r}{2\eta}\right) \frac{dp}{dx} \tag{3}$$

the following equation is obtained upon integration,

$$u = -\left(\frac{r^2}{4\eta}\right) \frac{dp}{dx} + C \tag{4}$$

where the boundary condition at the wall,

$$u(a) = 0 \tag{5}$$

allows the integration constant, C, to be evaluated. The equation

$$u = \frac{a^2 - r^2}{4\eta} \frac{dp}{dx} \tag{6}$$

indicates that the velocity profile is parabolic. If n is the number of molecules, the molecular flow in the cylindrical shell between r and r + dr is $2\pi nurdr$. The number of molecules per unit time flowing through the tube is then

$$G = n \int_0^a u 2\pi r dr = \frac{2\pi n}{4\eta} \frac{dp}{dx} \int_0^a (a^2 - r^2) r dr$$

$$= \frac{\pi a^4 n}{8\eta} \frac{dp}{dx} = \frac{\pi a^4}{8\eta kT} p \frac{dp}{dx} \tag{7}$$

where a is the radius of the tube, k is the Boltzmann constant, and T is the absolute temperature in degrees Kelvin.

In the steady state, G is independent of x such that

$$G \int_0^L dx = \frac{\pi a^4}{8\eta kT} \int_{p_1}^{p_2} p dp = \frac{\pi a^4}{8\eta kT} \frac{p_2^2 - p_1^2}{2} \tag{8}$$

where L is the length of the cylindrical tube. If the pressure drop from one end of the tube to the other is denoted by

$$\Delta p = p_2 - p_1, \tag{9}$$

and the average pressure is denoted by

$$\bar{p} = \tfrac{1}{2}(p_2 + p_1), \tag{10}$$

then the law of Poiseuille is obtained

$$G = \frac{\pi a^4 \bar{p} \Delta p}{8\eta kTL} \tag{11}$$

where the formula is strictly valid only if the mean free path of the gas is much less than the radius of the cylinder, i.e.,

$$\lambda << a. \qquad (12)$$

This is a necessary condition for the applicability of the shear stress calculation and the boundary condition.

As the pressure is lowered, however, with any given experimental arrangement, there must come a time when this boundary condition is no longer satisfied. As the pressure decreases, the mean free path of the gas will increase so that intermolecular collisions must, of necessity, lose their importance. Experimentally it was found that as the mean free path of the gas approached the diameter of the cylindrical tube, Poiseuille's law failed. This was not surprising in the sense that when the mean free path of the molecules greatly exceeded the dimensions of the apparatus, intermolecular collisions would be rare, and the determining factor in the behavior of the gas would be the collisions that a molecule would make with the walls of the apparatus. Each molecule would then act independently of all the other molecules in giving rise to the properties of the gas. Perhaps to emphasize the importance of the "independent" or "free" molecule, a gas under such conditions is said to exhibit "free-molecular" behavior, and to undergo "free-molecular" flow.

Early Investigations

In 1875 Kundt and Warburg (2) performed a series of experiments involving the damping of a vibrating disk by a surrounding gas. They found that at low pressures the damping decreased, and attributed the effect to a "slipping" of the gas over the walls of the tube which

augmented the flow. Their solution to the problem was to extend the Poiseuille equation by introducing an extra term containing a parameter called the "coefficient of slip" which physically represented a length through which the wall of the cylinder was displaced so that the gas velocity at this new boundary was zero. The value of the slip coefficient increased as the ratio of the diameter of the tube to the mean free path decreased (3).

James Clerk Maxwell (4), in 1879, utilized the results of an elaborate analysis that he had previously made of the stresses in a moving gas to calculate the magnitude of the slip distance in a gas from kinetic theory. It was shown that the value of the slip coefficient was always of the order of one mean free path and, in accordance with the experimental findings of Kundt and Warburg, varied at a given temperature in inverse ratio with the pressure. Maxwell postulated two types of molecular reflection which the gas could undergo against the wall of the container which depended upon the transfer ratio for momentum. For a smooth surface, specular reflection might occur where the molecule underwent no change in its tangential momentum. In such a case the transfer ratio was zero, and the coefficient of slip was equal to infinity since the molecule was unable to "cling" to the wall at all. On the other hand, if the molecules were diffusely reflected without regard to the direction of incidence and with complete loss of their initial average tangential momentum, the molecules would behave as if they were reflected according to the same cosine law that holds for the reflection of light from a rough surface. In such a case, the transfer

ratio would be unity because all of the momentum would be given up to the wall, and the slip coefficient would be on the order of the mean free path of the gas.

It is interesting that Maxwell speculated about the nature of the wall-molecule interaction and, at a time when the theory of such phenomena was in its infancy, mentioned the "rooftop effect" later to be considered in detail by De Marcus (5). In the general case, Maxwell interpreted a fractional value of the transfer ratio as meaning that a fraction of the surface reflects diffusely and the remainder specularly.

The importance that temperature seemed to play in the flow of rarefied gases through cylindrical tubes induced Osborne Reynolds (6) to conduct a series of experiments during which he discovered the fact that a temperature gradient imposed across porous disks caused a difference in pressures to develop in reservoirs on each side of the disks. Reynolds (6) writes concerning his experiments:

> I have, however, now ascertained, by experiments which will be described at length, that a difference of temperature may be a very potent cause of transpiration through porous plates. So much so that with hydrogen on both sides of a porous plate, the pressure on one side being that of the atmosphere, a difference of 160°F. (from 52°F. to 212°F.) in the temperature on the two sides of the plate secured a permanent difference in the pressure on the two sides equal to an inch of mercury; the higher pressure being on the hotter side. With different gases and different plates various results were obtained, which are however, as will be seen, connected by definite laws. I propose to call the motion of the gas caused by a difference of temperature "Thermal Transpiration."

Martin Knudsen (7) first calculated the quantity of gas streaming through a tube connecting two vessels filled with the same gas but at different temperatures. He was particularly concerned with the case of

of "molecular flow" at very low pressures, and used as a basic assumption the diffuse reflection of molecules from the walls of the tube in accordance with the cosine law of diffuse reflection. Knudsen's insight into the phenomenon of Thermal Transpiration becomes apparent when he writes of his earlier experiments (8):

> I considered this question to be of great importance in the correct use of the gas-thermometer and consequently of importance to all thermometry, especially that at low temperatures, and for this reason I undertook an experimental investigation of the phenomenon.

Since low pressure phenomena emphasize the importance of impacts between molecules and the walls of the vessel rather than intermolecular collisions, two points should be emphasized.

1. The various phenomena observed are very much a characteristic effect of the geometrical arrangement of an experimental apparatus.

2. It becomes necessary to scrutinize, from the molecular point of view, the nature of the energy exchange involved in wall-molecule collisions.

The Knudsen Equation

Consider two reservoirs connected by a capillary of diameter, D, as shown in Figure 1. The pressures in the two reservoirs are such that the mean free path is large in relation to a typical dimension of the reservoir. The number of wall collisions per square centimeter per second in Reservoir 2 is given by elementary kinetic theory (9) to be

$$N_2 = \frac{P_2}{(2\pi m k T_2)^{\frac{1}{2}}} \qquad (13)$$

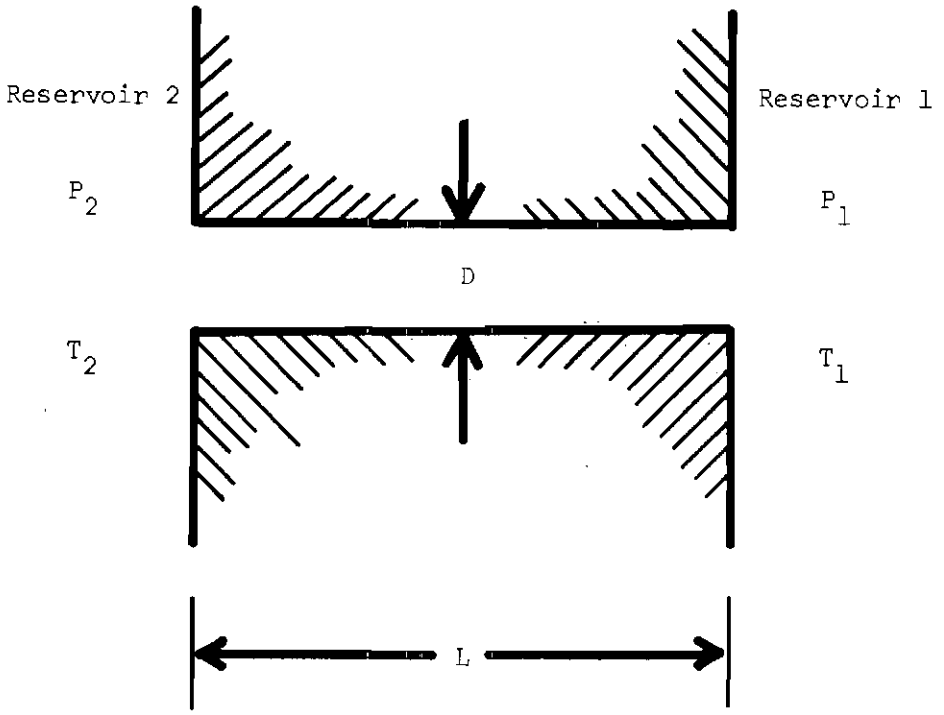

Figure 1. Diagram for the Discussion of Thermal Transpiration Through a Capillary

where N_2 is the number of wall collisions per square centimeter per second in Reservoir 2, P_2 is the pressure in Reservoir 2, m is the mass of a molecule of gas, k is the Boltzmann constant, and T_2 is the absolute temperature of Reservoir 2 in degrees Kelvin. The rate of flow from Reservoir 2 to Reservoir 1 is equal to the rate at which the molecules enter the capillary times the probability that they will leave through the other end of the capillary and is given by the expression

$$R_{21} = N_2 \cdot A \cdot Q_{21} \tag{14}$$

where

A = area available to the molecule for entrance to the capillary from Reservoir 2.

Q_{21} = probability that a molecule entering the capillary in Reservoir 2 will emerge from the capillary in Reservoir 1.

R_{21} = rate of flow of molecules from Reservoir 2 to Reservoir 1.

If D equals the diameter of the capillary, it follows that

$$R_{21} = \frac{P_2}{(2\pi mkT_2)^{\frac{1}{2}}} \cdot \frac{\pi D^2}{4} \cdot Q_{21}. \tag{15}$$

An expression for the rate of flow of gas from Reservoir 1 to Reservoir 2 can be obtained with a similar line of reasoning to give

$$R_{12} = \frac{P_1}{(2\pi mkT_1)^{\frac{1}{2}}} \cdot \frac{\pi D^2}{4} \cdot Q_{12}. \tag{16}$$

When a steady state condition has been reached, the two rates are equal

$$R_{21} = R_{12} \tag{17}$$

from which it follows that

$$\frac{P_2}{(2\pi mkT_2)^{\frac{1}{2}}} \cdot \frac{\pi D^2}{4} \cdot Q_{21} = \frac{P_1}{(2\pi mkT_1)^{\frac{1}{2}}} \cdot \frac{\pi D^2}{4} \quad Q_{12}. \tag{18}$$

This expression may be simplified to obtain the Knudsen limiting law in its most general form

$$\frac{P_1}{P_2} = \left(\frac{T_1}{T_2}\right)^{\frac{1}{2}} \quad \frac{Q_{21}}{Q_{12}}. \tag{19}$$

Under special circumstances such as totally diffuse reflection, where the scattering is independent of the position in the capillary, totally specular reflection, where the transmission probability is always unity, or a fixed degree of specular reflection, which is a combination of the two cases above, the forward and reverse transmission probabilities are equal. The Knudsen equation can then be written in its usual form:

$$\frac{P_1}{P_2} = \left(\frac{T_1}{T_2}\right)^{\frac{1}{2}}. \tag{20}$$

Knudsen (10) originated the term "thermomolecular pressure difference" to describe the effect of the above equation and wrote several papers

(11,12) in which he treated the effect not only in the low pressure region but also at pressures in the intermediate and high pressure range.

Experimental Considerations

Several workers (13-17) have made measurements of the thermal transpiration ratio, R, defined by the expression

$$R = \frac{P_1}{P_2} . \tag{21}$$

Typical of the results were those of Hobson, Edmonds, and Verreault (15). Experimental values of R for helium gas were measured by an absolute method in an ultra-high vacuum system over the pressure range 10^{-8} torr to 20 torr. The results are shown in Figure 2, where the limiting value of R = 0.512 is shown as a dashed line ($T_2 < T_1$). Two main results were found:

1. The lower limit for R is not reached in the pressure range studied.

2. The results obtained were essentially in agreement with the experimental results of other workers.

Table 1 shows the magnitude of the deviations observed by Hobson and co-workers. It seems clear that even in the region of very low pressures the Knudsen equation is not strictly obeyed.

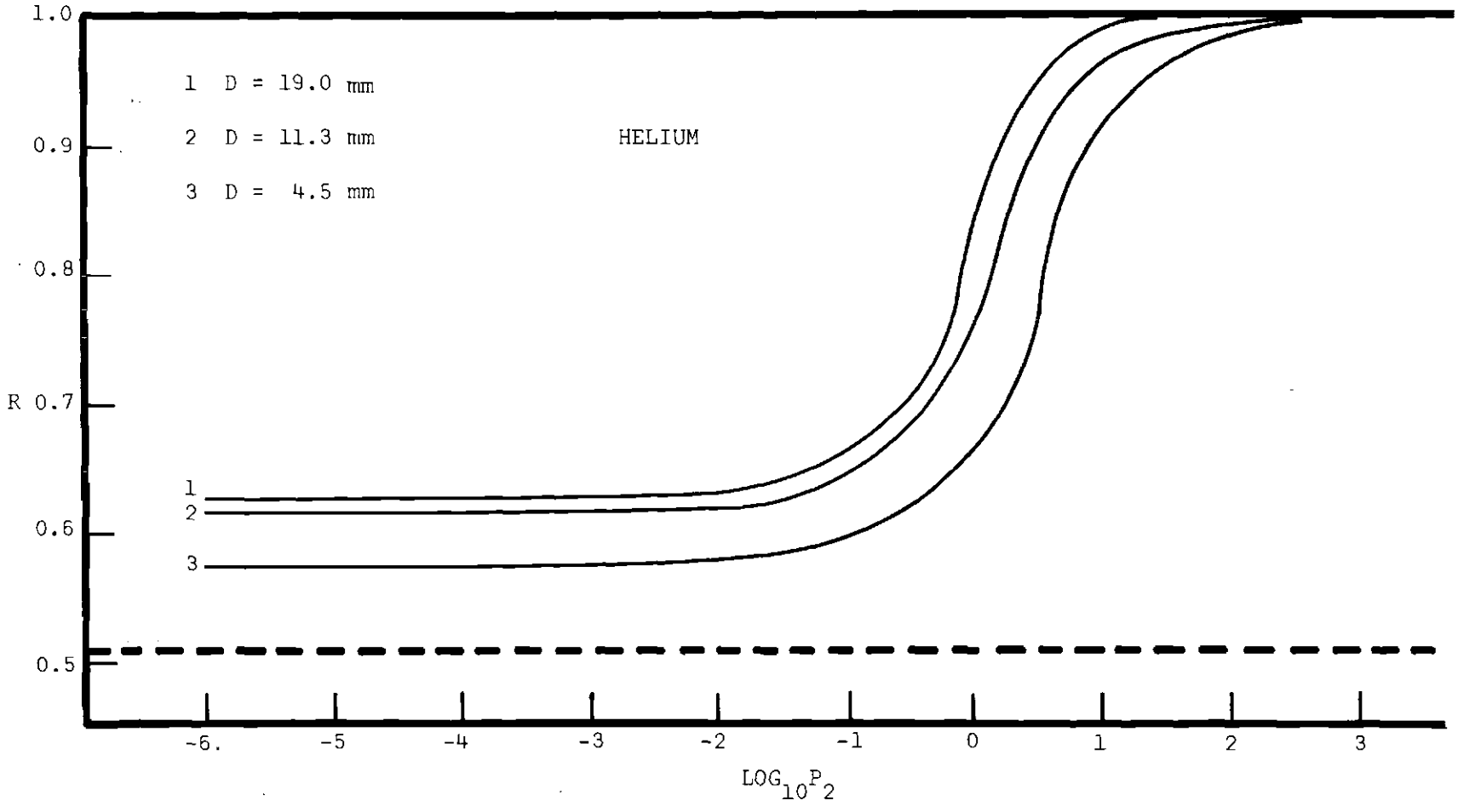

Figure 2. Measured Values of Thermal Transpiration Ratio Versus Pressure for Helium

Table 1. Low Pressure Values of Thermal Transpiration Ratio for Capillary Tubes of Different Diameters [The Percentage of Deviation from Theoretical Varied from 11.3 to 23.4.]

Gas	Experimental R[a]			$(T_1/T_2)^{1/2}$
	D=4.5 mm	D=11.3 mm	D=19.0 mm	
Helium	0.57	0.61	0.62	0.512
Neon	0.590	0.628	0.632	0.512

[a]Values of R taken from Reference 15.

In addition to measuring thermal transpiration ratios, workers have also been interested in investigating the scattering of molecules from a solid surface. Hurlbut (18) has performed extensive experiments with gas beams interacting with a number of practical technical surfaces such as polished steel, polished aluminum, and unpolished glass. The molecular beam apparatus was of conventional design consisting of a beam source (beams of nitrogen were used), defining orifices, a beam interrupter, a test region, and the usual vacuum apparatus. An ionization gauge was selected as the molecular beam detector because of its high inherent sensitivity and thermal stability. A dual ionization gauge was actually used which allowed the resolution of signals differing in amplitude by 8×10^{-11} torr in the presence of a background pressure on the order of 10^{-6} torr. An axisymmetric geometry was chosen to allow observation of the molecular flux over the entire available hemisphere. Very close adherence of the measured flux distributions to the cosine

scattering pattern was observed for each of the polished metal surfaces. At high angles of incidence for the molecular beam, however, there were indications of a specular lobe. In addition, a measurable fraction of the total number of incident molecules was scattered into directions lying about the specular ray for glass surfaces. These results are represented schematically in Figure 3 where the lobe of non-diffusely scattered molecules is shown around the specular ray. The fraction of molecules which were scattered specularly increased with increasing angle of incidence. Both Miller and Subbarao (18) and Yamamoti and Stickney (19) have reported that the faster moving molecules have a greater chance of being specularly reflected.

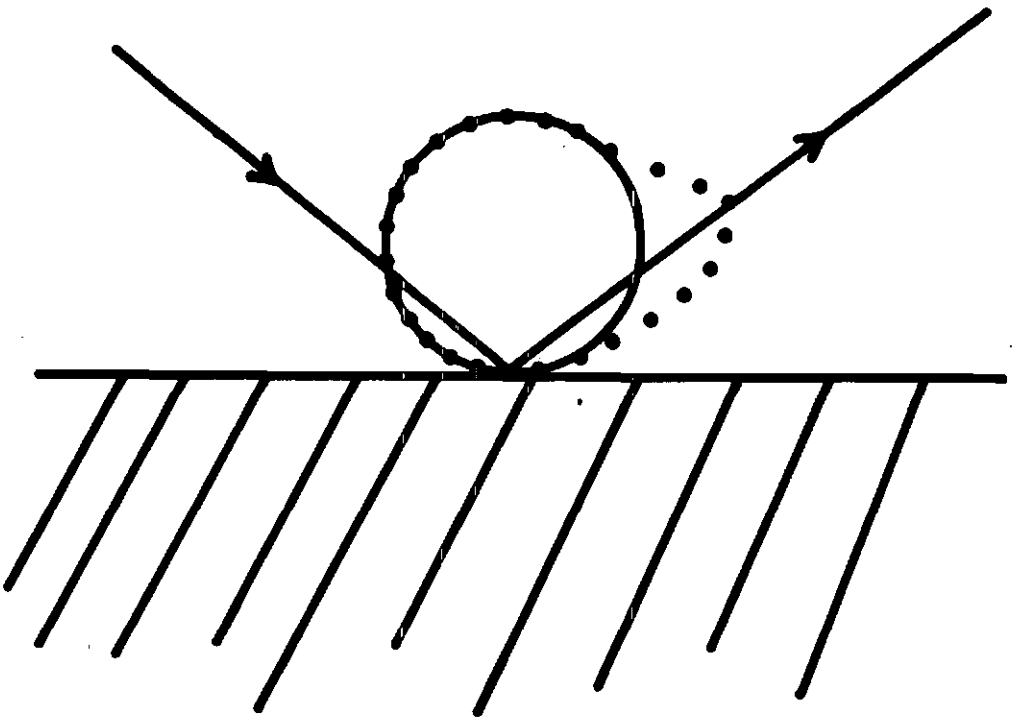

Figure 3. Schematic Representation of Molecular Beam Experiments Showing Specular Lobe Around Specular Ray

Statement of the Problem

The purpose of this dissertation is to investigate these deviations from the Knudsen limiting law. One way to explain the deviations is to postulate that the transmission probability, Q, varies in some way with temperature because of a small amount of specular reflection. This would require that

$$Q_{12} < Q_{21}$$

where

$$T_2 > T_1.$$

This would mean that a molecule traveling from the hot to cold side of the capillary has a greater chance of traversing a long tube than a molecule traveling from the cold to hot end. As has been pointed out, the assumption of completely diffuse reflection requires that $Q_{12} = Q_{21}$. However, if the specular reflection of a hot molecule striking a cold surface is slightly more probable than that of a cold molecule striking a hot surface, then $Q_{12} < Q_{21}$, where $T_2 > T_1$.

These considerations will be studied from two different approaches:

1. A computer model of thermal transpiration will be constructed in which the faster moving molecule has the greater probability of being specularly reflected. The variation of Q with temperature and degree of specular reflection can then be studied.

2. Flow measurements will be made on light gases in order to determine if any temperature dependence exists for the transmission probabilities. The temperatures will cover a range from 77.4°K. to 353.2°K.

CHAPTER II

THEORY

In general, there are two models which are used to describe the type of molecular scattering which may occur during the flow of a gas through a capillary tube under conditions where the mean free path of the gas is much greater than the diameter of the tube. When specular reflection occurs, the molecule which strikes the surface of the tube at some angle, θ, rebounds such that the velocity parallel to the surface is conserved, but the component of velocity perpendicular to the surface is reversed. The molecule thus rebounds with the angle of incidence equal to the angle of reflection and with its energy unchanged by the encounter with the wall. When diffuse reflection occurs, the molecule strikes the surface of the container with complete wall accommodation and forgets its past history, so that there is no special bias causing it to rebound along the specular ray. The molecules are then distributed in direction according to the cosine law, where the number of molecules leaving an element of surface in a direction which makes an angle θ with the normal to the surface is proportional to $\cos\theta$. In actual practice the wall surfaces are highly irregular on the submicroscopic scale, so that if a gas molecule, after reaching the surface, became temporarily trapped in a small pocket or adsorbed on the wall and later evaporated, one might expect that the direction of

reflection would have little relation to the direction from which the molecule came.

Consider Figure 4 which illustrates the two models of molecular scattering. The element of surface area, dS, is small enough to be treated as a smooth plane for molecular encounters. In an elastic collision between a molecule and the element of surface, the contact forces act at right angles to dS so that the component of molecular velocity parallel to dS is unchanged by the collision. Because the collision is elastic, the normal component of velocity is reversed by the collision and the molecule is specularly reflected from dS since the angle of reflection is equal to the angle of incidence. This situation is shown in Figure 4(a).

Now let $f^*(\vec{v})$ be the distribution function for molecular velocities such that $f^*(\vec{v})dvd\omega$ is the fraction of molecules with velocity vectors in the range of speeds dv and the range of directions $d\omega$ about $\vec{v}$. The Maxwell distribution function f(v) is introduced such that f(v)dv gives the fraction of molecules moving in any direction with speeds between v and v + dv. Evidently

$$f(v) = \int_0^{4\pi} f^*(\vec{v})d\omega \qquad (1)$$

where the integration is carried out over the entire solid angle of 4π. If the assumption is made that there is no preferred direction of motion, then the chance that the velocity vector is within the solid angle $d\omega$ is simply $d\omega/4\pi$. Hence

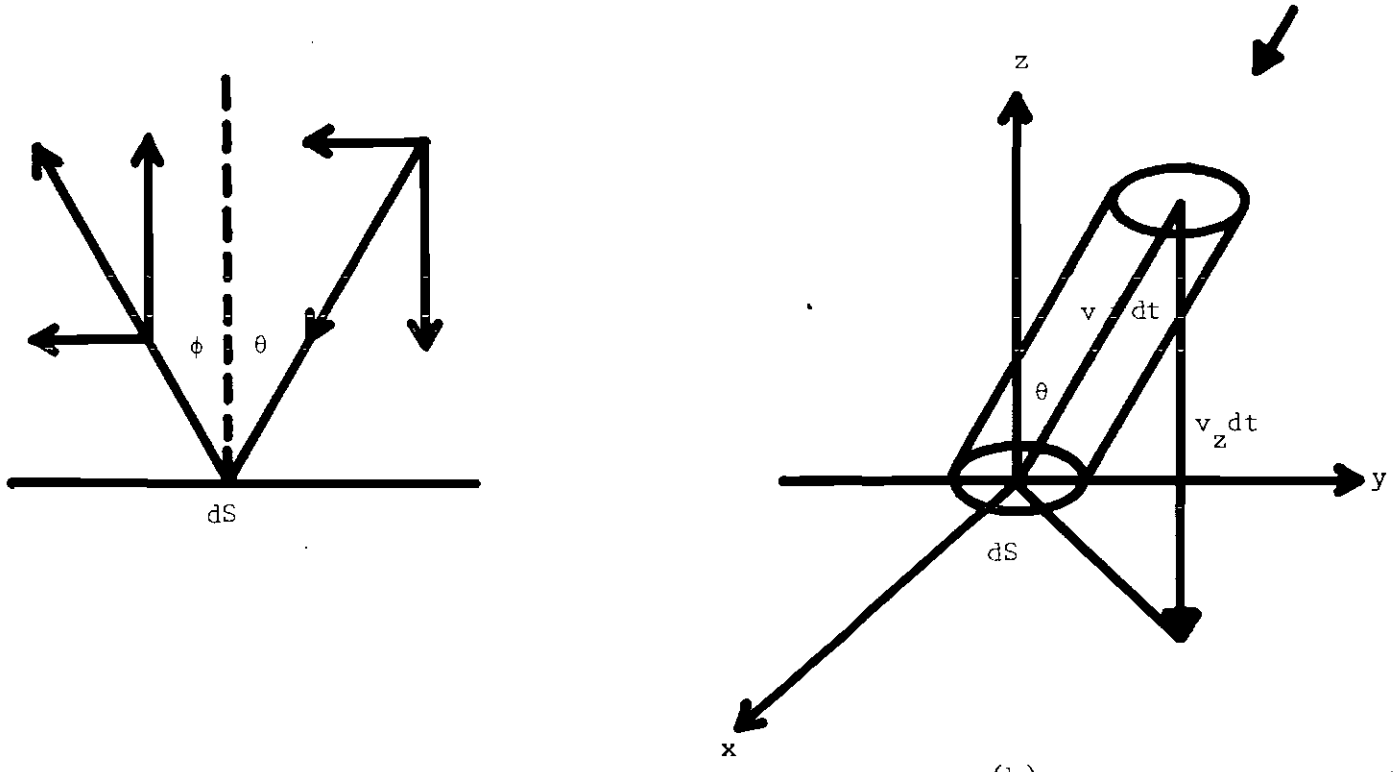

Figure 4. Models for Molecular Scattering

$$f^{*}(\vec{v})dvd\omega = f(v)dv(d\omega/4\pi) \qquad (2)$$

Figure 4(b) shows a group of molecules with velocity vectors in an infinitesimal neighborhood of $\vec{v}$ which strike dS during the time interval dt. These molecules would be contained at the beginning of the time interval in an oblique cylinder with base dS and slant length vdt whose axis is parallel to the vector $\vec{v}$. The altitude of the cylinder is $v_z dt$ and its volume is $v_z dtdS$. The number of molecules per unit volume with velocity vectors close to $\vec{v}$ within the range of speeds dv and the range of directions $d\omega$ is $nf^{*}(\vec{v})dvd\omega$ where n is the total number of molecules. The number of molecules with velocities close to v which strike dS during the time dt is therefore given by

$$nf^{*}(\vec{v})dvd\omega \cdot v_z dtdS. \qquad (3)$$

It immediately follows that the number of molecules with velocities close to $\vec{v}$ that strike the wall per unit area per unit time is given by

$$\begin{aligned} dN &= nv_z f^{*}(\vec{v})dvd\omega \\ &= nv\cos\theta f(v)dvd\omega/4\pi. \end{aligned} \qquad (4)$$

The number of molecules reflected from a unit area of the wall per unit time in a particular direction is equal to the number crossing a unit area in that direction and is found by integrating the above expression over all speeds

$$n\cos\theta \frac{d\omega}{4\pi} \int_0^\infty vf(v)dv = n\bar{v}\cos\theta \frac{d\omega}{4\pi} \qquad (5)$$

where $\bar{v}$ is the average molecular velocity. The cosine dependence upon this type of reflection is thus obtained. It is likely that the molecular scattering at the wall surface is some composite of the two reflection types, but the usefulness of the models lies in the fact that complicated problems are often simplified by their use.

The Transmission Probability

P. Clausing (21-24) first developed the picture of molecular transmission in terms of probabilities. Earlier workers, like Knudsen, had thought in terms of an average pressure at each point down the tube. In Clausing's approach, the transmission probability for molecules which enter the tube from the first vessel and emerge at the exit in the other vessel without having been back in the first is considered. The Clausing approach was extended by De Marcus (5,25-32) who was mainly interested in precise values of the Clausing probability factor for accurate vapor pressure measurements using a Knudsen cell. De Marcus described a very generalized and highly mathematical method for solving molecular flow problems in terms of integral equations developed by Clausing. In his analysis of the equations, De Marcus shows how various techniques such as "squeezing" and "scissoring" may be used to obtain approximate solutions for the transmission probability.

In the squeezing technique he shows how solutions may be squeezed between two functions by an iteration process yielding both an upper and lower bound. In the scissoring process the integral equation is first

reduced to one involving only half the integration interval before the squeezing method is used. When the probability kernel is symmetrical, and the flow is independent of the distance along the capillary, the Clausing integral equation may be solved by a variational technique which has been used to solve for transmission probabilities in the case of circular tubes, parallel plates, and a bed of spheres. Values of the transmission probability obtained by De Marcus have been tabulated with an improved accuracy over those given by Clausing. The first part of this work follows the formalism used by De Marcus.

Development of the Integral Equation

Consider an infinitesimal length of capillary tube with surface areas, dS and dS', and widths, dx and dx', respectively, as shown in Figure 5. Suppose only diffuse reflection occurs. The collision density at x may be calculated by considering the molecular contributions from the following sources:

1. the number of molecules which enter the tube and make a first bounce at x;
2. the number of molecules from all other points in the capillary which leave some point, say x' in area dS', and arrive at the point x within the ring of area dS.

The collision density, n(x), or the number of collisions per unit of surface in unit time, is to be found as the solution to a linear integral equation which expresses the fact that in a steady state the rate of impingement of molecules on a surface element of the walls of a flow system is equal to the rate of departure. For actual calculations

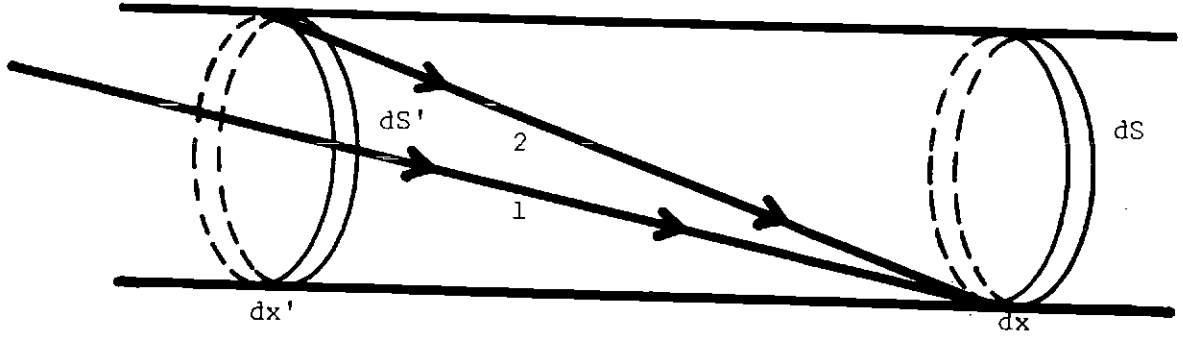

Figure 5. Circular Capillary Tube Showing Surface Areas for the Calculation of Molecular Density

it is convenient to normalize the problem such that one molecule per second enters the capillary entrance, and if it succeeds in traversing the length of the capillary tube, exits into a perfect vacuum. The fact that the integral equation is linear allows the solution to any other problem to be synthesized from such normalized solutions. Considering one dimensional systems, i.e., systems with only one entrance and one exit, where a single space coordinate is sufficient to describe the collision density, the following functions may be defined:

$n(x)$ rate of collisions per unit length of the distance x measured from the entrance which fall between x and x + dx.

$n_1(x)$ rate of first collisions per unit length of the distance x measured from the entrance which fall between x and x + dx.

$N_1(x)$ probability that the first collision of a molecule entering the flow system will occur at some distance greater than x from the entrance.

$K(y,x)$ probability per unit length of the distance x measured from the entrance that a molecule which has collided with the walls of the system at y will make its next collision between x and x + dx.

$P(x;L)$ probability per unit length of the distance x measured from the entrance that a molecule which has collided at x will leave the system at the exit where x = L.

$P(x;0)$ probability per unit length of the distance x measured from the entrance that a molecule which has collided at x will leave the system at the entrance where x = 0.

Q probability that a molecule which enters the system at x = 0 will exit at x = L, i.e., the transmission probability.

In order to obtain the value of the collision density at x, it is necessary to integrate over all of the rings which make a contribution to the density at x as well as to consider all of the molecules which make

their first diffuse collision at x upon entering the capillary tube. The formula for the collision density becomes

$$n(x) = n_1(x) + \int_0^L K(y,x)n(y)dy \tag{6}$$

where L is the length of the capillary tube. The molecular current flowing, or the transmission probability, can also be written by considering the number of molecules which pass completely through the tube without a collision, i.e., the molecules which make their first diffuse collision beyond L, and the molecules which make a diffuse collision at x and then pass out of the tube at x = L. The resulting equation is

$$\begin{aligned} Q &= \int_L^\infty n_1(x)dx + \int_0^L n(x)P(x;L)dx \\ &= N_1(L) + \int_0^L n(x)P(x;L)dx. \end{aligned} \tag{7}$$

Since $N_1(x)$ is the probability that a molecule which enters the flow system at x = 0 makes its first collision beyond x and $n_1(x)dx$ is the probability that a molecule entering the capillary at x = 0 will make its first collision at x, it follows that

$$n_1(x) = -\frac{dN_1(x)}{dx}. \tag{8}$$

It should be noted that in one dimensional systems such as Knudsen flow in circular capillaries, the properties of the flow system are independent of x so that the kernel function is of the displacement type

$$K(y,x) = K(x,y) = K(|x-y|) = K(|y-x|) \tag{9}$$

such that the kernel depends only upon the distance between x and y and not on the separate variables. Thus the normalized Clausing equation is sometimes written as

$$n(x) = n_1(x) + \int_0^L K(|x-y|)n(y)dy \tag{10}$$

to indicate the displacement character of the kernel.

The Case of Specular Reflection

The equations given above apply only to the case of diffuse scattering. With appropriate modification the concepts may be extended to include the case of specular reflection (29,32).

For the case of specular reflection, the following functions may be defined:

- $s(x)$ rate of diffuse collisions per unit length of the distance x measured from the entrance which fall between x and x + dx.
- $s_1(x)$ rate of first diffuse collisions per unit length of the distance x measured from the entrance which fall between x and x + dx.
- $S_1(x)$ probability that the first diffuse collision of a molecule entering the flow system will occur at some distance greater than x from the entrance.
- $\Gamma(y,x)$ probability per unit length of the distance x measured from the entrance that a molecule which has diffusely collided with the walls of the system at y will make its next diffuse collision between x and x + dx.

$\pi(x;L)$ probability per unit length of the distance x measured from the entrance that a molecule which has diffusely collided at x will leave the system at the exit where $x = L$.

$\pi(x;0)$ probability per unit length of the distance x measured from the entrance that a molecule which has diffusely collided at x will leave the system at the entrance where $x = 0$.

Q probability that a molecule which enters the system at $x = 0$ will exit at $x = L$, i.e., the transmission probability.

The formulas for the collision density

$$s(x) = s_1(x) + \int_0^L \Gamma(y,x)s(y)dy \tag{11}$$

and the transmission probability

$$\begin{aligned} Q &= \int_L^\infty s_1(x)dx + \int_0^L s(x)\pi(x;L)dx \\ &= S_1(L) + \int_0^L s(x)\pi(x;L)dx \end{aligned} \tag{12}$$

follow immediately from the definitions. Also as before,

$$s_1(x) = -\frac{dS_1(x)}{dx}. \tag{13}$$

It can be seen that there is a correspondence between the functions for diffuse reflection and those which allow both diffuse and specular reflection:

$$S_1(x) \longleftrightarrow N_1(x)$$

$$s_1(x) \longleftrightarrow n_1(x)$$

$$\Gamma(y,x) \longleftrightarrow K(y,x) \qquad (14)$$

$$\pi(x;0) \longleftrightarrow P(x;0)$$

$$\pi(x;L) \longleftrightarrow P(x;L).$$

As De Marcus has pointed out, usually only one of the functions in each hierarchy need be evaluated due to the relations which exist among the formulas. He went on to develop a method of obtaining a variational solution for the transmission probability which involved the adjustment of parameters to maximize a functional.

Modification of the Integral Equation

The purpose of the first part of this dissertation was to study the influence of temperature and specular reflection on the transmission probability with an appropriate computer model. For the purposes of the Monte Carlo calculations it was more expedient to define the transmission probability in terms of a new function $f(x,L)$ which represented the probability that a molecule which underwent its first diffuse collision at x would eventually pass out the exit of the capillary at $x = L$. The integral equation for the transmission probability then assumes the form

$$Q = \int_{L}^{\infty} s_1(x)dx + \int_{0}^{L} s_1(x)f(x,L)dx$$

$$= S_1(L) + \int_{0}^{L} s_1(x)f(x,L)dx \qquad (15)$$

where, as will be shown later, the functions $s_1(x)$ and $S_1(x)$ may be evaluated analytically.

CHAPTER III

DESIGN OF THE COMPUTER MODEL

The Monte Carlo method (33-35) consists of the generation of a sequence of values of a random variable, X, whose expected value is the solution to the problem at hand. The expected value of X is then estimated from the sequence by

$$\hat{X} = \frac{1}{N} \sum_{i=1}^{N} X_i \qquad (1)$$

where $\hat{X}$ is the estimated value of the expectation of X, X_i is the i^{th} generated value of the random variable, and N is the number of values in the sequence. By the central limit theorem the distribution of the random variable X_i tends to the normal distribution about $\hat{X}$ as N becomes large. The accuracy of a Monte Carlo calculation is proportional to $1/N^{\frac{1}{2}}$.

The computer model was based upon the following considerations:

1. Gas molecules are either diffusely reflected with complete accommodation with the wall, or specularly reflected with no accommodation with the wall.

2. The energies of the molecules impinging on the capillary wall would be distributed according to the Maxwell-Boltzmann distribution of molecular velocities as applied to an effusing gas:

$$F_3(E) = \left(\frac{1}{kT}\right)^2 Ee^{-E/kT} . \qquad (2)$$

Since this equation is somewhat awkward to use in the already time-consuming Monte Carlo calculations, it is assumed for convenience that the energies of the molecules are distributed according to a simple exponential:

$$F(E) = \frac{1}{kT} e^{-E/kT} . \qquad (3)$$

Although it is true that the distribution law will give the wrong average energy of the molecules, it can still be used to give a desired degree of specular reflection at that temperature by the appropriate selection of other parameters in the model. For convenience, the energy in the distribution formula is given in terms of the Boltzmann constant; that is,

$$\epsilon = E/k . \qquad (4)$$

3. In order to decide when specular reflection occurs, the notion of an activation energy for specular reflection is introduced. The probability that a molecule of translational energy, ϵ, will be reflected specularly is arbitrarily given by

$$P(\epsilon) = 1 - e^{-\epsilon/\epsilon_0}, \qquad (5)$$

where ϵ_0 is an arbitrary parameter to control the amount of specular reflection. This expression has the following advantages:

a. It is a simple, manageable function.

b. $P(\epsilon)$ increases monotonically with energy.

c. Even for large values of ϵ, 1 - P is finite.

The degree of specular reflection can be calculated by considering a uniform gas at temperature T. Of the molecules striking the wall of the container, a fraction

$$\int_0^\infty P(\epsilon)F(\epsilon)d\epsilon = \frac{T}{T + \epsilon_0} \tag{6}$$

will be specularly reflected, where the parameter ϵ_0 may be adjusted accordingly.

4. The probability of diffuse reflection is, accordingly,

$$1 - P(\epsilon) = e^{-\epsilon/\epsilon_0} . \tag{7}$$

If a particle is reflected diffusely, it is reflected from the walls according to the cosine law where the probability of a particle entering an elementary solid angle is proportional to the cosine of the angle with respect to the normal to the surface.

5. The particles move independently of each other so that there are no intermolecular collisions.

6. The equation to be solved is the expression for the transmission probability,

$$Q = S_1(L) + \int_0^L s_1(x)f(x,L)dx \tag{8}$$

where

$$s(x) = s_1(x) + \int_0^L \Gamma(y,x)s(y)dy \ . \tag{9}$$

In the computer model, only the value of f(x,L) need be evaluated as a function of the distance from the entrance of the capillary, x.

It should also be noted that if the model were used to study temperatures considerably higher than those used in this study, the the three dimensional molecular velocity distribution should probably be used in place of the simplified expression.

Consider a beam of molecules in a Maxwellian temperature distribution striking the wall of the capillary. The distribution of molecular energies is given within the approximations of the model by

$$F(\epsilon) = \frac{1}{T} e^{-\epsilon/T} \ . \tag{10}$$

The fraction of molecules undergoing at least n successive specular reflections, after a diffuse reflection at temperature T is

$$\int_0^\infty [P(\epsilon)]^n \cdot F(\epsilon)d\epsilon = r_1 r_2 r_3 \ldots r_n \tag{11}$$

where

$$r_n = \frac{nT}{nT + \epsilon_0} \ , \tag{12}$$

since $P^{n-1}F$ is the distribution of ϵ in the specularly reflected ray after n - 1 reflections. Therefore, the fraction of molecules which undergo n - 1 successive specular collisions followed by a diffuse one is given by

$$\int_0^\infty [P(\epsilon)]^{n-1}F(\epsilon)d\epsilon - \int_0^\infty [P(\epsilon)]^{n}F(\epsilon)d\epsilon = r_1r_2r_3\ldots r_{n-1}(1-r_n). \tag{13}$$

Derivation of the Function $\Gamma(y,x)$

$\Gamma(y,x)$ is the probability per unit length that a molecule which has diffusely collided at y will suffer its next diffuse collision between x and x + dx. Now the function $\Gamma(y,x)$, like $K(y,x)$, is symmetrical about y in spite of the temperature gradient along the wall because the reflection law is independent of the temperature of the wall at the point of reflection and depends only on the past history of the molecule being reflected. Thus,

$$\Gamma(x,y) = \Gamma(y,x) = \Gamma(|x-y|) = \Gamma(|y-x|), \tag{14}$$

as before. Since the model allows specular reflection to occur, there may be any number of specular jumps between one diffuse reflection and the next. Specular reflection may be terminated by a diffuse reflection.

Consider a length of capillary where the contributions of all types of jumps must be summed in order to arrive at the value of $\Gamma(y,x)$, as shown in Figure 6. The definition of $\Gamma(y,x)$ requires that a molecule which collides diffusely at x make its next diffuse collision at y. Since there are an infinite number of ways for a molecule to make two diffuse collisions with intervening specular collisions, the formula for the kernel is evidently an infinite series. The first term arises from the fact that a diffuse jump may occur with no intervening specular collisions and is indicated by path number 1. The molecule will proceed along path 1 but will diffusely reflect. Since the probability of specular reflection was r_1, the probability of diffuse reflection was $(1-r_1)$. The probability kernel for the jump is $K(|x-y|)$, and the effective area of dx as seen from dy in terms of dx is 1. Therefore the first term of the infinite series is

$$(1)(1-r_1)K(|x-y|). \tag{15}$$

The molecule can also collide diffusely at dx if it leaves from dy toward the mirror image of dx on the opposite wall, undergoing one intervening specular reflection in the process. The mirror image of dx is only half as large as dx itself and the probability kernel now depends upon only half the original distance, or the distance from y to the mirror image. The probability that the molecule would undergo diffuse reflection with one intervening specular jump would be $(r_1-r_1r_2)$, and the probability kernel would be $K(|\frac{1}{2}(x-y)|)$. The second term in the series thus becomes

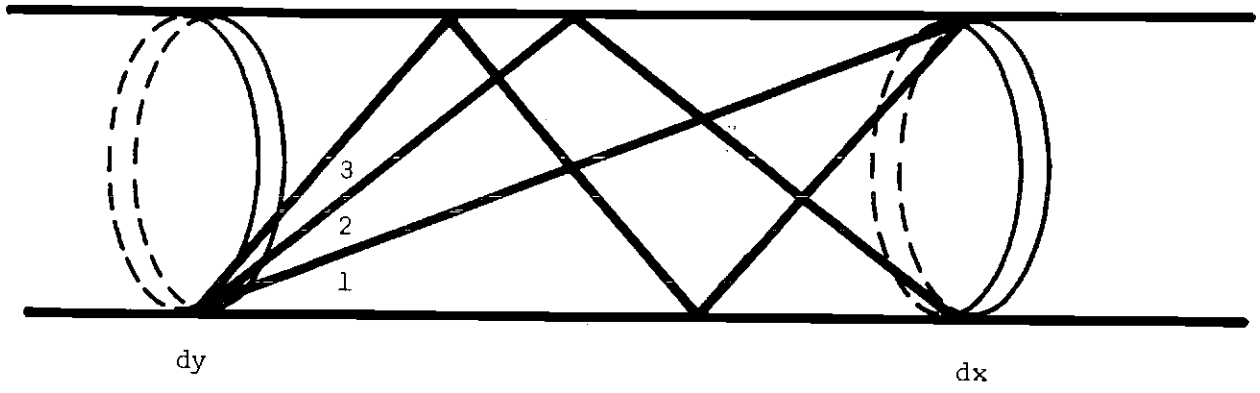

Figure 6. Summation of Specular Ray Contributions to Obtain Series Formula for $\Gamma(y,x)$

$$(\tfrac{1}{2})(r_1-r_1r_2)K\left(\left|\frac{x-y}{2}\right|\right). \tag{16}$$

Similarly, the molecule may arrive at dx by proceeding to the doubly reflected image of the opposite wall with a probability equal to

$$\left(\frac{1}{3}\right)(r_1r_2-r_1r_2r_3)K\left(\left|\frac{x-y}{3}\right|\right), \tag{17}$$

since the mirror image this time is only 1/3 dx. The trend of the series is obvious and the series may be summed to obtain

$$\begin{aligned}\Gamma(y,x) &= (1-r_1)K(|x-y|) + \tfrac{1}{2}\, r_1(1-r_2)K\left(\left|\frac{x-y}{2}\right|\right) \\ &= \frac{1}{3}\, r_1r_2(1-r_3)K\left(\left|\frac{x-y}{3}\right|\right) \\ &\quad + \ldots \qquad .\end{aligned} \tag{18}$$

In the case of no specular reflection,

$$\lim_{\epsilon_0 \to +\infty} \Gamma(y,x) = K(|x-y|). \tag{19}$$

Development of the Entrance Formula

The equation for the collision density is

$$s(x) = s_1(x) + \int_0^L s(y)\Gamma(y,x)dy. \tag{20}$$

Consider the equilibrium conditions where a capillary is connected to two reservoirs filled with a rarefied gas at a uniform temperature and pressure. The integral equation for this situation is

$$s(x) = s_1(x) + s_1(L-x) + \int_0^L s(y)\Gamma(y-x)dy \qquad (21)$$

where the following functions are defined:

$s_1(x)$ rate of first diffuse collisions per unit length of the distance x measured from the entrance of the first reservoir.

$s_1(L-x)$ rate of first diffuse collisions per unit length of the distance L - x measured from the entrance of the second reservoir

$s(x)$ rate of diffuse collisions per unit length of x measured from the entrance.

$\Gamma(y,x)$ probability per unit dx that a molecule which has diffusely collided at y will suffer its next diffuse collision at x.

The temperature is constant in this case. The last two values will be denoted as $s_0(x)$ and $\Gamma_0(y,x)$ to indicate the set-up at equilibrium. The collision density per unit x must be that of a uniform gas,

$$s(x) = \tfrac{1}{4}\, n\bar{v}\pi D \qquad (22)$$

where D is the capillary diameter and $\bar{v}$ is the average velocity of the gas. Considering the diffuse collision density only, and normalizing to one entering molecule, we obtain

$$s_0(x) = \frac{\frac{1}{4}\, n\bar{v}\pi D(1-r_1)}{\frac{1}{4}\, n\bar{v}\,\frac{\pi D^2}{4}} = \frac{4}{D}\,(1-r_1). \tag{23}$$

It then follows that

$$s_0(x) = \frac{4}{D}\,(1-r_1) = s_1(x) + s_1(L-x) + \int_0^L \Gamma_0(y,x) \cdot \frac{4}{D}\,(1-r_1)dy\ . \tag{24}$$

Removing the constants from the integral,

$$s_0(x) = s_1(x) + s_1(L-x) + \frac{4}{D}\,(1-r_1) \int_0^L \Gamma_0(y,x)dy \tag{25}$$

and dividing the integral into two parts,

$$s_0(x) = s_1(x) + s_1(L-x) + \frac{4}{D}\,(1-r_1)\left[\int_0^x \Gamma_0(y,x)dy + \int_0^{L-x} \Gamma_0(y,x)dy\right] \tag{26}$$

we obtain, with the substitution, $u = |x-y|$,

$$\frac{4}{D}(1-r_1) = s_1(x) + s_1(L-x) + \frac{4}{D}(1-r)\left[\int_0^x \Gamma_0(u)du + \int_0^{L-x} \Gamma_0(u)du\right]. \tag{27}$$

Setting L = 2x, it follows that

$$\frac{4}{D}(1-r_1) = s_1(x) + s_1(x) + \frac{4}{D}(1-r_1)\left[\int_0^x \Gamma_0(u)du + \int_0^x \Gamma_0(u)du\right] \tag{28}$$

since we are dealing with an equilibrium gas. Simplifying,

$$s_1(x) = \frac{2}{D}(1-r_1) - \frac{4}{D}(1-r_1)\int_0^x \Gamma_0(u)du \tag{29}$$

and taking the derivative, we obtain

$$\frac{ds_1(x)}{dx} = -\frac{4}{D}(1-r_1)\Gamma_0(x). \tag{30}$$

Since

$$\lim_{\epsilon_0 \to \infty} s_1(x) = n_1(x) \tag{31}$$

it follows that

$$\frac{dn_1(x)}{dx} = -\frac{4}{D} \cdot K(x) \tag{32}$$

or

$$\frac{dn_1(x/m)}{dx} = -\frac{4}{D} \cdot \frac{1}{m} \cdot K(x/m). \tag{33}$$

Solving this expression for the kernel function in terms of the derivative of $n_1(x/m)$ with respect to x, we obtain

$$\frac{1}{m} K(x/m) = -\frac{D}{4} \frac{dn_1(x/m)}{dx} \tag{34}$$

from which it follows that

$$\frac{ds_1(x)}{dx} = (1-r_1)\left[(1-r_1)\frac{dn_1(x)}{dx} + r_1(1-r_2)\frac{dn_1(x/2)}{dx}\right. \tag{35}$$

$$\left. + r_1r_2(1-r_3)\frac{dn_1(x/3)}{dx} + \ldots\right].$$

Integrating this expression, the $s_1(x)$ function is obtained as

$$s_1(x) = (1-r_1)[(1-r_1)n_1(x) + r_1(1-r_2)n_1(x/2) \tag{36}$$

$$+ r_1r_2(1-r_3)n_1(x/3) + \ldots].$$

Since

$$s_1(x) = - \frac{dS_1(x)}{dx} , \tag{37}$$

it is apparent that

$$S_1(x) = (1-r_1)[(1-r_1)N_1(x) + 2r_1(1-r_2)N_1(x/2) + 3r_1r_2(1-r_3)N_1(x/3) + \ldots]. \tag{38}$$

Since $n_1(x)$ and $N_1(x)$ are simply related, it remains only to calculate one or the other. The analytical expressions may then be combined with the computer calculation of $f(x,L)$ to obtain the transmission probabilities.

Derivation of the Expressions for $n_1(x)$ and $N_1(x)$

$N_1(x)$ is by definition the probability that a molecule emitted into the capillary at the entrance circle $x = 0$ will pass through the capillary beyond x without collision. If the radius of the capillary is denoted by a, then $N_1(x)$ is the probability of a molecule passing through a circle of area πa^2 whose center is on the axis of the capillary at x and whose plane is normal to the capillary axis. Consider a sphere at the end of a capillary of radius a which contains both the periphery of the entrance circle and the circle at x as shown in Figure 7. The equation of the sphere is

$$\left(x' - \frac{x}{2}\right)^2 + y'^2 + z'^2 = a^2 + \frac{x^2}{4} \tag{39}$$

where primes have been added to x, y, and z to avoid confusion with the distance x.

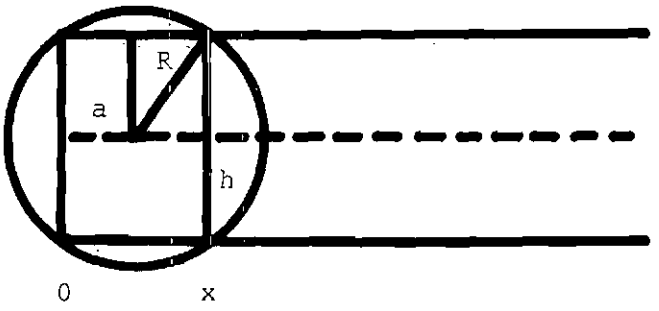

Figure 7. Sphere Located at End of Capillary of Radius, a, Which Contains Both the Periphery of the Entrance Circle at x = 0 and the Circle at x

A molecule which passes from the entrance circle through the circle at x without striking the capillary walls will also pass through the cap of the sphere without collision. Conversely, a molecule emitted from the inner surface of the spherical cap at x and passing directly out the entrance would also pass through the entrance cap of the sphere. Hence we can consider emission with the cosine law from inside the spherical cap at x instead of emission from the circle at x = 0 and collision with the circle at x. It is a property of the cosine law that emission from any point on the inner surface of a sphere gives a uniform probability over the surface of the sphere. The fraction of molecules which strike the zone is

$$\frac{2\pi Rh}{4\pi R^2} \tag{40}$$

where R equals the radius of the sphere and h is the height of the zone. If the molecules entering are normalized to unity per unit area, then the number falling beyond x can be calculated:

$$N_1(x) = \frac{2\pi Rh}{4\pi R^2} \cdot \frac{2\pi Rh}{\pi a^2} = \frac{h^2}{a^2} \quad . \tag{41}$$

From geometrical considerations it can be shown that

$$h = \sqrt{a^2 + \frac{x^2}{4}} - \frac{x}{2} = \frac{1}{2}\sqrt{x^2 + 4a^2} - x. \tag{42}$$

Since $2a = D$,

$$N_1(x) = \frac{1}{D^2}\left[2x^2 - 2x(x^2+D^2)^{\frac{1}{2}} + D^2\right] \tag{43}$$

from which it follows that

$$n_1(x) = \frac{2}{D}\left[(x^2+D^2)^{\frac{1}{2}} + \frac{x^2}{(x^2+D^2)^{\frac{1}{2}}} - 2x\right]. \tag{44}$$

It remains only to evaluate f(x,L) from the Monte Carlo computer routine.

The Computer Model

The function f(x,L) is defined as the probability that a molecule which has made a first diffuse collision at x will eventually pass through a capillary of length L and emerge at the exit. The problem thus reduces to calculating the number of molecules of a statistical

sample which exit the tube as a function of how far down the tube the calculation was begun.

The calculations were performed on a Burroughs 5500 digital computer. Random numbers were generated with a power residue formula where successive random numbers are given by

$$R_{n+1} = CR_n (\text{modulo } 8^{13}) \tag{45}$$

and C=541755813883. R_0 was equal to 1. The random number was computed in double precision to 26 octal digits and then normalized to the unit interval with a division by 8^{13}. The period of the random number sequence used was 2^{37}. The random variables were related to the uniformly distributed numbers by integrating the appropriate distribution function. Let r be a random variable which follows a distribution function P(r), over the range $0 < r < a$. Each value of r may be obtained by the relation

$$R_n = \int_0^{r_n} P(t)dt \tag{46}$$

where the R_n are adjusted to fall in a range determined by $0 < r < a$.

Calculation of the Jump Distance

Consider the point (x,y,z) in the diagram of Figure 8. In terms of spherical coordinates the x and y coordinates of the point are given by

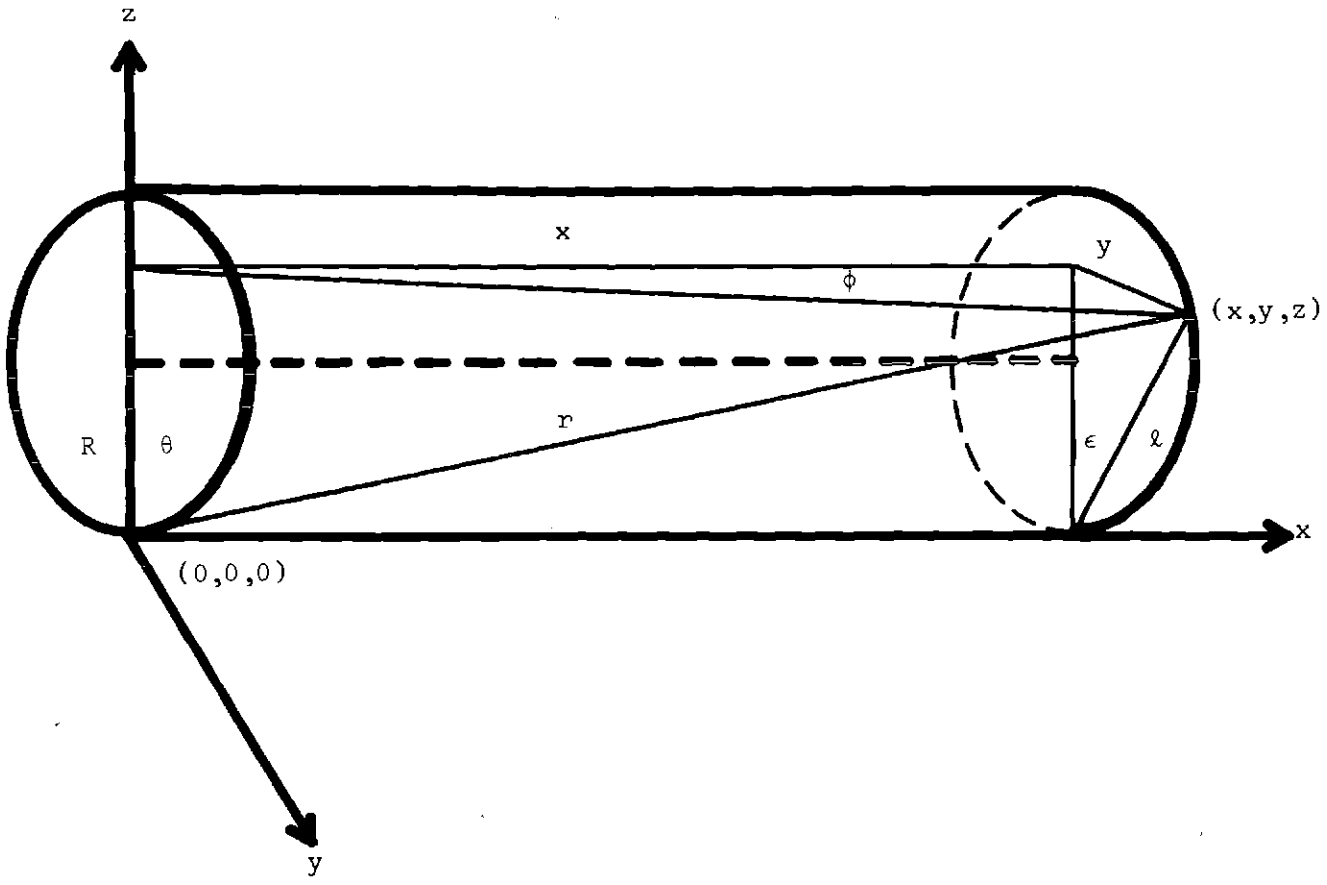

Figure 8. Diagram for the Calculation of a Molecular Jump Distance

$$x = r\sin\theta\cos\phi$$
$$y = r\sin\theta\sin\phi \quad . \tag{47}$$

From geometrical considerations at the face of the cylinder, it can be shown that

$$\ell = 2R\cos\epsilon \tag{48}$$

where R is the radius of the cylinder and ϵ is the angle between z and ℓ. From the Pythagorean Theorem,

$$\ell^2 = z^2 + y^2 = 4R^2\cos^2\epsilon \tag{49}$$

and since

$$\cos\epsilon = z/\ell \tag{50}$$

it follows that

$$\ell = 2R(z/\ell). \tag{51}$$

Hence

$$\ell^2 = 2Rz = z^2 + y^2. \tag{52}$$

Squaring y and z we obtain

$$y^2 + z^2 = r^2(\cos^2\theta+\sin^2\theta\sin^2\phi) \tag{53}$$

from which it follows that

$$r^2(\cos^2\theta+\sin^2\theta\sin^2\phi) = 2Rr\cos\theta. \tag{54}$$

Solving for r we obtain

$$r = \frac{2R\cos\theta}{(\cos^2\theta+\sin^2\theta\sin^2\phi)}. \tag{55}$$

Combining the expressions for r and x, we obtain the distance of a molecular jump along the axis of the capillary:

$$\Delta x = \frac{2R\cos\theta\sin\theta\cos\phi}{(\cos^2\theta+\sin^2\theta\sin^2\phi)}. \tag{56}$$

Operation of the Model

By using a sequence of random variables uniformly and independently distributed in the interval [0,1], a set of molecular histories which satisfy the given physical assumptions can be generated. A random variable, I, is defined such that I = 1 when a molecular history is terminated by the molecule leaving through the exit of the capillary, and I = 0 when a molecular history is terminated by the molecule leaving through the entrance of the capillary. The expected value of I is f(x,L), and the estimate given by the previous equation becomes

$$f(x,L) = \hat{I} = \frac{1}{N}\sum_{i=1}^{N} I_i, \qquad N_{exit} = \sum_{i=1}^{N} I_i \tag{57}$$

where N_{exit} is the number of molecular histories which terminated with the molecule leaving the capillary exit and N is the number of molecular histories generated.

The calculation of a molecular history begins by starting the molecule at some position, say, $x = x_0$, down a capillary tube of length, L, across which is placed a temperature gradient defined by two temperature reservoirs, T_1 and T_2, respectively. The temperature along the tube may be calculated from the relation

$$T = T_2 - (T_1/L)x \tag{58}$$

where x is the distance along the tube, and $T_2 > T_1$.

Two random numbers are chosen and the θ and ϕ values of the molecular jump are calculated as

$$\begin{aligned} R_n &= \sin\theta \qquad 0 \le \theta \le \pi \\ R_n &= \sin\phi \qquad 0 \le \phi \le \pi/2 \end{aligned} \tag{59}$$

where the distribution function for θ has been integrated to obtain the proper cosine law dependence on the angle. The energy of the molecule is then calculated in units of the Boltzmann constant

$$\epsilon = -T\ln R_n \tag{60}$$

where T has been evaluated in accordance with the temperature gradient equation above. The length of the molecular jump may be calculated from

$$\Delta x = \frac{\sin\theta\cos\theta\cos\phi}{1 - \sin^2\theta\cos^2\phi} \tag{61}$$

where D is assumed to be 1 and the L/D ratio is controlled by proper choice of the capillary length. To prevent any coupling between the θ and ϕ angles, a random number was used to determine the direction of the jump. Hence,

$$\begin{aligned} 0 \le R_n < 0.5 \qquad & \Delta x = |\Delta x| \\ 0.5 \le R_n \le 1 \qquad & \Delta x = -|\Delta x| . \end{aligned} \tag{62}$$

The nature of the jump was determined from the relation

$$R_n > e^{-\epsilon/\epsilon_0} \tag{63}$$

where the jump was considered to be specular if

$$\epsilon < \epsilon_0 \ln \frac{1}{R_n} \tag{64}$$

and diffuse if

$$\epsilon \geq \epsilon_0 \ln \frac{1}{R_n} . \tag{65}$$

When the molecular collision proved to be specular, random numbers were chosen until the nature of the jump was changed. The length of the total jump was then calculated based upon the number of intervening specular reflections and the position of the molecule in the tube was updated accordingly. If the collision was determined to be diffuse, of course, there were no intervening specular reflections to consider in determining the new position of the molecule. After each calculation of the position of the molecule in the tube, a check was made to see whether or not the molecule had left either the entrance or exit. If the molecule remained in the tube, the calculations were resumed. Otherwise, the calculated history was stored and another molecule begun. The calculation was terminated after a predetermined number of molecular histories had been generated.

A flow diagram of the program is shown in Figure 9. The distance of the first diffuse collision down the tube is given by x_0, the length of the tube by L, the number of molecular histories to be generated by M, the temperature of the two reservoirs by T_1 and T_2, respectively, and the parameter of specular reflection by ϵ_0. Conventional flow-charting methods were used in preparing the diagram.

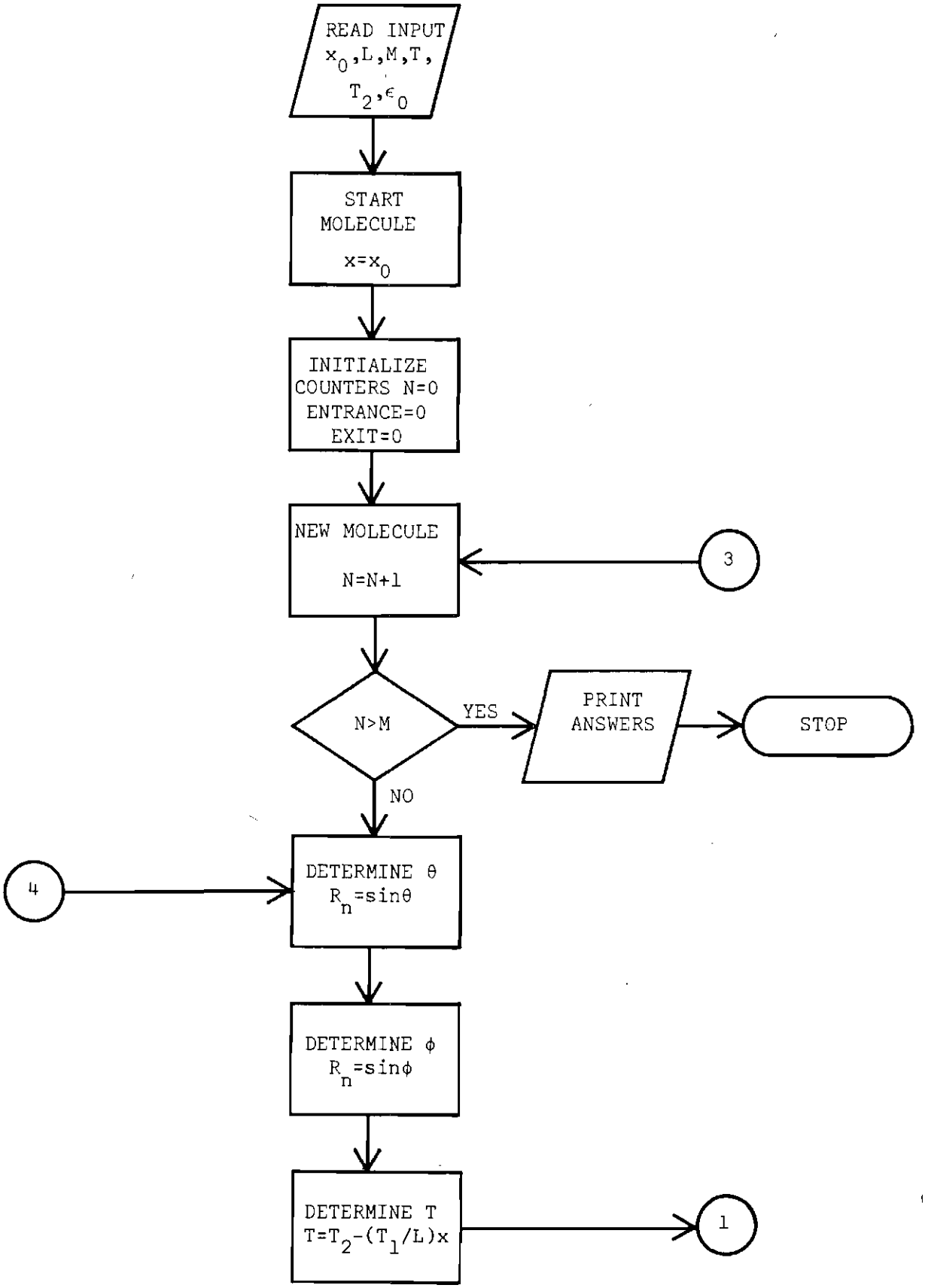
READ INPUT
x_0,L,M,T,
T_2,ϵ_0
START
MOLECULE
$x=x_0$
INITIALIZE
COUNTERS N=0
ENTRANCE=0
EXIT=0
NEW MOLECULE
N=N+1
3
N>M
YES
PRINT
ANSWERS
STOP
NO
4
DETERMINE θ
R_n=sinθ
DETERMINE φ
R_n=sinφ
DETERMINE T
$T=T_2-(T_1/L)x$
1

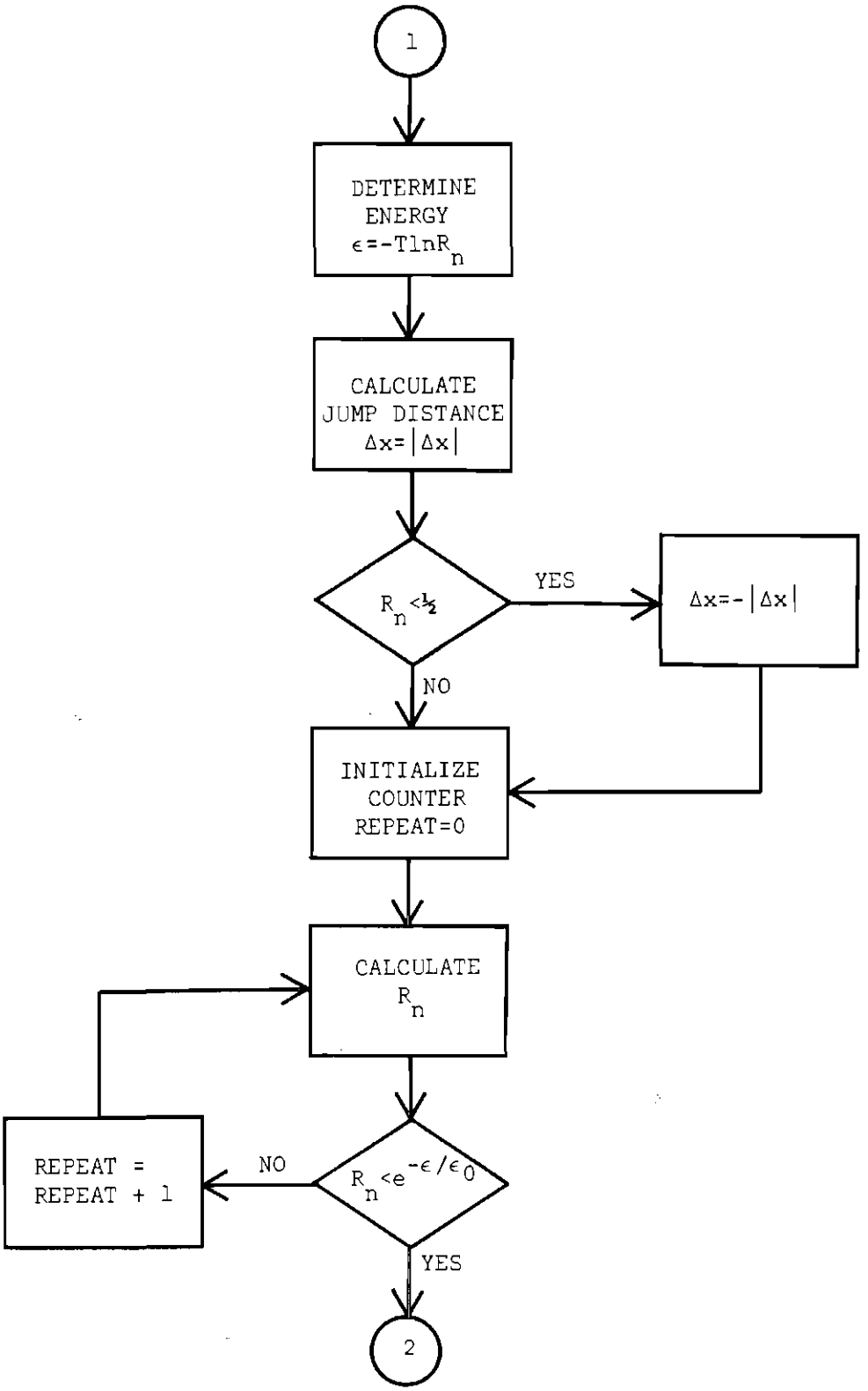
1
DETERMINE ENERGY $\epsilon=-T\ln R_n$
CALCULATE JUMP DISTANCE $\Delta x=|\Delta x|$
$R_n<\frac{1}{2}$
YES
$\Delta x=-|\Delta x|$
NO
INITIALIZE COUNTER REPEAT=0
CALCULATE R_n
$R_n<e^{-\epsilon/\epsilon_0}$
NO
REPEAT = REPEAT + 1
YES
2

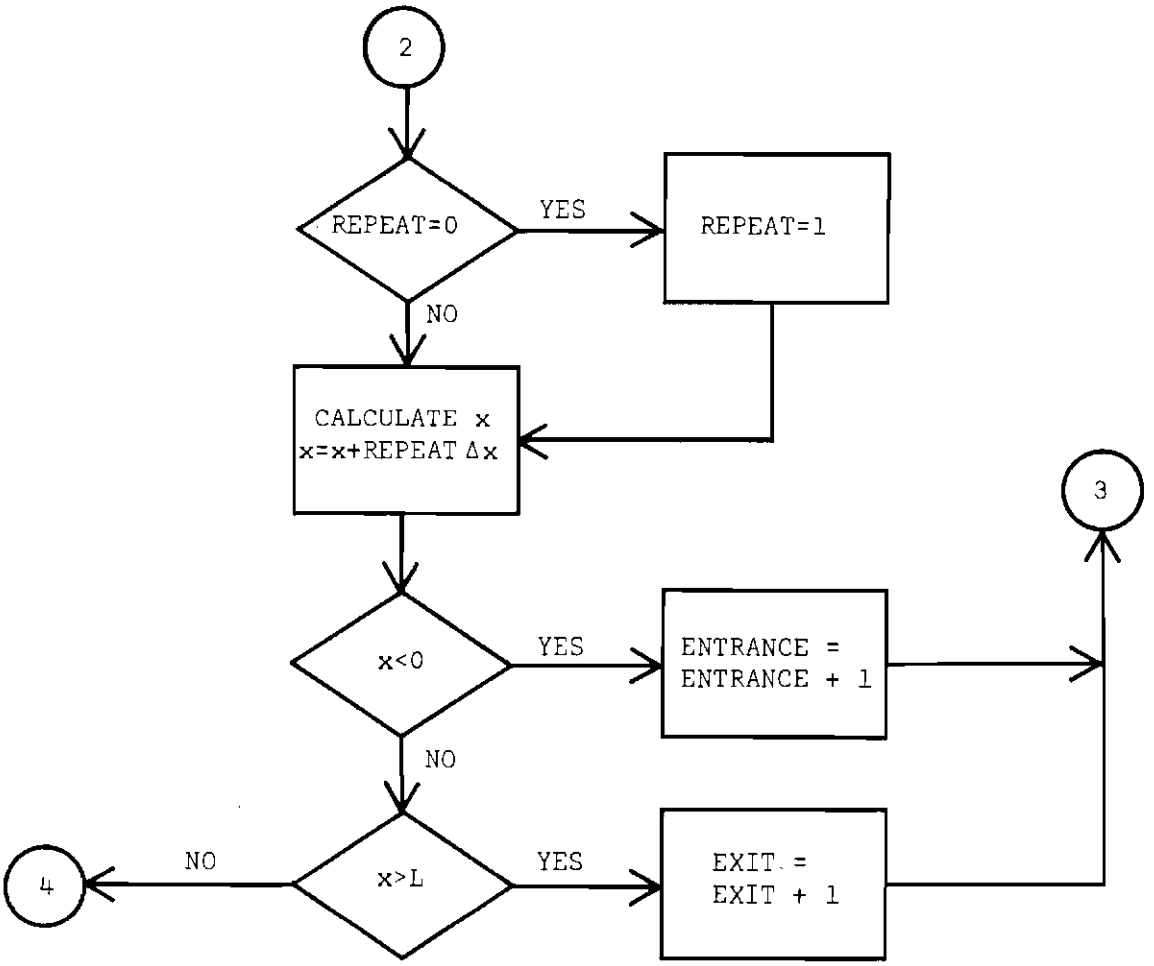
2
REPEAT=0
YES
REPEAT=1
NO
CALCULATE x
x=x+REPEAT Δx
3
x<0
YES
ENTRANCE =
ENTRANCE + 1
NO
4
NO
x>L
YES
EXIT =
EXIT + 1

CHAPTER IV

THEORY OF CAPILLARY FLOW IN TUBES

The early experiments of Kundt and Warburg (2) indicated that certain low pressure phenomena could be accounted for by assuming that a rarefied gas was able to "slip" over the walls of its container. It was assumed that any such slipping was proportional to the velocity gradient next to the wall of the container, at least as long as the velocity gradient was small. With this assumption, it is relatively easy to correct the Poiseuille flow equation for the existence of slip. Again assume a long straight tube of circular cross-section where the velocity of the gas across any cross-section is a function of the radial distance, r, from the axis. As before (1), in order to make steady flow possible, the net force due to the pressure on the ends of the mass of gas must be equilibrated by the viscous drag over its sides. Equating forces in the x-direction we again obtain

$$\frac{du}{dr} = -\left(\frac{r}{2\eta}\right) \frac{dp}{dx} , \tag{1}$$

so that upon integrating, we get

$$u = -\left(\frac{r^2}{4\eta}\right) \frac{dp}{dx} + C \tag{2}$$

where C is the integration constant still to be determined from a consideration of the boundary conditions imposed upon the gas flow at the walls of the container. Now the velocity of the gas next to the wall is no longer zero as in simple Poiseuille flow, but is proportional to the velocity gradient

$$u = \xi \frac{du}{dz} = - \xi \frac{du}{dr} \tag{3}$$

where z is considered normal to the wall of the cylinder, and ξ is considered to be a constant, usually termed the coefficient of slip. Since

$$u = - \frac{r^2}{4\eta} \frac{dp}{dx} + C \tag{4}$$

it follows immediately that, when r = a, the radius of the capillary,

$$u = \left(\frac{\xi a}{2\eta}\right) \frac{dp}{dx} . \tag{5}$$

It then follows that the integration constant, C, must be of such a value that

$$u = \frac{1}{4\eta} (a^2 - r^2 + 2\xi a) \frac{dp}{dx} . \tag{6}$$

The molecular flow through the cylinder may now be calculated as in Poiseuille flow:

$$G = n \int_0^a u 2\pi r dr = \frac{2\pi n}{4\eta} \frac{dp}{dx} \int_0^a (a^2 - r^2 + 2\xi a) r dr$$

$$= \left[\frac{\pi a^4 n}{8\eta} + \frac{\pi a^3 n \xi}{2\eta} \right] \frac{dp}{dx} \tag{7}$$

$$= \left[\frac{\pi a^4 p}{8\eta kT} + \frac{\pi a^3 \xi p}{2\eta kT} \right] \frac{dp}{dx} .$$

As before, G is independent of x in the steady state such that

$$G \int_0^L dx = \frac{\pi a^4}{8\eta kT} \int_{p_1}^{p_2} p dp + \frac{\pi a^3 \xi'}{2\eta kT} \int_{p_1}^{p_2} dp \tag{8}$$

where L is the length of the cylinder and $\xi' = \xi p$. Performing the indicated integration, one obtains

$$G = \frac{\pi a^4 \bar{p} \Delta p}{8\eta kTL} + \frac{\pi a^3 \xi' \Delta p}{2\eta kTL} \tag{9}$$

$$= \frac{\pi a^4 \Delta p}{8\eta kTL} \left[\frac{\bar{p}}{} + \frac{4\xi'}{a} \right]$$

where $\Delta p = p_2 - p_1$, the pressure drop from one end of the tube to the other, and $\bar{p} = \frac{1}{2}(p_1 + p_2)$, the average pressure. The coefficient of slip can be seen to have the units of length, and if the above expression is compared to the Poiseuille formula, can be pictured by noting that the motion is the same as if the cylinder wall were displaced backward a distance ξ with the velocity gradient extending uniformly to zero velocity at the new boundary. Present (1) has shown that

$$\xi \sim \frac{2}{3}\lambda \tag{10}$$

by considering momentum balances and the average distance that a molecule travels since its last collision before reaching the wall of the cylinder.

The flow of a gas when the mean free path of the gas greatly exceeds the diameter of the cylinder is also amenable to theoretical treatment. Such flow is termed free-molecular flow, or Knudsen flow, after the investigator who formulated much of the early theory.

Consider a long tube of circular circular cross-section with walls which are perfectly diffusing, such as the one shown in Figure 10.

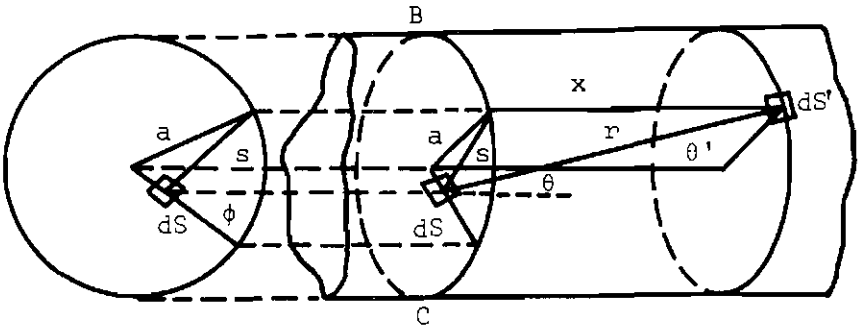

Figure 10. Coordinate System for Calculating Free Molecular Flow in Long Tube

The two ends are maintained at different pressures, and the temperature is uniform throughout the cylinder. Let the pressure be so low that

$$\lambda >> a \tag{11}$$

where λ is the mean free path of the gas, and a is the radius of the tube. Thus the flow of the gas is determined by the collisions with the wall, rather than by intermolecular collisions, which under the above condition would rarely occur.

Consider the flow of molecules across a cross-section BC of the tube. The molecules which cross an element of area dS of this cross-section come from various points along the wall of the tube where they underwent reflection, say, form an element of area, dS', on the wall a distance x from the plane containing the area BC, and also a distance r from dS in a direction making an angle θ with the normal to dS and an angle θ' with the normal to dS'. Now consider Figure 11 which shows the element of area, dS', in greater detail.

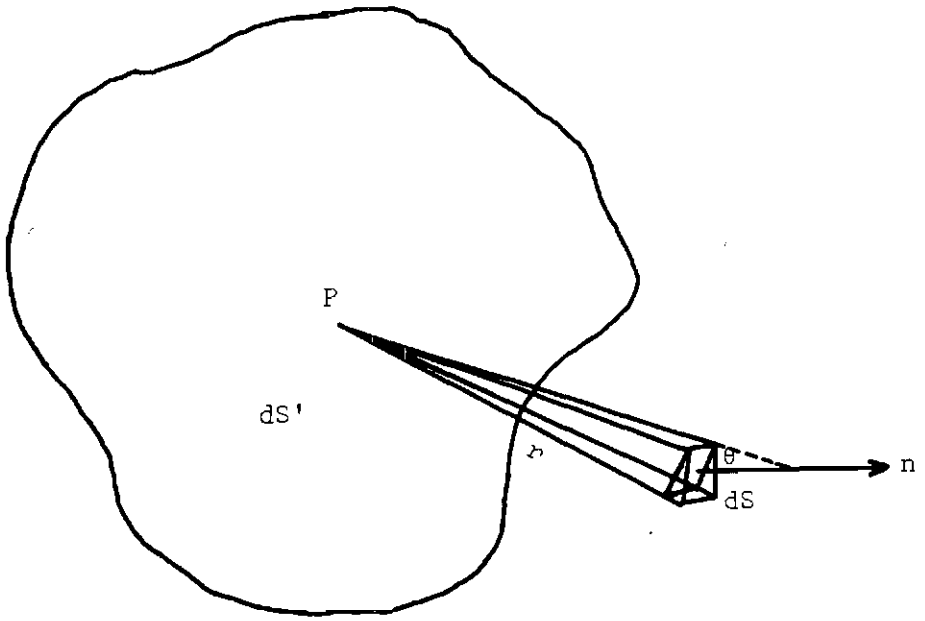

Figure 11. Element of Solid Angle for Calculating Number of Molecules Passing the Unit Area in a Direction Lying Within the Element

It was shown in Chapter II that the number of molecules leaving the unit of area, dS', per second, in a direction lying within an element of $d\omega$ of solid angle was given by

$$\frac{1}{4\pi} n\bar{v}\cos\theta' dS' d\omega \tag{12}$$

where $d\omega$ is the solid angle subtended by dS at dS' and has the value

$$d\omega = \frac{dS\cos\theta}{r^2} . \tag{13}$$

Choose the x axis parallel to the tube and locate the xy plane in the cross-section containing dS. If s is the projection of r on the xy plane, then the distance x from the xy plane to the cross-section through the element of area dS' is given by

$$x = r\cos\theta = s\cot\theta. \tag{14}$$

The molecular density is an unknown function of this distance, x, and can be expressed as n(x). If it is assumed that the density changes slowly with respect to the distance along the tube, the molecular density may be expanded in a Taylor's series around the point x = 0:

$$n(x) = n(0) + x\left(\frac{dn}{dx}\right)_0 + \tfrac{1}{2}x^2\left(\frac{d^2n}{dx^2}\right)_0 + \ldots . \tag{15}$$

Now in terms of spherical coordinates, the element of solid angle, $d\omega'$,

may be written as

$$d\omega' = \sin\theta d\theta d\phi \tag{16}$$

so that the net number of molecules crossing the element of area dS per unit time is given by the expression

$$dN = -\frac{\bar{v}dS}{4\pi}\int_0^{2\pi} d\phi \int_0^{\pi} n(x)\cos\theta\sin\theta d\theta \tag{17}$$

where the integration limits on θ correspond to a tube of infinite length.

If the Taylor's series expansion for the molecular density, n(x), is inserted into the above equation, the higher derivative terms above the first are neglected, and it is remembered that

$$x = s\cot\theta, \tag{18}$$

we obtain

$$dN = -\frac{\bar{v}dS}{4\pi}\int_0^{2\pi} d\phi \left[n(0) \int_0^{\pi} \cos\theta\sin\theta d\theta \right. \tag{19}$$

$$\left. + \left(\frac{dn}{dx}\right)_{x=0} s \int_0^{\pi} \cot\theta\cos\theta\sin\theta d\theta \right].$$

It is clear that the first integral in θ vanishes because of the limits of integration, since

$$\int_0^{\pi} \cos\theta\sin\theta d\theta = \tfrac{1}{2}\sin^2\theta\Big|_0^{\pi} = 0. \tag{20}$$

The second integral in θ may also be easily evaluated to give

$$\int_0^{\pi} \cot\theta\cos\theta\sin\theta d\theta = \int_0^{\pi} \cos^2\theta d\theta = \tfrac{1}{2}\theta + \tfrac{1}{4}\sin 2\theta\Big|_0^{\pi} = \pi/2 . \tag{21}$$

It then follows that

$$dN = -\frac{\bar{v}dS}{8}\left(\frac{dn}{dx}\right)_0 \int_0^{2\pi} sd\phi, \tag{22}$$

or

$$N = -\frac{\bar{v}}{8}\left[\int dS \int_0^{2\pi} sd\phi\right]\frac{dn}{dx} . \tag{23}$$

Since the cross-section of the tube is circular, the integral in dS may be integrated by remembering that the element of area dS is equal to dxdy (see Figure 12). Thus

$$\int sdS = \int_{-a}^{a} dx \int_{-(a^2-x^2)^{\frac{1}{2}}}^{(a^2-x^2)^{\frac{1}{2}}} [(a^2-x^2)^{\frac{1}{2}}-y]dy = 2\int_{-a}^{a} (a^2-x^2)dx = \frac{8}{3}a^2. \tag{24}$$

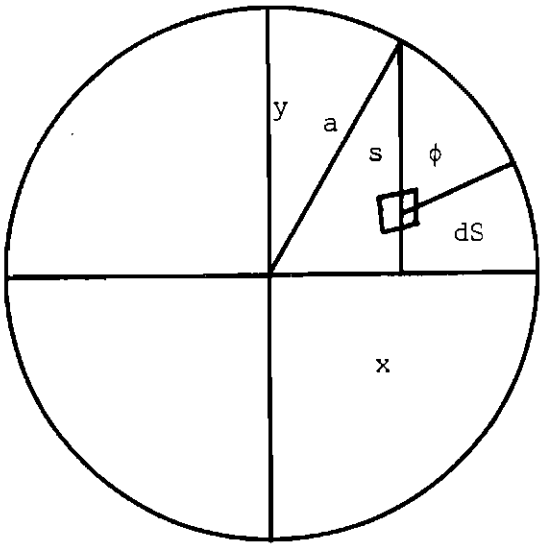

Figure 12. Element of Area for Circular Cross-Section of Capillary Tube

It then follows that

$$\int_0^{2\pi} d\phi \int s\,dS = \frac{16}{3}\pi a^3 \tag{25}$$

so that

$$N = -\frac{2}{3}\bar{v}\pi a^3 \frac{dn}{dx} . \tag{26}$$

In a steady flow, the number of molecules flowing per unit time must be constant along the tube, so that the density gradient is uniform and can be replaced by $\Delta n/L$ where Δn is the difference in density between the ends and L is the length of the tube. Since $\Delta n = \Delta p/kT$, the flow rate in moles is given by

$$F(\text{moles}) = \frac{2\pi a^3}{3}\left(\frac{8RT}{\pi M}\right)^{\frac{1}{2}}\frac{\Delta p}{LRT}\,. \qquad (27)$$

Present (1) has shown that consideration of the second term in the Taylor series expansion leads to the same result because the resulting θ integral vanishes. Knudsen flow through a tube differs from Poiseuille flow in several respects. The former varies as the cube of the radius whereas the latter varies as the fourth power. Similarly, Poiseuille flow is proportional to the pressure difference between the ends of the tube and the average of the end pressures, whereas Knudsen flow is proportional to the pressure difference alone. It is also clear that if the specific flow $F/\Delta p$ is plotted against the average pressure, $\bar{p}$, a straight line should be obtained in the slip flow region, the intercept of which should yield a value of the slip coefficient. Since the work of Knudsen (36), Iuchi and Kanki (37), Liu (38), Fryer (39), and Scott and Dullien (40) indicates a minimum in the flow curve at low pressures, it is apparent that the slip equation cannot be valid over the entire pressure range. The gas flow in the three pressure regimes in terms of molecules per unit time can now be summarized:

$$F = \frac{\pi a^4 \bar{p}\Delta p}{8\eta kTL} \qquad \text{(Poiseuille Flow)}$$

$$F = \frac{\pi a^4 \bar{p}\Delta p}{8\eta kTL} + \frac{\pi a^3 \Delta p}{m\bar{v}L} \qquad \text{(Slip Flow)} \qquad (28)$$

$$F = \frac{2\pi a^3}{3}\left(\frac{8kT}{\pi m}\right)^{\frac{1}{2}}\frac{\Delta p}{LkT} \qquad \text{(Knudsen Flow).}$$

or, for small values of r/λ,

$$F\left(\frac{r}{\lambda}\right) = e^{-(2r/\lambda)} . \tag{31}$$

It then follows that for a long capillary tube of circular cross-section, the flow equation becomes

$$G' = \left[1-e^{-\sinh^{-1}(2r/\lambda)}\right](A\bar{p}+B) + Ce^{-\sinh^{-1}(2r/\lambda)} \tag{32}$$

where the constants A, B, and C may be evaluated from kinetic theory and are given by

$$A = \frac{\pi r^4}{8\eta kTL}$$

$$B = \frac{4\pi r^3}{3m\bar{v}L} \tag{33}$$

$$C = \frac{16r^3}{3m\bar{v}L}$$

In a typical flow measurement, the decay of the pressure in the system with time is usually followed. The number of molecules per unit time, G, is given by

$$G = -\frac{dN}{dt} = -\frac{1}{N}\frac{dN}{dt} \cdot N = -\frac{d\ln P}{dt} \cdot N, \tag{34}$$

Since PV = NkT, it follows that

$$-\frac{d\ln P}{dt} \equiv K = \frac{G}{N} = \frac{GkT}{PV} . \tag{35}$$

The variable in Scott and Dullien's equation is given in terms of G as

$$G' = \frac{G}{p} , \tag{36}$$

so that the constant defined above becomes

$$K = G' \frac{kT}{V} . \tag{37}$$

Expressing $F(r/\lambda)$ as

$$F\left(\frac{r}{\lambda}\right) = e^{-\sinh^{-1}(D/\lambda)} = \left(\frac{D}{\lambda} + \left[\left(\frac{D}{\lambda}\right)^2 + 1\right]^{\frac{1}{2}}\right)^{-1} \equiv F \tag{38}$$

we obtain finally,

$$K = \frac{kT}{V}\left[\left(1 - \frac{1}{F}\right)(A\bar{p}+B) + \frac{1}{F} C\right]. \tag{39}$$

Upon simplification,

$$K = \frac{kT}{V} C + \frac{kT}{V} (B-C)(1-F) + \frac{kT}{V} (1-F)A\bar{p} \tag{40}$$

and substitution for the constants derived from kinetic theory we obtain

$$K = K_0\left[1 - \left(1 - \frac{\pi}{4}\right)(1-F) + \frac{3\pi}{128}(1-F)\left(\frac{D}{\lambda}\right)\right], \qquad (41)$$

where the quantity, D/λ, is considered to be a mean value.

Flow Into a Perfect Vacuum

Consider now the flow of a gas through a capillary under conditions where the gas exits into a vacuum as is depicted in Figure 13.

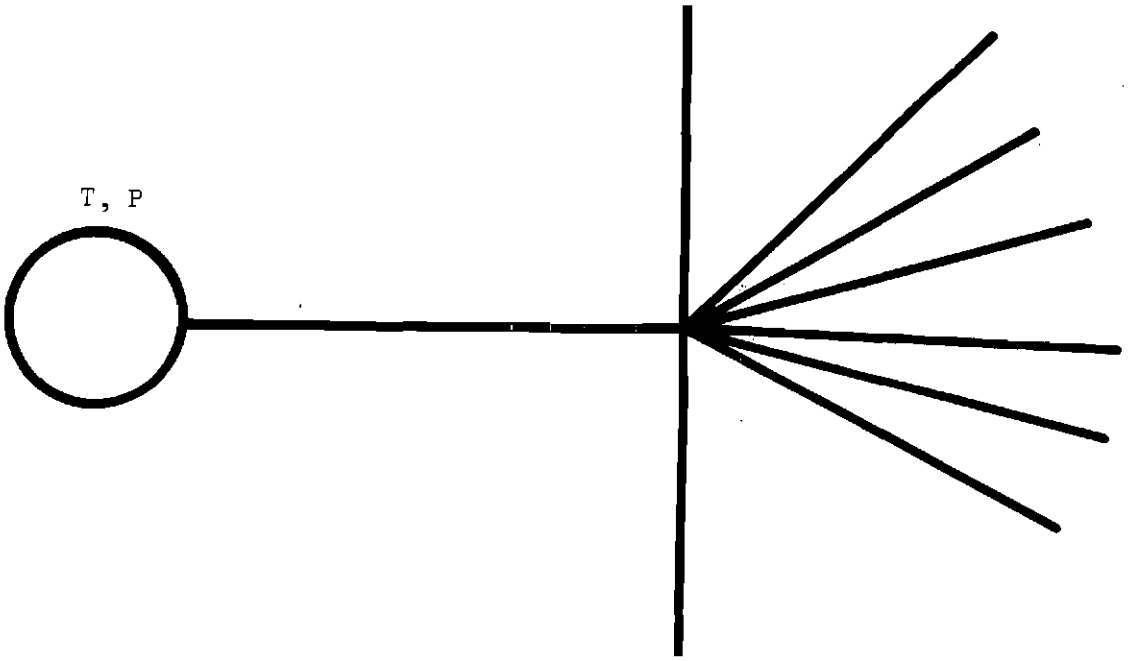

Figure 13. Flow of Gas Through a Capillary into a Perfect Vacuum

The number of molecules flowing into the vacuum is equal to the number of molecules entering the capillary multiplied by the transmission probability, Q. The usual kinetic energy expression,

$$\nu = \tfrac{1}{4}n'\bar{v}, \qquad (42)$$

denotes the number of molecules colliding per second per unit area of the wall of the container, where n' is the number density of the contained gas. It then follows that

$$-V \frac{dn'}{dt} = \tfrac{1}{4} n' \bar{v} \cdot A \cdot Q \tag{43}$$

where A is the cross-sectional area of the capillary and V is the volume of the gas reservoir. Since

$$P = n'kT, \tag{44}$$

it follows that

$$\frac{dn'}{dt} = \frac{1}{kT} \frac{dP}{dt} , \tag{45}$$

so that upon substitution for $\bar{v}$ and A, the following expression may be written

$$-V\left(\frac{1}{kT} \frac{dP}{dt}\right) = \tfrac{1}{4}\left(\frac{1}{kT} P\right)\left(\frac{8kT}{\pi m}\right)^{\frac{1}{2}}\left(\frac{\pi D^2}{4}\right) Q \tag{46}$$

where D is the capillary diameter and k is the Boltzmann constant. Rearranging this expression,

$$- \frac{dP}{P} = \left[\frac{1}{V}\left(\frac{\pi kT}{2m}\right)^{\frac{1}{2}} \frac{D^2}{4} Q\right] dt \tag{47}$$

we obtain finally

$$-\frac{dP}{P} = \left[\frac{1}{V}\left(\frac{\pi RT}{2M}\right)^{\frac{1}{2}}\frac{D^2}{4}Q\right]dt = k'Qdt. \qquad (48)$$

Thus it follows, in agreement with the formula derived from the work of Scott and Dullien, that

$$\frac{d\ln P}{dt} = -k \qquad (49)$$

and that $K = k$. Obviously a measure of the rate constant in the flow equation is also a measure of the transmission probability, Q.

CHAPTER V

EXPERIMENTAL

The evidence from the Monte Carlo calculations suggests that the transmission probability is relatively insensitive to a temperature gradient across a capillary. In addition, the calculations also indicate that specular reflection may play a role in the divergence of the forward and reverse transmission probabilities. Isothermal flow measurements may therefore provide some insight to the deviations from the Knudsen limiting law which have been observed experimentally.

In order to measure the temperature dependence of the transmission probability, it is necessary to measure the flow constant, k, of the expression

$$\frac{d\ln P}{dt} = -k'Q = k \qquad (1)$$

at different temperatures for different gases.

After a suitable calibration, thermal conductivity can be used to give an indication of the pressure of a system (41). In fact, if only the rate of change of the pressure with time is desired, it is not necessary to calibrate the apparatus against an absolute standard such as a McLeod gauge.

The Hot Wire Manometer

In 1906 M. Pirani (42) showed that the pressure of a system could best be measured by following the rate of heat loss from a thin hot wire--thus the term "hot wire manometer." In the usual set-up, the heat loss of the hot wire is measured electrically with a Wheatstone bridge network which performs the double function of heating the wire and measuring the resistance. A simplified circuit diagram of a Pirani gauge is shown in Figure 14.

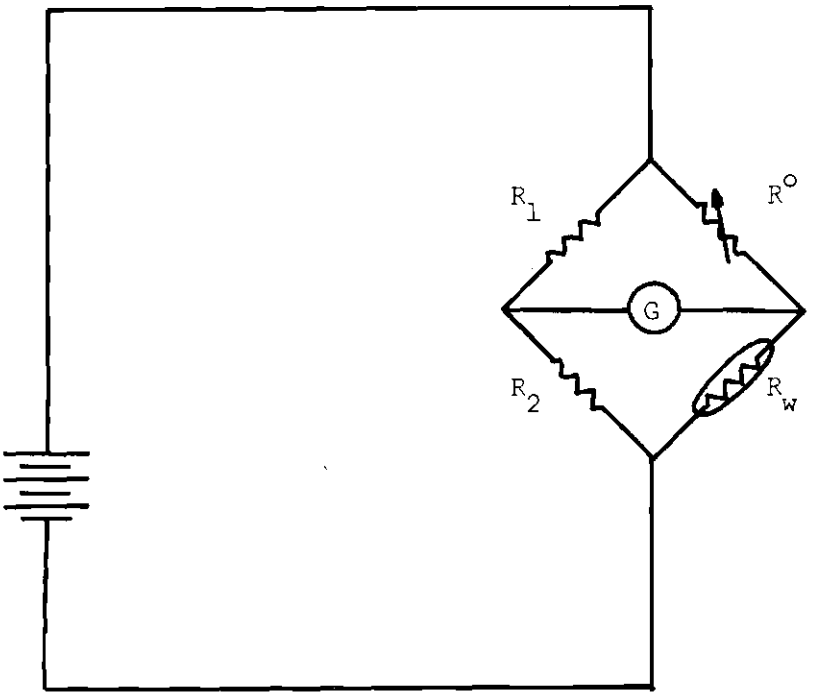

Figure 14. Simplified Wheatstone Bridge Circuit Showing Hot Wire Manometer

The hot wire with resistance R_w is placed in a bridge having one variable resistance (R°) and two arms of equal resistance (R_1 and R_2).

At a low pressure, say below a micron, where conduction is negligible, the voltage applied to the bridge may be set to some convenient value. The variable resistor, R°, may then be adjusted until the galvanometer indicates a null, at which time the bridge is balanced. An increase of pressure, by increasing the heat loss, lowers the wire temperature and unbalances the bridge. Likewise, a decrease in pressure, by decreasing the heat loss, raises the wire temperature and again unbalances the bridge. In either case, when the bridge is rebalanced by altering the value of R°, the resistance of the hot wire, and therefore its temperature, must be at the original value. Since the electrical energy into the gauge must equal the heat energy out of the gauge, the voltage across the hot wire is an indication of the pressure when the bridge is balanced. That this is so can be seen by considering the thermal equilibrium equation

$$\text{electrical input} = \text{radiation term} + \text{conduction term} + \text{end support term}$$

Since the conduction term is proportional to the pressure and the radiation term and the end support term are both proportional to the temperature difference between the wire and the gas, the Pirani gauge should obey the equation

$$E^2 = AP + B \qquad (2)$$

provided the temperature difference is constant. If the voltage reading across R_w at zero pressure is denoted by E_0, a simple relationship,

$$E^2 - E_0^2 = AP$$

exists between the voltage and the pressure of such a system. The flow constant, k, can thus be evaluated by measuring the voltage across R_w as a function of time and plotting $\ln(E^2-E_0^2)$ versus the time to evaluate the slope, k.

Experimental Apparatus

The control circuit for the Pirani gauge is shown in Figure 15. The bridge was designed on the "constant current" principle so that the temperature of the wire, and hence the value of ΔT, could be controlled through an adjustment of the bridge balance resistors. It was thus possible to set the bridge balance so that a particular ratio of E/E^o, where E is the voltage across the hot wire, and E^o is the voltage across the adjacent arm of the bridge, was indicative of a particular value of ΔT, since the temperature of the wire could be obtained from a suitable calibration chart.

The Pirani gauge chosen for the experiment was a Pyrex glass tube, GAV-004, bakeable to 400°C., purchased from Bendix, Inc., Rochester, New York. The gauge was approximately 5 inches in length and had a volume of about 4 cubic centimeters. The coiled wire inside was fixed between two tungsten pins which extended outside the gauge about ¼ inch. The external connection to the Wheatstone bridge was made with a

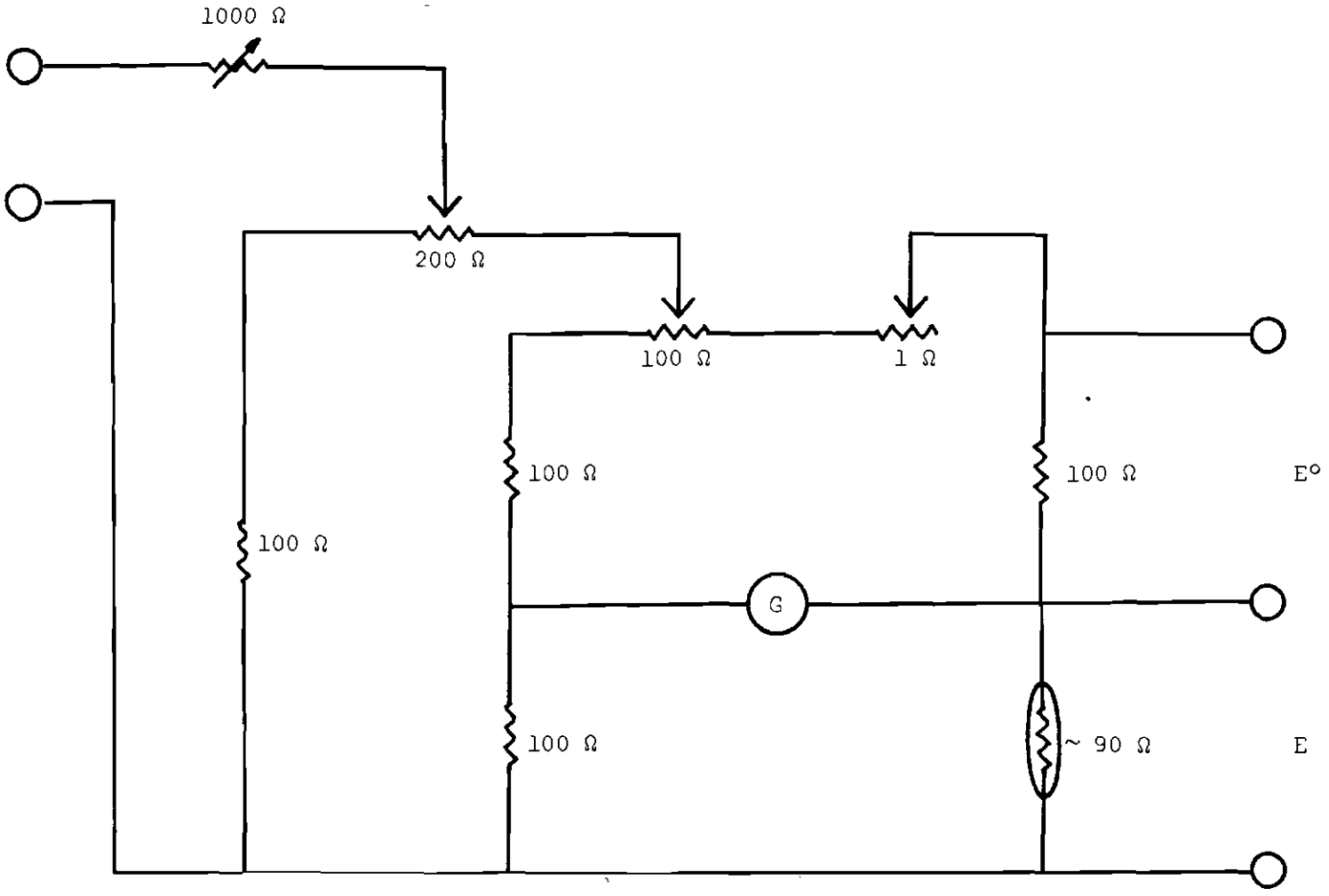

Figure 15. Control Circuit for Pirani Gauge

GAV-006 matching cable connector also purchased from the Bendix Corporation.

The Pirani gauge was sealed to the gas reservoir used in the experiments as shown in Figure 16. The gas sample cell was designed so that both isothermal and temperature gradient measurements could be made with the same reservoir and the same capillary tube. A length of precision capillary (diameter 0.0204 centimeters) was obtained from Ace Glass, Inc., in Vineland, New Jersey. Using successively finer grinding powders, and the rough grinder in the glass blowing lab, a taper was placed on one end of the capillary such that a good seal was obtained with the 5/12 Pyrex female joint. The length of the finished capillary tube was 5.70 centimeters. The special tube could then be placed in either of the 5/12 females in the flow cell. In the lower position the entire reservoir could be immersed in a temperature-controlled water bath for isothermal studies. In the upper position, the lower part of the cell could be maintained at one temperature and the upper end of the capillary at another, using the glass cup around the outer piece of glass as the second temperature reservoir, for temperature gradient experiments. The flow cell was designed to minimize the pressure differential across the ground glass taper of the capillary by placing the seal inside the primary vacuum reservoir. The ends of the capillary tube were always well defined due to the ground glass taper which was used to join the capillary tube to the flow cell. Glassblowing would have distorted the capillary in the area near the seal.

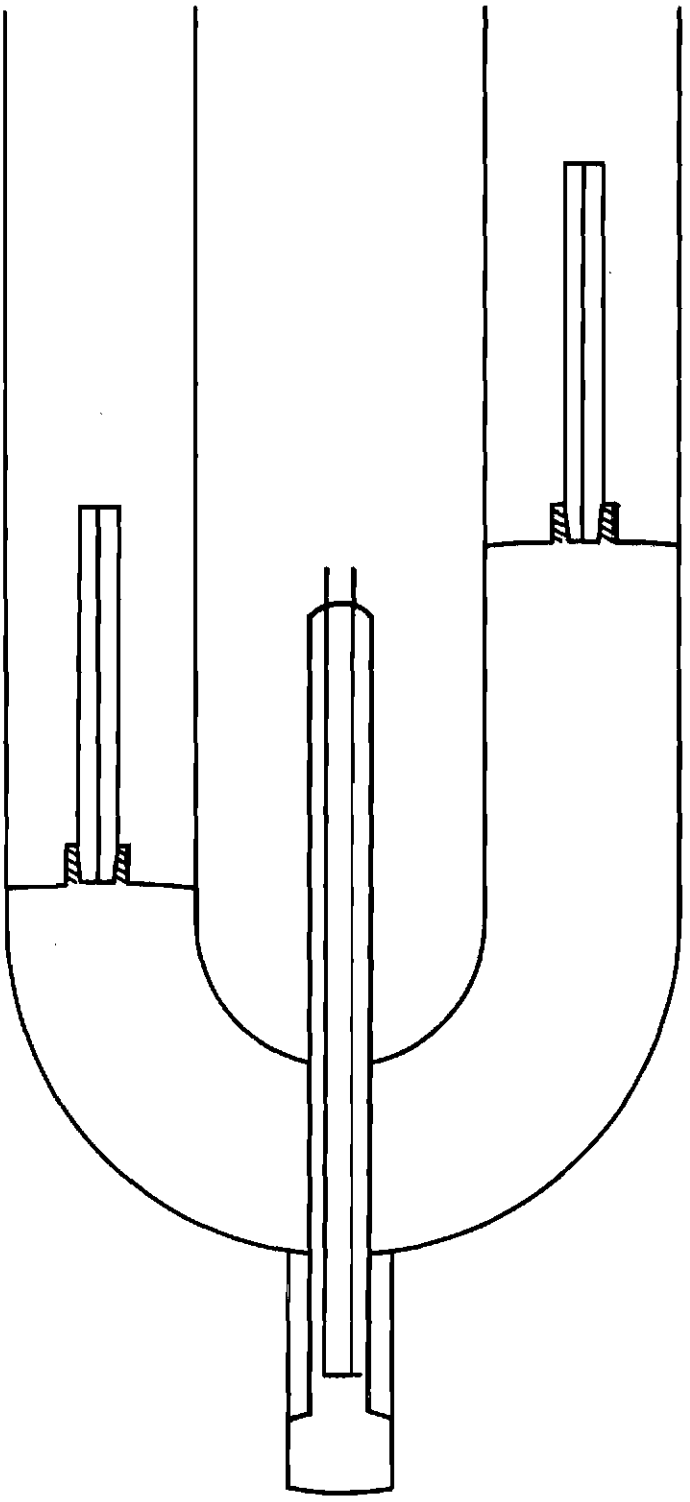

Figure 16. Gas Sample Cell: Pirani Gauge and Capillary Detail

The temperature was controlled within ± 0.01°C. with a Haake Series N Constant Temperature Circulator, Model NBS, purchased from Brooklyn Thermometer Company in Farmingdale, New York. The Model NBS circulator has a built-in, dual-purpose pump which applies both pressure and suction at the same time by means of aspiration. The rate of flow of the circulator could be modified by varying the size of the nozzle outlet, the diameter of the circulating hose, or by clamping the circulating hose. A continuously variable heating control allowed selection of a heater output from 0 to 2000 watts. The use of the Haake K-60 Heat Exchanger allowed temperatures down to -60°C. to be obtained. Two contact thermoregulators were used:

1. 1-070040: range -60 to +30 degrees Centigrade, and
2. 1-070043: range 0 to +100 degrees Centigrade.

The voltage across the Pirani gauge during a run was monitored with a high accuracy digital voltmeter, Model 8104, purchased from California Instruments in San Diego, California. The accuracy of the instrument after 15 minutes warm-up was ±0.02 per cent of full scale ±0.03 per cent of the reading with a stability of 0.02 per cent of full scale per month. The resolution was 0.01 per cent of full scale, and in the range used, the linear settling time to the specified accuracy was 250 milliseconds.

The null point of the Wheatstone bridge circuit was indicated by the Model 104W1 Brown Electronik Null Indicator purchased from the Minneapolis-Honeywell Regulator Company in Philadelphia, Pennsylvania. The indicating meter was a D'Arsonval galvanometer movement with scale

markings of -4 to 0 to +4. Divisions were spaced 1 centimeter apart with subdivisions between +1 and -1 in millimeters. The instrument was designed for precision Wheatstone bridge circuits and had an input filter to reduce the effect of normal external stray currents. The current sensitivity was 1.0×10^{-9} amp/mm and the voltage sensitivity was 1.0×10^{-6} v/mm. The indicating meter, which reads the final value in less than one-half second after an unbalance occurs, is critically damped and is independent of external circuit resistance.

Pressure measurements on portions of the assembly other than the flow reservoir were made with an Ionization Vacuum Gauge Type GIC-110B with two sensing tubes, one a thermocouple tube Type GTC-004 and the other an ionization gauge tube Type GIC-017, all purchased from the Bendix Corporation. For absolute calibration a precision McLeod gauge manufactured by Hastings-Raydist, Inc., in Hampton, Virginia, was used. Two scales were available on the gauge covering a range of 20 torr to 1.0×10^{-5} torr with a sensitivity of 5×10^{-4} at 1 centimeter height differential.

The voltage supply for the bridge circuit was a charge retaining battery, Type DD-5-1, purchased from the WISCO Division of ESB Incorporated in Racine, Wisconsin. Such batteries are ideal for use with instruments requiring stable voltage with infrequent charging or attention. The capacity of the battery was rated at 500 amp hrs with a rate of 1.0 amperes. The cut-off voltage was 1.95 volts.

All of the circuitry was protected against sudden stray current surges after power failure with an electrical latch. A diagram of the

circuit is shown in Figure 17. A failure in the line current causes the latch to disconnect the protected circuit and to switch the power to the alarm outlet. The pilot light is not illuminated when a power failure has occurred. The latch may be reset by depressing the start switch.

The Vacuum Assembly

The flow cell was attached to the vacuum assembly in such a way that a gas pipette could be used to measure out known quantities of a gas from a primary reservoir at a given pressure and introduce the gas into the flow cell. The primary reservoir could be filled with a gas at pressures ranging from about 50 torr to atmospheric pressure. In this way the reservoir of the flow cell could be filled with gas either for an actual measurement or for purposes of calibration. The entire assembly could be evacuated to a pressure of less than 1.0×10^{-6} torr with the aid of a mercury diffusion pump coupled with a CENCO roughing pump purchased from Central Scientific Company. In cases where the temperature circulator was not used, the temperature was measured with a copper-constantan thermocouple which had been previously calibrated against the sublimation temperature of carbon dioxide using the method of Scott (43). A diagram of the vacuum assembly is shown in Figure 18. A dry ice trap was used after the diffusion pump except during the flow measurements at 77.4°K. when liquid nitrogen was used.

Experimental Procedure

Typically a flow experiment was carried out under isothermal conditions where the initial and final pressures of the run were adjusted

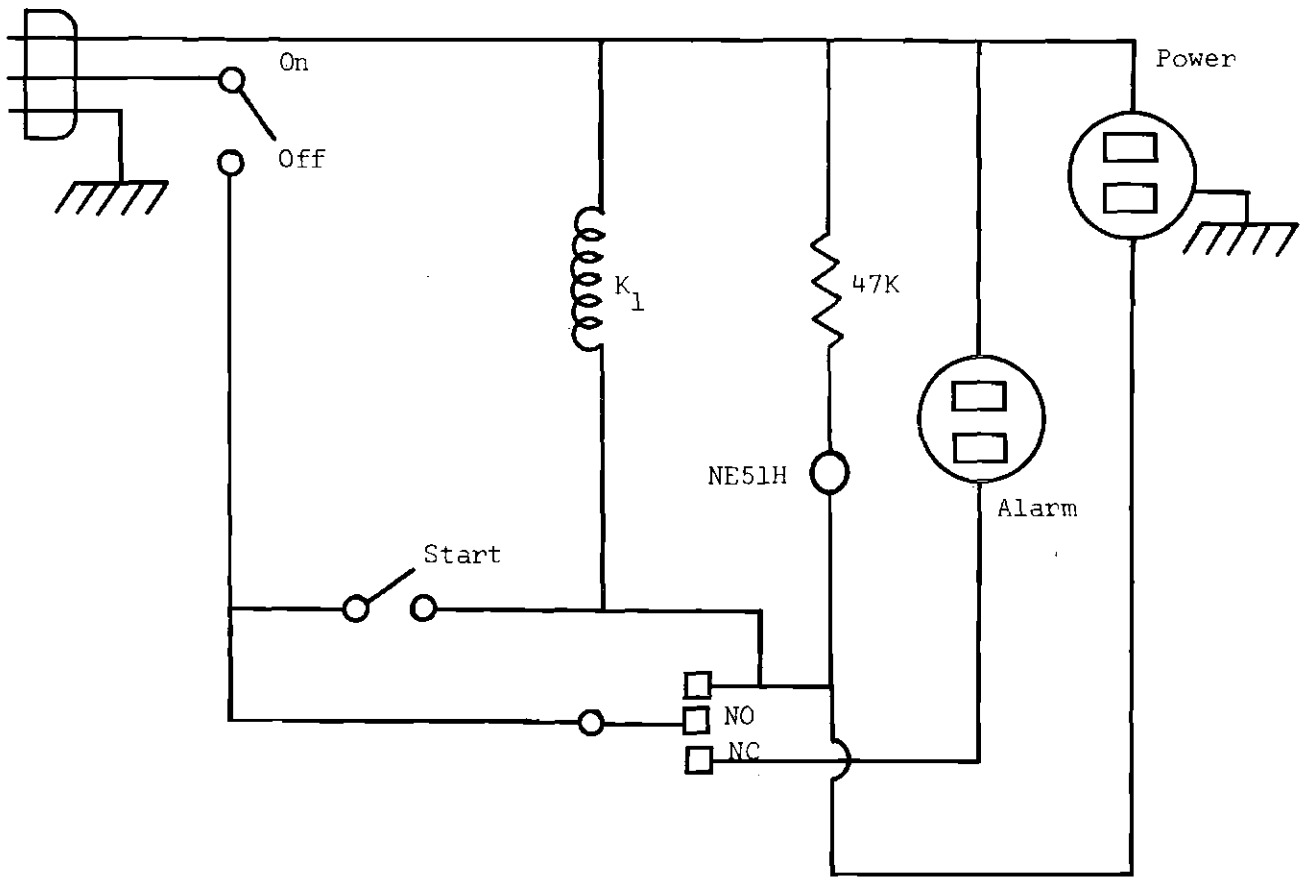

Figure 17. Circuit Diagram for Electrical Latch

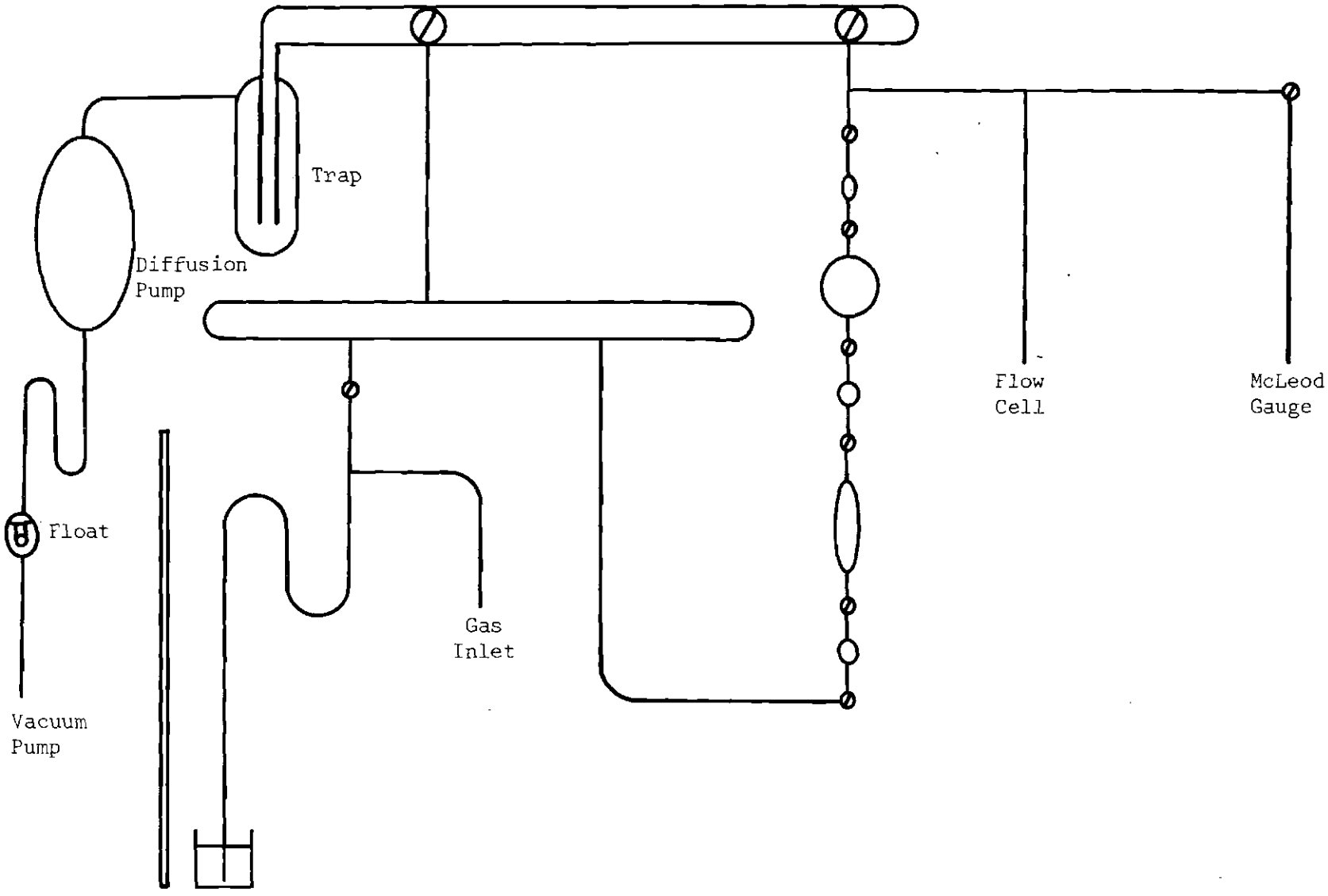

Figure 18. Vacuum Assembly

so that runs for different gases took place over the same range of mean free paths. Calibration curves of voltage across the Pirani gauge versus pressure read from the McLeod gauge were made for each gas at each temperature. Once the temperature bath had been adjusted to the desired value, a quantity of gas was introduced into the part of the vacuum system which included the flow reservoir and the McLeod gauge by means of the gas pipette. The system was then allowed to come to equilibrium for several hours before the pressure reading was made. Values of the initial and final mean free paths were chosen, first, to start the run under conditions of Knudsen flow, and, second, to terminate the runs in reasonable lengths of time. Accordingly, each run was started at a mean free path of 0.204 centimeters (10 times the capillary diameter) and stopped at a mean free path of 0.75 centimeters (36.8 times the capillary diameter). Voltages corresponding to the appropriate pressures could be determined from the calibration charts. The flow reservoir was then filled with a chosen gas and the voltage monitored until the desired voltage reading had been passed. The system was then opened to the vacuum and when the voltage reading on the digital voltmeter indicated that the starting value had been reached, a timer was started. Readings were then taken of the voltage as a function of time until the final value of the voltage was reached. At that time the run was terminated and another run begun by once again filling the reservoir with the desired quantity of gas. The voltage readings were taken only when the galvanometer indicated that the bridge was balanced. Since the readings were continually changing during the run due to the decrease

of pressure in the reservoir, and since the galvanometer had to be adjusted throughout the run while the measurements were being made, the digital voltmeter was a distinct advantage. When a potientiometer was tried in place of the digital voltmeter, it was not possible to monitor the experiment, to adjust the bridge current, and to take voltage readings simultaneously. Since it took at least a few seconds to measure a value of the voltage with the potentiometer, the pressure had changed and the bridge had become unbalanced by the time the measurement was completed. An uncertainty was thus always associated with runs made in this manner and the digital voltmeter was used exclusively to monitor the voltage.

The reading at "zero" pressure was always taken after several weeks of pumping and flushing the flow reservoir with a light gas such as hydrogen. The stability of this reading over various runs of different gases at different times added confidence to the correctness of this value. In addition, the runs were made under conditions where the "zero" pressure reading made sometime after the completion of a run or a series of runs could be compared with the value obtained before the reservoir was filled initially. It was therefore possible to monitor the characteristics of the Pirani gauge from day to day.

Choice of Gases

The gases chosen for the flow measurements were argon, helium, hydrogen, and deuterium. The light gases were chosen for their tendency to undergo specular reflection during a flow experiment as opposed to argon, which was expected to undergo little of this type of reflection

under typical experimental conditions. The deuterium gas was not as pure as desired, but it was used because its behavior should show general trends of interest. Table 2 summarizes the gases chosen for the experiments. The gases were contained in individual lecture bottles and were purchases from the Matheson Gas Products Company in Morrow, Georgia. The purity of each gas in Table 2 is expressed in mole per cent.

Table 2. Molecular Weight, Purity, and Grade of Gases Used in Flow Experiments

Gas	Molecular Weight	Purity	Grade
Argon	39.948	99.998	Prepurified
Helium	4.0026	99.995	High Purity
Deuterium	4.032	98.0	Technical
Hydrogen	2.016	99.95	Prepurified

Each lecture bottle was provided with a leak-free packless valve with handwheel control to provide good metering characteristics. For finer control during metering, a Model 3300 pressure regulator was used to introduce the gases into the system. The external thread on the bottle allowed the regulator to be placed in any convenient position for introducing the gas into the system.

CHAPTER VI

RESULTS AND DISCUSSION

The Monte Carlo program was designed to evaluate the term f(x,L) as a function of the distance down the capillary. The temperature of the entrance and exit reservoirs were 300°K. and 100°K., respectively. The results are summarized in Tables 3-6, where the L/D ratio and the value of ϵ_0 are indicated in each table.

Table 3. Results of Monte Carlo Run for L/D = 1, ϵ_0 = 900, and N = 500

x	f(x,L)
0.0	0.252
0.2	0.336
0.4	0.428
0.6	0.580
0.8	0.708
1.0	0.770

Table 4. Results of Monte Carlo Run for L/D = 10, ϵ_0 = 900, and N = 1000

x	f(x,L)
0	0.065
1	0.177
5	0.547
9	0.866
10	0.953

Table 5. Results of Monte Carlo Run for L/D = 10, ϵ_0 = 2100, N = 1000

x	f(x,L)
0	0.049
1	0.147
5	0.512
9	0.859
10	0.963

Table 6. Results of Monte Carlo Run for L/D = 50, ϵ_0 = 900, and N = 1000

x	f(x,L)
0.0	0.012
0.4	0.027
1.0	0.047
4.0	0.096
10.0	0.206
25.0	0.468
40.0	0.780
46.0	0.892
49.0	0.969
50.0	0.991

Figure 19 shows graphically the results for the three cases where the specular parameter was set at 900. This parameter was adjusted to give a somewhat higher degree of specular reflection (about 10 per cent) than might normally be expected so that any obvious trends in the performance might be recognized.

The transmission probabilities for each case were calculated by evaluating the integral equation

$$Q = S_1(L) + \int_0^L s_1(x)f(x,L)dx \qquad (1)$$

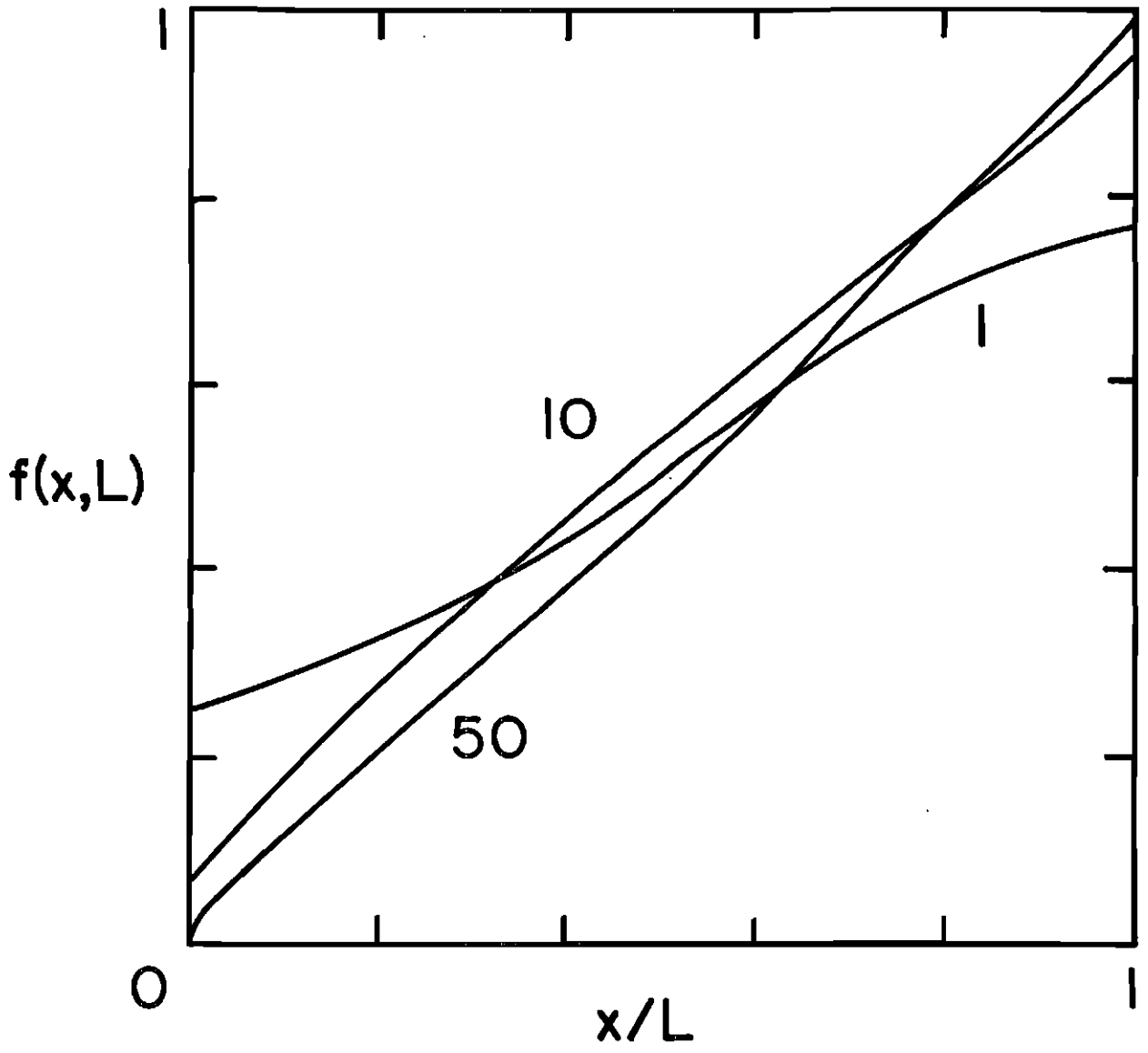

Figure 19. Exit Function for Various Capillary Length to Diameter Ratios

where the value of the integral was determined using the trapezoidal rule. The forward transmission probability, Q_{21}, was obtained by considering the entrance temperature to be at 300°K., while the exit temperature was maintained at 100°K. For the case of the reverse transmission probability, Q_{12}, the definitions of entrance and exit were interchanged. Recursion formulas for $S_1(x)$ and $s_1(x)$ were found to be useful in this calculation:

$$s_1(x) = (1-B_1)\left[\sum_{n=1}^{\infty} A_n(1-B_n)n_1\left(\frac{x}{n}\right)\right]$$

$$S_1(x) = (1-B_1)\left[\sum_{n=1}^{\infty} nA_n(1-B_n)N_1\left(\frac{x}{n}\right)\right]$$

$$A_n = (A_{n-1})(B_{n-1})$$

$$B_n = \left(\frac{n}{n+c}\right)$$

$$c = \epsilon_0/T$$

In addition, values of the transmission probability for isothermal conditions were calculated using the variational solution of De Marcus (29). In terms of the model, this solution becomes

$$Q = 8\left[\frac{ABL-AC-B^2}{4AL^2-C}\right] \qquad (3)$$

where

$$A = 1 + S_1(L)$$

$$B = \int_0^L S_1(x)dx \tag{4}$$

$$C = \int_0^L xS_1(x)dx.$$

Explicit expressions may be written for A, B, and C:

$$A = (1-r_1)[(1-r_1)N_1(L)+2r_1(1-r_2)N_1(L/2)$$
$$+3r_1r_2(1-r_3)N_1(L/3)+\ldots] + 1$$

$$B = (1-r_1)[(1-r_1)I(L)+4r_1(1-r_1)I(L/2) \tag{5}$$
$$+9r_1r_2(1-r_3)I(L/3)+\ldots]$$

$$C = (1-r_1)[(1-r_1)J(L)+8r_1(1-r_2)J(L/2)$$
$$+27r_1r_2(1-r_3)J(L/3)+\ldots]$$

where

$$N_1(x) = [2x^2-2x(x^2+1)^{\frac{1}{2}}+1]$$

$$I(L/n) = \int_0^{L/n} N_1(x)dx \tag{6}$$

$$J(L/n) = \int_0^{L/n} xN_1(x)dx$$

and r_n has its usual significance. It readily follows that

$$I(L/n) = \frac{1}{3}\left[2K^3-2(K^2+1)^{3/2}+3K+2\right] \tag{7}$$

and

$$J(L/n) = \frac{1}{4}\left\{2K^4-2K(K^2+1)^{3/2}+K(K^2+1)^{1/2} + \ln\left[K+(K^2+1)^{1/2}\right]+2K^2\right\} \tag{8}$$

where $K = L/n$.

Table 7 shows the results of the transmission probability calculation under both the temperature gradient and isothermal conditions. The standard deviation of the Monte Carlo results was calculated from the usual formula

$$\sigma = \left[\frac{f(x,L)\left(1-f(x,L)\right)}{N}\right]^{\frac{1}{2}} \tag{9}$$

where a weighted average was used to calculate the standard deviation for Q. Since the trapezoidal rule was used to evaluate the integral in the equation for the transmission probability, the standard deviation was weighted according to the individual contributions to the integral. Thus, for L = 10, we obtain

$$\sigma = \left[\tfrac{1}{4}\,\sigma_0^2 + \frac{25}{4}\,\sigma_1^2 + 16\,\sigma_5^2 + \frac{25}{4}\,\sigma_9^2 + \tfrac{1}{4}\,\sigma_{10}^2\right]^{\frac{1}{2}} \tag{10}$$

Table 7. Transmission Probabilities for Free Molecular Flow in Capillaries

L/D	T_1	T_2	ϵ_0	Q	σ
1	-	-	∞	0.514	-
1	300	300	900	0.695	-
1	300	100	900	0.719	0.007
1	100	100	900	0.558	-
1	100	300	900	0.539	0.008
10	-	-	∞	0.109	-
10	300	300	2100	0.142	-
10	300	100	2100	0.140	0.010
10	100	100	2100	0.118	-
10	100	300	2100	0.113	0.009
10	300	300	900	0.232	-
10	300	100	900	0.245	0.011
10	100	100	900	0.133	-
10	100	300	900	0.123	0.009
50	-	-	∞	0.0253	-
50	300	300	900	0.0691	-
50	300	100	900	0.0653	0.0044
50	100	100	900	0.0322	-
50	100	300	900	0.0300	0.0040

where

$$\sigma_x = \left[\frac{f(x,10)\left[1-f(x,10)\right]}{N}\right]^{\frac{1}{2}} \qquad (11)$$

and N is the number of Monte Carlo trials.

Figure 20 shows the transmission probabilities as a function of the "critical energy" of specular reflection. The upper curve represents the case where the entrance and exit temperatures were 300°K. and 100°K., respectively. In the lower curve of Figure 20 the values of the entrance and exit temperatures were reversed. It is evident that as the degree of specular reflection increases, the values of the forward and reverse transmission probabilities diverge more and more, and the deviation from the Knudsen limiting law occurs as anticipated. It has been pointed out earlier that for diffuse reflection, a fixed amount of specular reflection, or for completely specular reflection, the forward and reverse transmission probabilities are equal and in these cases the curves would not be expected to diverge.

Figure 21 depicts a unified plot of capillary transmission probabilities as a function of the degree of specular reflection at the entrance temperature. The value of the parameter r_1 is used to characterize this temperature. The solid curve is for the case of no temperature gradient. Apparently the existence of a temperature gradient along the tube has only a secondary effect on the value of the transmission probability. The temperature of the entrance reservoir must then play the decisive role in the variation of the transmission probabilities

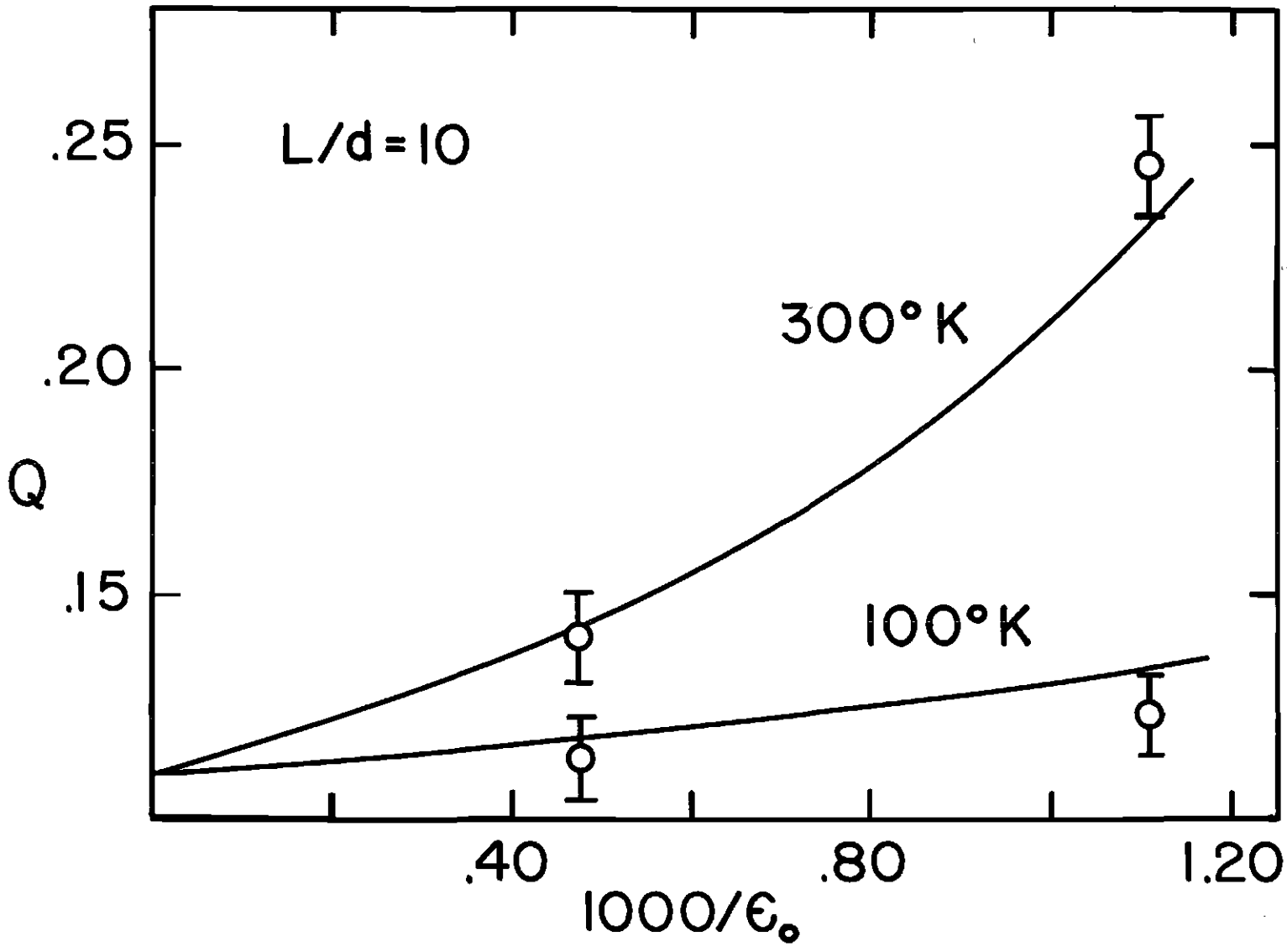

Figure 20. Transmission Probabilities as a Function of the Critical Energy for Specular Reflection [Solid curves are for no temperature gradient. Circles are Monte Carlo values for a capillary with a uniform temperature gradient between 300°K. and 100°K.]

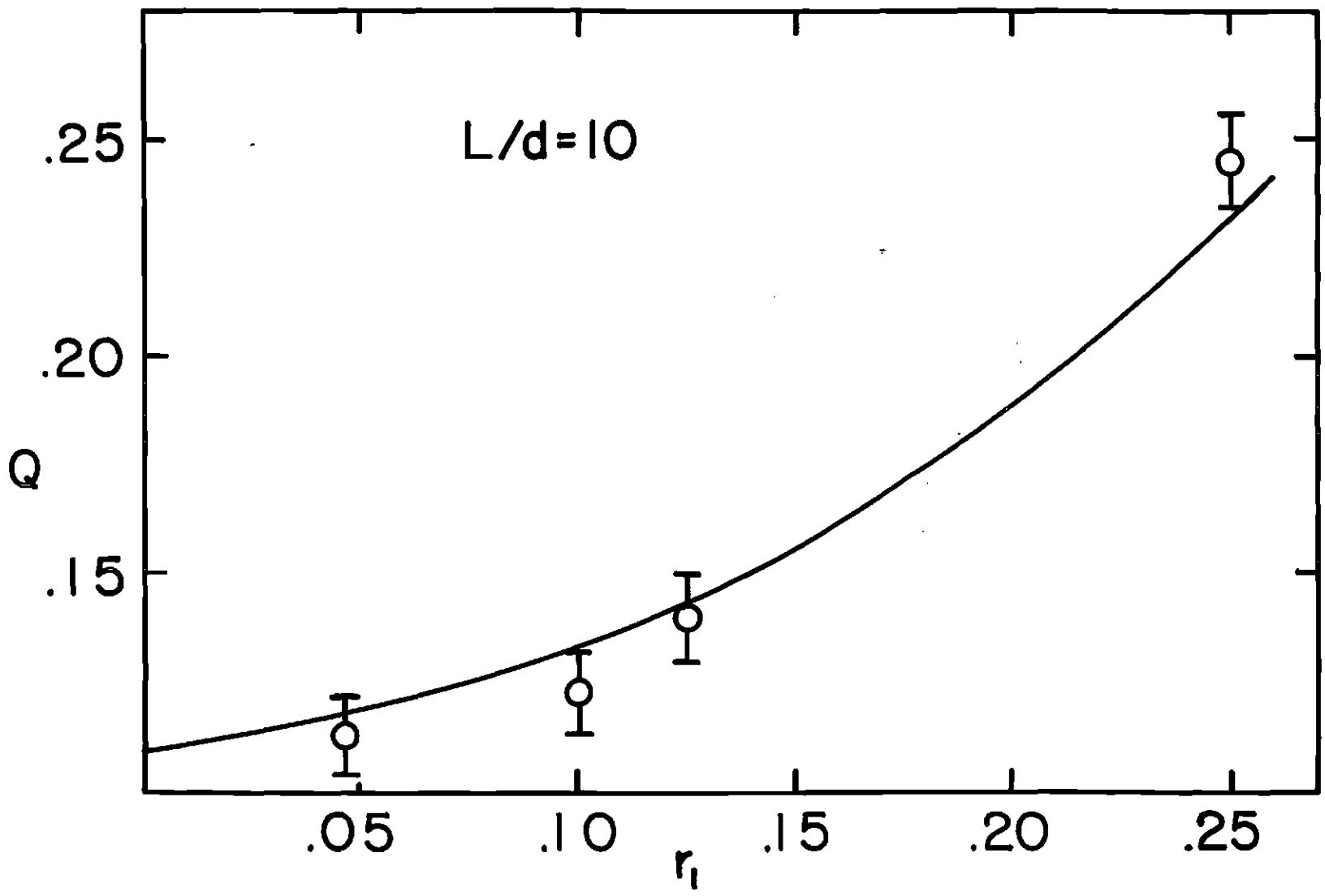

Figure 21. Unified Plot of Transmission Probabilities as a Function of the Degree of Specular Reflection at the Entrance Temperature [Solid curve is for no temperature gradient. Circles are Monte Carlo Values.]

with temperature. The flow experiments were designed to investigate this temperature dependence.

Results of Flow Measurements

The rate constant for each run was determined by plotting $\ln(E^2-E_0^2)$ versus the time and determining the slope. The results for each gas at the four temperatures used in the experiment are tabulated in Table 8 where the rate constants have been multiplied by 1000 for convenience.

Table 8. Rate Constants Determined from Flow Measurements

Gas	k_{77}	k_{194}	k_{298}	k_{353}
Ar	0.15799	0.25190	0.31552	0.34466
D_2	-	0.80929	1.0255	1.1270
H_E	0.51808	0.83109	1.0429	1.1575
H_2	0.69920	1.1395	1.4356	1.5843

Because the supply of deuterium gas was exhausted, no runs were made for this gas at liquid nitrogen temperatures. Each point in the table represents an average of at least 3 runs and as many as 20 runs. During the first part of the experimental work a large number of flow measurements were made to ensure that the calculated slopes were reproduceable. Since consistent results were obtained from the sets of data which were gathered over a period of several weeks, the number of runs thought appropriate for each gas was reduced to around five. In several cases,

only three runs were made because of experimental difficulties. It was found, for example, that the phenolic connector between the Pirani gauge and the electrical cable to the Wheatstone bridge was damaged after a few week's exposure to high temperatures. Consequently the number of runs for several gases at high temperatures was reduced to expedite the taking of data. Replacing the electrical connection was a long and tedious task since the flow cell had to be removed from the vacuum assembly and the protective Tygon sheath around the electrical connection carefully removed to prevent damage to the gauge. Such an operation also required a complete pumpdown and outgassing of the system after repairs which were rather time consuming.

Extrapolation to Zero Pressure

In order to remove the pressure dependence of the rate constants in Table 8, the values could either be adjusted to correspond to the same average mean free path or extrapolated to zero pressure to obtain the pressure independent rate constant, k_0. The latter procedure was adopted.

The equation governing the flow of gases in the pressure range of interest is the modified form of the Scott and Dullien equation, derived in Chapter IV. With arbitrary constants, α and β, this equation may be expressed in the form

$$k = k_0\left[1+\alpha(1-F)+\beta(1-F)\left(\frac{D}{\lambda}\right)\right] \qquad (12)$$

where

$$F = \left[D/L + \left((D/L)^2 + 1\right)^{\frac{1}{2}}\right]^{-1}. \qquad (13)$$

In these expressions D is the diameter of the capillary tube, L is the capillary tube length, and λ is the mean free path computed from the average pressure of the run. Under the conditions of each run, this equation can be expressed as

$$k = k_0 \Delta \qquad (14)$$

where Δ is a factor which can be computed from the circumstances of the measurement. Several very long runs of helium and argon were made starting at a pressure of about 0.4 torr and ending at a pressure of about 1.0×10^{-4} torr. The resulting data were then divided into intervals where the pressure decreased by about a factor of two each time, and rate constants were computed for each interval. The rate constants and average pressures were then fitted to the above equation with a non-linear least squares computer program to determine the constants α and β. Values of Δ computed from the experimentally determined parameters differed from those determined using the theoretical constants by less than one-half of 1 per cent. Table 9 summarizes the results of the rate constant extrapolation where the pressure independent rate constants have also been multiplied by the factor 1000 for convenience.

Table 9. Rate Constants from Flow Measurements Extrapolated to Zero Pressure

Gas	$k_{0_{77}}$	$k_{0_{194}}$	$k_{0_{298}}$	$k_{0_{353}}$
Ar	0.15967	0.25489	0.31826	0.34823
D_2	-	0.81775	1.0342	1.1360
He	0.52453	0.83986	1.0515	1.1666
H_2	0.71669	1.1514	1.4481	1.5964

Calculation of the Experimental Transmission Probability

In a form that explicitly indicates the dependence of the rate constant on the molecular weight of the gas, the temperature, and the transmission probability, the formula for the rate constant can be written

$$k_0 = \left[\frac{1}{V}\left(\frac{\pi R}{2}\right)^{\frac{1}{2}}\frac{\overline{D^2}}{4}\right]\left(\frac{T}{M}\right)^{\frac{1}{2}} Q \qquad (15)$$

where V is the volume of the gas reservoir and R is the ideal gas constant. The volume of the gas reservoir was determined by mercury displacement to be 40.748 cm^3. The diameter of the glass capillary was also determined by filling it with mercury and calculating the diameter from the increase in weight. The value of D was found to be 0.0203 centimeters in agreement with the manufacturer's specification. The expression for the transmission probability then takes the form

$$Q = k_0\left(\frac{M}{T}\right)^{\frac{1}{2}}\left[\frac{1}{V}\left(\frac{\pi R}{2}\right)^{\frac{1}{2}}\frac{D^2}{4}\right]^{-1} \qquad (16)$$

$$= 34.611\ k_0\left(\frac{M}{T}\right)^{\frac{1}{2}} .$$

Values of the transmission probability calculated for each temperature are given in Table 10 multiplied by a factor of 100.

Table 10. Values of the Transmission Probability Computed from Flow Measurements

Gas	Q_{77}	Q_{194}	Q_{298}	Q_{353}
Ar	0.3971±8	0.4003±5	0.4032±6	0.4054±7
D_2	-	0.4084±2	0.4161±7	0.4199±10
He	0.4129±7	0.4175±6	0.4217±5	0.4300±3
H_2	0.4004±4	0.4064±11	0.4121±4	0.4175±4

The results are also shown graphically in Figure 22, where the value of the transmission probability is plotted versus the absolute temperature. A smooth curve is obtained in each case and it seems clear that the transmission probability is temperature dependent. The average error associated with the transmission probability was determined by calculating the average error of the rate constant for each series of runs and using a maximum differential error analysis to calculate the error in the transmission probability. The error was found to be on the order of 0.15 per cent.

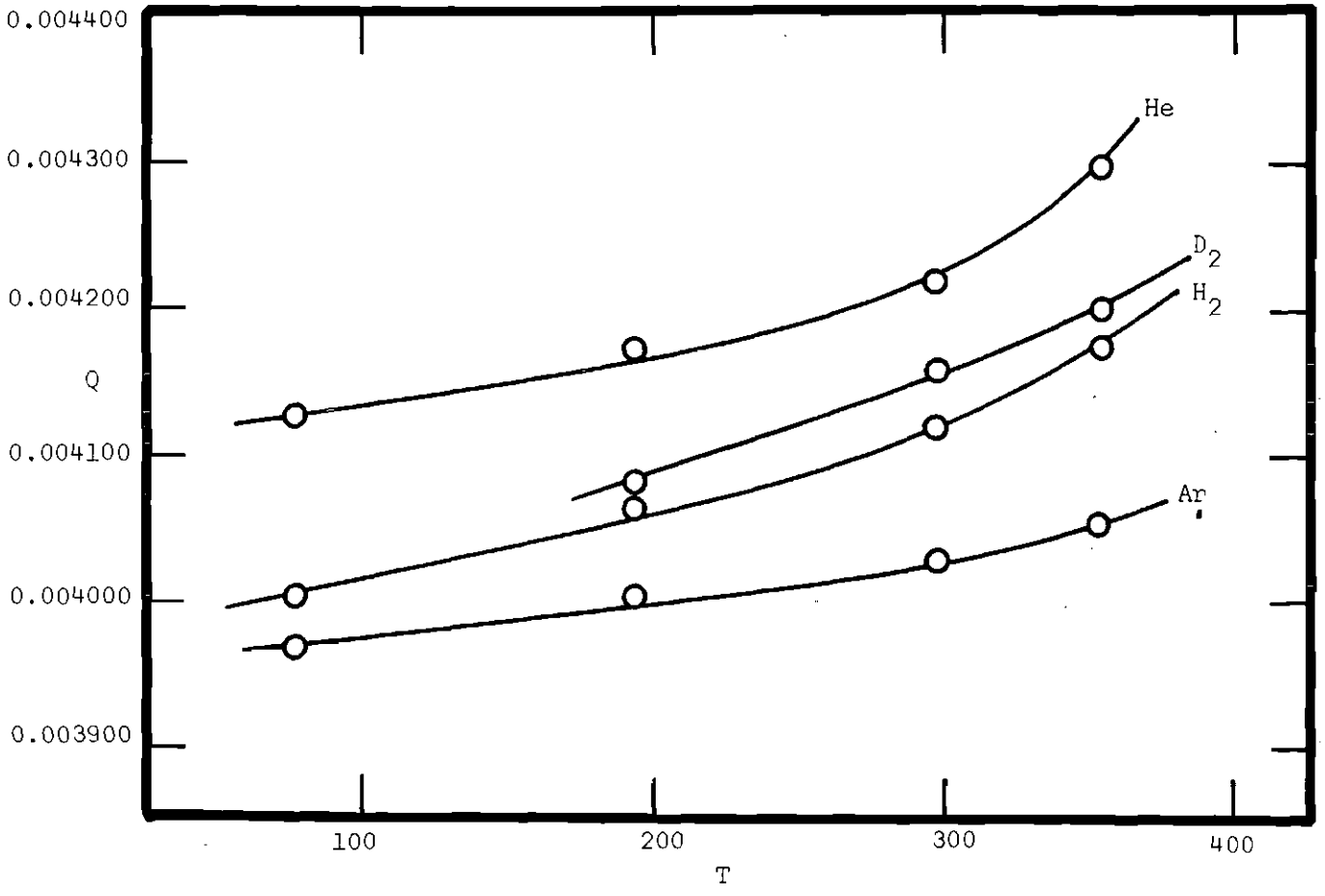

Figure 22. Transmission Probability Versus Temperature

These results represent an improvement over the determinations of Berman and Lund (13) for a number of gases. In their experimental set-up they studied the flow of gases through a short nickel capillary as well as through a porous disk and an orifice. Although most of their measurements were made at 25°, additional measurements previously made at 0°, 8°, and 50° were also presented. The supplementary measurements were made primarily with the orifice and porous disk. The results were presented relative to the experimental transmission probability of argon at 25°. The results of Berman and Lund for capillary flow, as well as the results of this experimental work are presented in Figure 23. The Berman and Lund results are contained in the area between the vertical dotted lines in the temperature range from 0° to 50°. The two data points for helium taken by Berman and Lund were so closely spaced that within the stated error in the ratio (±0.007) it was not possible to detect a temperature dependence in the value of the transmission probability. In addition, their data for argon, helium, and xenon consisted of one point each at 25° and were therefore inconclusive. It was also difficult to attribute a temperature dependence to the neon and krypton data within the error specified. The question of the temperature dependence of the transmission probability was therefore unresolved.

The solid curves for helium, hydrogen, deuterium, and argon represent the findings of this work. It is now clear that there is a considerable temperature effect for each gas. The range of temperatures has been extended to include those from -196° to 80° and the error in the ratios has been reduced by about a factor of 2.

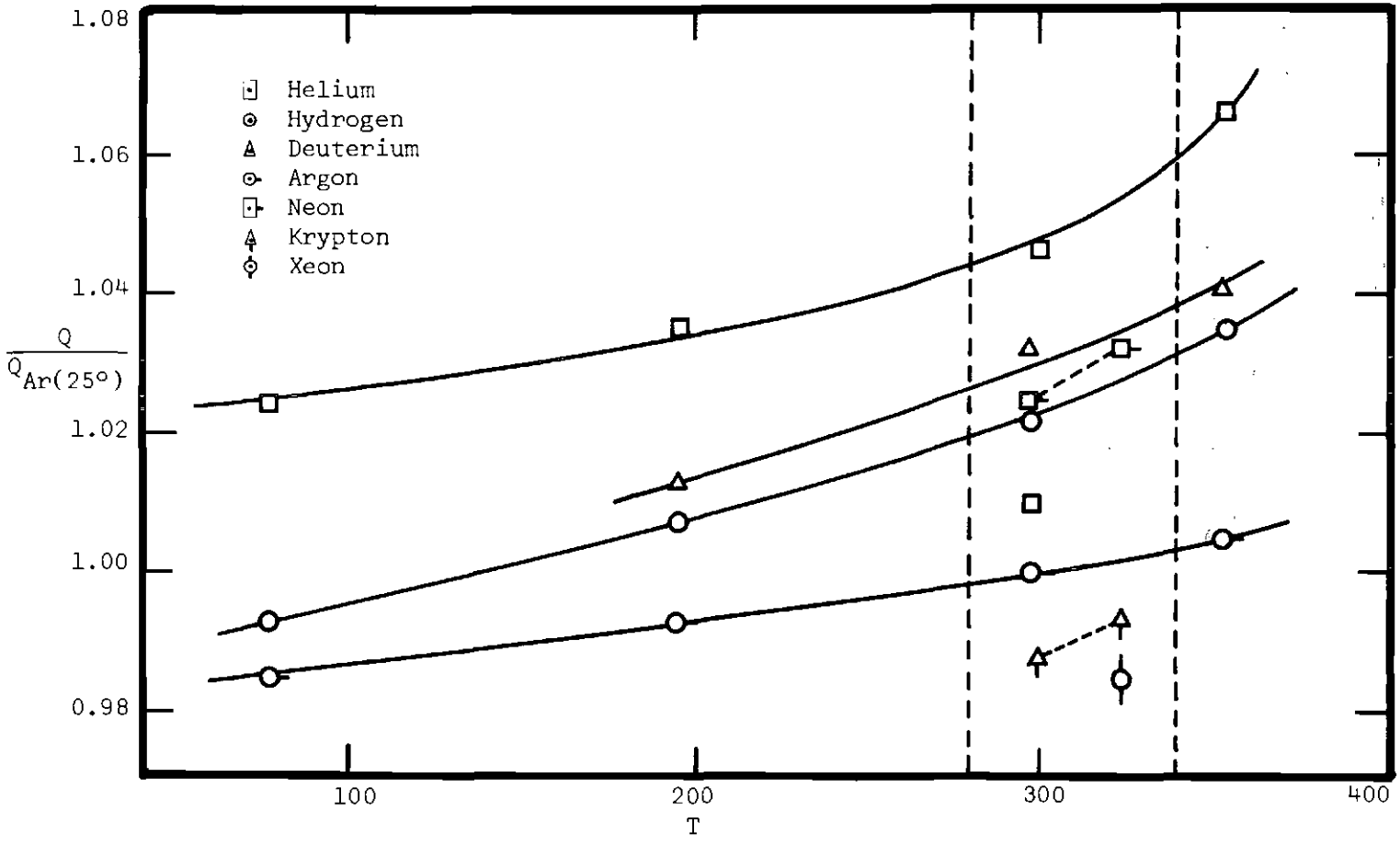

Figure 23. Unified Plot of Transmission Probability Ratio Versus Temperature

Berman and Lund (13) have also indicated that the interaction parameter, ϵ, as tabulated by Hirshfelder (44), is a convenient term which can be related to the transmission probability. The parameter, ϵ, corresponds to the depth of the minimum in the potential energy curve of the gas, and can be related theoretically to gas transport properties. A plot of the transmission probability versus ϵ/kT for the experimental findings of this study is given in Figure 24, where ϵ is the force constant for the Lennard-Jones (6-12) potential, k is the Boltzmann constant, and T is the absolute temperature. A table of values for ϵ/k is given in Hirshfelder's book on page 1110, Table 1-A. That the values of the transmission probability are characteristic of the gas can be seen more clearly in Figure 25, where the transmission probabilities are plotted against $\ln(\epsilon/kT)$ to change the scale of the values of ϵ/kT. Although Berman and Lund obtained anomalous results with helium, such results were not observed in this work.

The variation of the transmission probability with temperature has important considerations with regard to the use of the Knudsen formula for correcting experimental data for the effects of thermal transpiration. The experimental tests of the Knudsen equation at ultra-high vacuum consist of the data by Edmonds and Hobson (14), and Hobson, Edmonds and Verreault (15). Deviations from the limiting law in the case of helium have been referred to in Chapter I. The tabulations of Edmonds and Hobson are particularly informative because of the interesting trend which is apparent in the data. These data are presented in Table 11 where it is clear that as the L/D ratio increases,

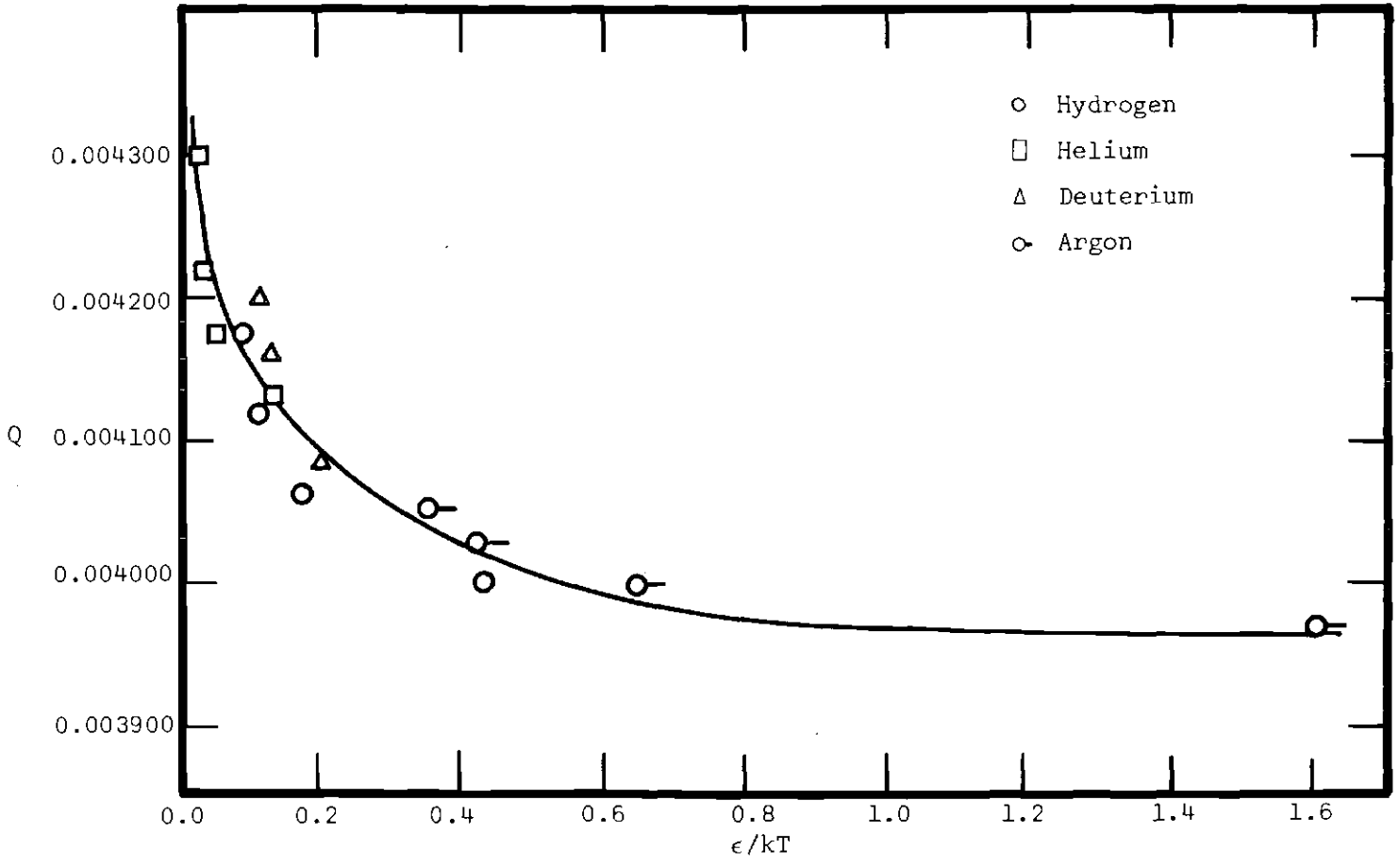

Figure 24. Transmission Probability Versus ϵ/kT

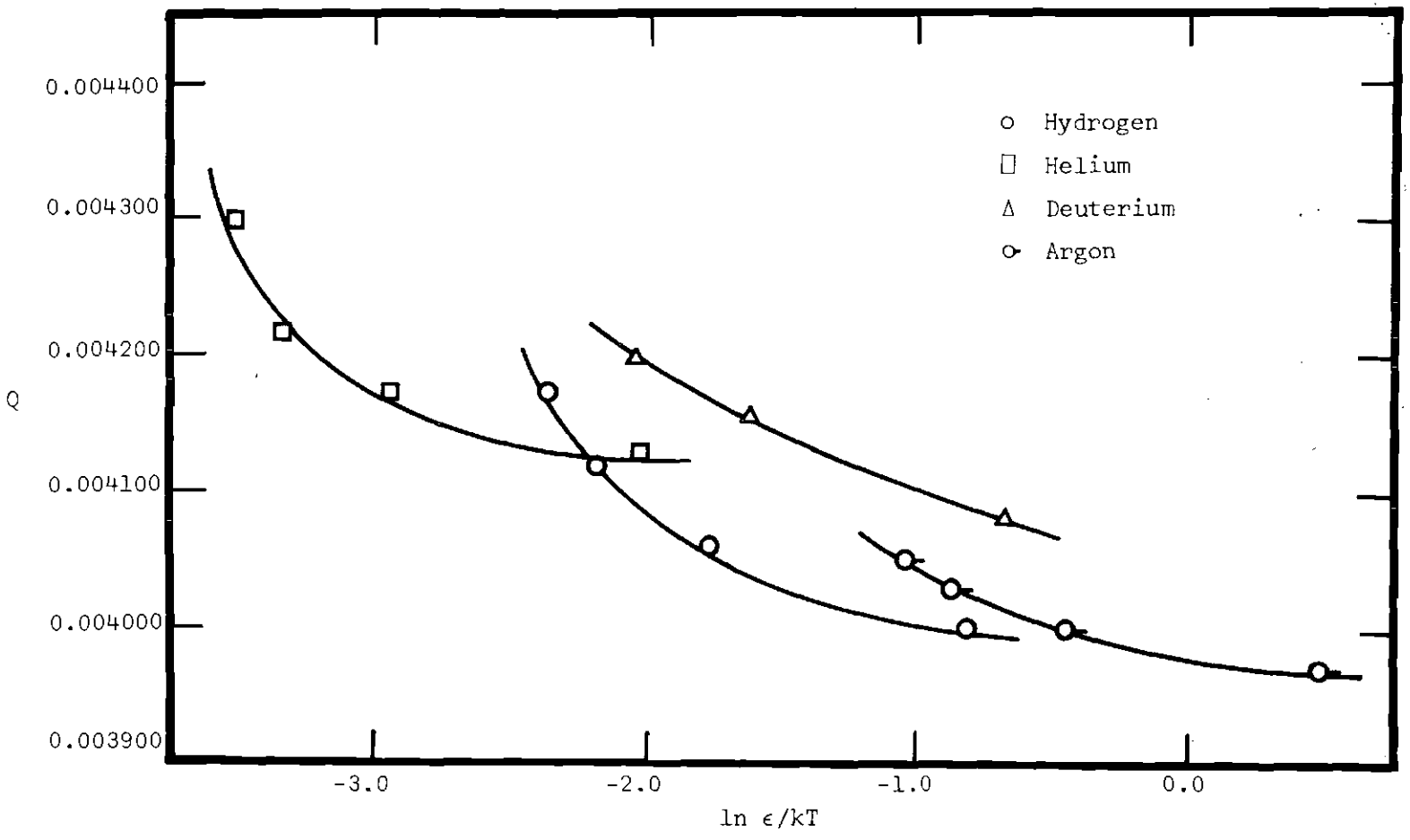

Figure 25. Transmission Probability Versus ln(ϵ/kT)

the experimentally-measured values of the thermal transpiration ratio approach closer and closer to the value predicted by the limiting law.

Table 11.[a] Values of the Transmission Probability Ratio for Neon and Helium for Tubes of Different L/D Ratios

Neon		Helium	
L/D	Q_{21}/Q_{12}	L/D	Q_{21}/Q_{12}
5.79	1.248	5.79	1.222
7.96	1.238	7.96	1.215
11.1	1.156	11.1	1.132
23.7	1.142	23.7	1.136
214.3	1.050	214.3	1.038

[a]Computed from information in References 14 and 15.

Between the two temperatures of 77.4° and 295°, the data indicate that for helium the measured value of R is 0.530 for a tube with an L/D ratio of 214.3. From Figure 22, the ratio of the transmission probabilities for helium obtained in this work for the two temperatures of interest is 1.021 which would give a theoretical value of 0.523 from the generalized Knudsen equation. The L/D ratio of the tube used to measure the transmission probabilities was about 280. Table 11 indicates that a value of R measured with such a tube might be less than 0.530. If the decrease amounted to as little as 0.5 per cent, the theoretical prediction would be within the bounds of the experimental error given for the transpiration measurements.

Table 11 might explain the greater temperature effect which is hinted at in Figure 23 for neon and krypton, since the measurements were made for a capillary with a very small L/D ratio. It should also be pointed out that the trend in Table 11 is the opposite of what is predicted by the computer model. It would be interesting to know whether or not this is the result of the sensitivity of the transmission probability to backscattering near the ends of the tube. Backscattering, where the impinging molecule is preferentially scattered in the direction of incidence, is thought to play a role in the deviations of experimentally-determined transmission probabilities from the theoretical predictions of the Clausing equations. Deviations on the order of 15 per cent were observed in this work.

Calculation of the Theoretical Transmission Probability

The "long tube" formula for the transmission probability was first derived by Knudsen (7) from an asymptotic expansion for Q. That this formula is "just" correct has been shown by De Marcus (28) and by Berman (45), both of whom have indicated that the magnitude of the second order term is slightly above the usual criterion for disregarding a term in an expansion. For the capillary tube used in these experimental measurements, the long tube formula gives a transmission probability of 0.004771. The more exact variational solution of De Marcus (26), which gives an upper bound to the transmission probability, gives a value of 0.004712 for Q which is about 1 per cent below that of the long tube formula.

A number of workers have indicated that transmission probabilities calculated from experimental measurements are lower than those calculated from theory, especially for long tubes, and that as the ratio of capillary length to capillary diameter increases, the diagreement between experiment and theory becomes more severe (13,46-51).

Berman and Lund (13) have indicated that deviations of about 4 per cent occur using porous media in pressure decay experiments. Their capillary was made by drilling a hole in a small thin nickel disk. The dimensions were such that the tube was quite short with an L/D ratio of about 1.33. Their conclusion was that the transmission probabilities obtained in the experimental measurements were lower than those which would be expected from kinetic theory considerations which assume diffuse scattering of molecules after a wall collision. Helium, neon, argon, krypton, and xenon were used in the study and all of the gases showed such deviations.

Flow measurements have also been made by Hanley and Steele (46) under isothermal conditions using a pressure decay method and a system of 25 stainless steel capillaries of length 10.00 centimeters and of diameter 0.015 centimeters. The L/D ratio in these experiments was therefore equal to 667. Deviations of considerable magnitude were observed, with indications that the deviations might decrease with increasing temperature. The results were expressed in terms of a dimensionless flow rate D^* where

$$D^* = D/a\bar{v} \tag{17}$$

and D equals the number of molecules passing through unit area of the tube in unit time, a equals the capillary radius, and $\bar{v}$ equals the average molecular speed of the gas. Values of D^* were plotted against a/λ and extrapolated to zero pressure. The theoretical value of D^* may be calculated from the following considerations.

From the definition of D it follows that

$$D = \left(-\frac{dn'}{dt}\right)\left(\frac{1}{\pi a^2}\right)\left(\frac{L}{p/kT}\right) \tag{18}$$

where it is assumed that the gas density is equal to the number density. In this expression, n' equals the number of molecules, t equals the time, k equals the Boltzmann constant, p equals the pressure, and T equals the absolute temperature. Since

$$\left(\frac{dn'}{dt}\right) = \frac{1}{4} n'\bar{v}AQ \tag{19}$$

where A is the cross-sectional area and Q is the transmission probability, it follows that

$$D = \frac{2}{3}\bar{v}a \tag{20}$$

from which it follows immediately that

$$D^* = \frac{2}{3} \tag{21}$$

in the limit of zero pressure. At 273°K., Hanley and Steele observed deviations from this value on the order of 30 per cent, indicating qualitative agreement with Lund and Berman (13). They attributed the results to the nature of the molecule-wall interaction and indicated that any theoretical treatment of the problem should consider the differences in the gas-gas and gas-surface interactions.

Hanley (47) has also found the same order deviations in the unsteady state where the system approaches equilibrium in a manner quite unlike that predicted by theory. The experimental set-up consisted of 23 stainless steel capillaries of length 10.00 centimeters and radius 0.0073 centimeters, resulting in an L/D ratio of 1369 for the experimental apparatus. The transpiration flow rate under isothermal conditions was related to the variation of pressure with time through phenomenological expressions derived from linear nonequilibrium thermodynamics.

Some recent work by Steele and Hanley (48) has indicated that a form of the Dusty Gas Model of Mason, Evans, and Watson (47) can be combined with the flow expressions of nonequilibrium thermodynamics to give at least qualitative agreement with experimental measurements. The values of D^{*} so calculated were about 10 per cent from the experimental values and about 30 per cent from the theoretical values computed from the Clausing integral equations.

The extensive measurements of Lund and Berman (49,50) concerning flow and self-diffusion in capillaries have clearly indicated that experimental measurements deviate from the predictions of existing

theories based on the diffuse scattering of molecules and that such deviations can be correlated with a monotonically increasing function of the ratio of observed to theoretical free molecule transports. The authors have developed a model for describing transport under a partial pressure gradient as well as transport under a total pressure gradient in capillaries of arbitrary length to diameter ratio over a pressure range extending from the free molecular to the continuum pressure regimes.

The model was formulated using empirical functions which were developed from least squares procedures and a wide variety of experimental data. The results indicated that free molecule "end corrections," essentially leading to an effective lengthening of the capillary tube, were necessary to obtain proper correlation with the experimental data.

A wide variety of experimental data on the pressure dependence of the flow of gases through capillaries was examined using this model in order to study systematically the dependence of the discrepancies between theory and experiment on the capillary length to radius ratio, on the gas which was flowing, and to some extent, on the nature of the capillary surface.

In the data analysis, a parameter C, defined as the ratio of the theoretical transmission probability Q to the experimental probability Q_m, was introduced into the flow equations and determined from nonlinear least square techniques for each set of capillary transport data. It was found that in almost every case, the value of C was greater than

unity, indicating a measured transmission probability which was lower than that predicted by theory. It was reasoned that some measure of wall roughness might correlate with the parameter C since a number of experiments and theoretical calculations have shown that the transmission probability can be reduced substantially by such roughness. Davis, Levenson, and Milleron (35), for example, found from theoretical Monte Carlo calculations that some surface structures can reduce the conductance by as much as 20 per cent.

If the deviations from the theoretical transmission probability are to be associated with the geometrical structure of the wall, then the magnitude of the deviations must depend upon the fraction of the transmitted particles which have made wall collisions, f_w. Since the probability of traversing a capillary tube of length L and diameter D is given by

$$N_1(L) = \frac{1}{D^2}\left[2L^2 + D^2 - 2L(L^2+D^2)^{\frac{1}{2}}\right] \tag{22}$$

the fraction transmitted with at least one collision is given by (51)

$$f_w = 1 - \left(\frac{N_1(L)}{Q}\right) \tag{23}$$

where Q is the transmission probability. An excellent correlation between 1/C and f_w was found by the authors for data from many sources. The intercept of the curve at $f_w = 1$, corresponding to the value of 1/C for an infinite length tube, was 0.915. Some values of C obtained by

the authors for various L/D ratios are shown in Table 12. The effect of artificially roughing one of the tubes with an L/D ratio of 1.55 changed the average value of C from 1.075 to 1.126. It was concluded by the authors that the transmission probability of a capillary tube of given length to diameter ratio must be primarily determined by the detailed geometric structure of the surface and not by the gross chemical nature of the capillary walls. It seems likely that a complete calculation of the theoretical transmission probability will necessitate a detailed consideration of both diffuse and specular reflection as well as some degree of backscattering. De Marcus (5) has indicated how this may be done in the case of parallel plates. In view of the evidence from the literature, values of experimental transmission probabilities which are lower than those computed from existing theoretical models are not surprising.

Table 12. Values of Experimentally Determined Parameter, C, as a Function of the Ratio of Capillary Length to Capillary Radius

L/a	C
0.319	1.017
0.945	1.040
2.029	1.053
2.035	1.047
3.099	1.075
5.944	1.101
11.839	1.086

CHAPTER VII

CONCLUSIONS AND RECOMMENDATIONS

This dissertation represents an investigation of the Knudsen limiting law by means of a Monte Carlo computer model and flow measurements through capillary tubes at low pressures. The model was designed to indicate the behavior of Clausing transmission probabilities when a temperature dependent molecular scattering law for diffuse and specular reflection was introduced. Flow measurements were made through a capillary tube to investigate the temperature dependence of the transmission probability. Some conclusions of this research are listed below.

1. The computer model indicates that the transmission probability is relatively insensitive to a temperature gradient across a capillary. Figure 21 on page 95 shows a unified plot of transmission probabilities as a function of the degree of specular reflection at the temperature of the entrance reservoir. The solid line represents the variational solution of De Marcus for the case of no temperature gradient. There seems to be no significant deviation of the values of the non-isothermal transmission probabilities from those of the variational solution. This plot would also seem to indicate that the transmission probability depends primarily upon the temperature of the entrance reservoir.

2. The computer model predicts that as the degree of specular reflection increases, the forward and reverse transmission probabilities

diverge. This trend is indicated in Figure 20 on page 94 where the transmission probabilities are plotted as a function of the specular parameter, ϵ_0. The upper curve represents the case where the entrance reservoir is at 300°K.; the lower curve represents the case where the entrance reservoir is at 100°K. The solid curve is again for the case of no temperature gradient as computed from the variational solution of De Marcus. For a specular parameter of 2100, the forward and reverse transmission probabilities differed by about 12 per cent.

3. Experimental measurements have shown that the values of the transmission probability are temperature dependent over a much wider range than previously reported. Figure 22 on page 101 shows the experimental transmission probabilities plotted as a function of the temperature. The greatest temperature dependence occurred in the case of hydrogen and the least in the case of argon. According to the computer model, this temperature dependence would indicate that a degree of specular reflection is occurring for each of the gases studied. The measurements covered a temperature range on the order of 276°K.

4. The experimental measurements indicated that the transmission probability is characteristic of the gas since separate curves were obtained for each gas. Argon, which because of its molecular weight and force constant might be expected to undergo the least amount of specular reflection, always had a transmission probability which was lower than each of the other gases over the entire temperature range. The position of the deuterium curve is somewhat uncertain because of the 2 per cent uncertainty in the molecular weight. Since any impurity is likely to

have a molecular weight which is greater than that of deuterium, the actual curve may be somewhat lower than the one indicated in Figure 22.

5. Values of the experimentally-measured transmission probabilities correlate well with the Lennard-Jones force constants for each gas as previously indicated by Lund and Berman. Figure 24 on page 105 shows a unified plot of the transmission probability versus ϵ/kT for all of the gases. This correlation can be seen more clearly if the natural logarithm of ϵ/kT rather than ϵ/kT is used in the plot as shown in Figure 25 on page 106. The agreement seems satisfactory, particularly when it is realized that the force constant is more properly a measure of molecule-molecule interactions than wall-molecule interactions.

6. Flow experiments provide an experimental means of measuring Clausing transmission probabilities with an average error of about 0.15 per cent. If a Pirani gauge is used to measure the pressure, the critical issue is the accurate measurement of the voltage across the wire. A high accuracy digital voltmeter is almost a necessity since the use of an ordinary potentiometer would increase the error by at least an order of magnitude.

7. The experimental values of the transmission probability are lower than those predicted by the variational solution of De Marcus. The indications are that backscattering plays an important role in this disagreement and that a full theoretical treatment of the problem must include some degree of backscattering. This seems to be especially important in the case of capillary tubes with large L/D ratios.

8. Deviations from the Knudsen limiting law on the order of 1 to 5 per cent may be accounted for because of the temperature dependence of the transmission probability.

During the course of this research, several topics for further investigation presented themselves. Such topics represent extensions of this work or additions to work already in the literature. Several of the more interesting proposals are listed below.

1. There are indications from published data by a number of workers that deviations from the Knudsen limiting law decrease as the L/D ratio of the capillary increases. It would be interesting to make measurements of the thermal transpiration ratio, R, for a series of capillaries covering a wide range of L/D values with a special emphasis upon very long tubes in order to see how closely the limiting law is approached in such cases.

2. The variational solution for the transmission probability gives an upper bound to the value. On the other hand, the squeezing technique yields both an upper and lower bound for the transmission probability. Both methods of solution have been shown to agree for very short tubes, but no comparisons have been made in the case of much longer tubes where the L/D ratio is much larger. It would be useful to have the results of such calculations.

3. For the case of infinite parallel plates, De Marcus has shown that the introduction of backscattering into the Clausing integral equations results in lowered theoretical transmission probabilities. In addition, the indication is that this decrease becomes larger

percentage-wise as the L/D ratio increases. The few examples calculated were for rather small L/D ratios (D in this case represents the plate separation) and in each case evaluation of the transmission probability involved the solution of two coupled integral equations by numerical methods. A Monte Carlo solution to the problem of backscattering might throw considerable light on the disagreement between theory and experiment which exists in the literature at present. Such a study should cover a wide range of L/D ratios, with particular emphasis on long tubes where the disagreement is most severe.

4. Measurements of the transmission probability from flow experiments should be extended to higher temperatures where the value of dQ/dT would be expected to be greater than in the range of temperatures studied in this work. It would also be interesting to include additional gases, such as neon, krypton, and nitrogen in the study.

5. It would be useful to make measurements of the thermal transpiration ratio, R, and the transmission probability, Q, using the same capillary for two temperatures of interest. Since both measurements would be made at the same L/D ratios for the same condition of the capillary surface, the amount of disagreement between the measured and theoretical values of R, and the size of the correction indicated by the ratio of the two values of the transmission probability could be particularly informative.

APPENDIX A

PRESSURE RELATION FOR PIRANI GAUGE

Since the electrical energy into the gauge must equal the heat energy out of the gauge, the following thermal equilibrium equation may be written:

$$\text{electrical input} = \text{radiation term} + \text{conduction term} + \text{end support loss term} \tag{1}$$

Let us consider each term separately:

1. Radiation

According to Stephen's Law the radiation loss is proportional to the fourth power of the temperature of the wire. Thus, it follows that the radiation energy loss is given by

$$\dot{Q}_r = K_r(T_w^4 - T_g^4) \tag{2}$$

where $\dot{Q}_r$ is the change in heat energy due to radiation, K_r is the radiation constant for the wire, T_w is the temperature of the wire, and T_g is the temperature of the gas. The dot over the variable, Q, means change with respect to time. If it is assumed that $T_w \sim T_g$ such that

$$\Delta T = T_w - T_g << T_g \tag{3}$$

then the expression may be expanded to give

$$\begin{aligned} \dot{Q}_r &= K_r(T_w^4 - T_g^4) = K_r([T_g+\Delta T]^4 - T_g^4) \\ &= K_r(T_g^4 + 4T_g^3\Delta T + 6T_g^2\Delta T^2 + 4T_g\Delta T^3 + \Delta T^4 - T_g^4). \end{aligned} \tag{4}$$

Rearranging the equation and remembering that ΔT is small, we obtain finally

$$\dot{Q}_r = 4K_r T_g^3(T_w - T_g) = K_r'\Delta T \tag{5}$$

showing that the radiation loss is proportional to the temperature difference between the wire and the gas.

2. Conduction

Consider a wire of diameter d stretched along the axis of a tube of diameter D (see Figure 26). If the gas molecules have, on the average, temperatures of T_g' and T_w' for arrival and departure at the wire, respectively, then the rate of energy transfer from wire to gas may be written as

$$\dot{Q}_c = K_c n(T_w' - T_g') \tag{6}$$

where n equals the number of molecules striking the wire in unit time. Since the number of molecules striking the wire is also proportional to the pressure of the gas, this equation may also be written as

$$\dot{Q}_c = K_c' P(T_w' - T_g') \tag{7}$$

where P is the pressure. Now the temperature of the reflected gas molecules, T_w', depends upon the temperature of the wire surface, the type of surface, the temperature of the incident molecules, and the type of molecules.

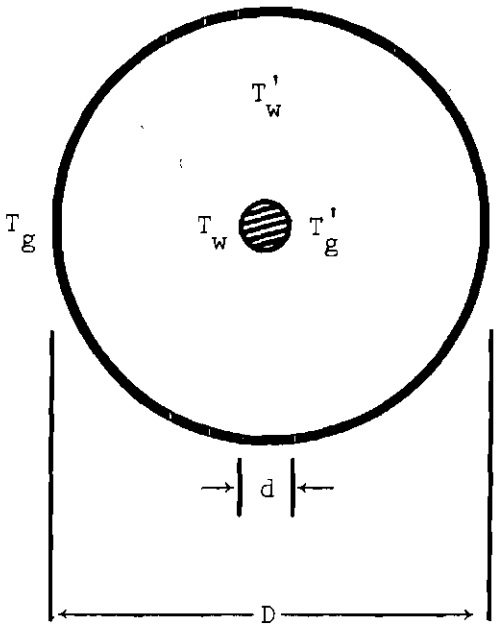

Figure 26. Heat Conductivity Element: Thin Wire of Diameter, d, Mounted Along Axis of Cylinder of Diameter, D

If we define an accommodation coefficient, α, such that

$$\alpha = \frac{T'_w - T'_g}{T_w - T'_g} , \tag{8}$$

then the previous equation becomes

$$\dot{Q}_c = \alpha K'_c P(T_w - T'_g) \tag{9}$$

where T'_g, the temperature of the incident molecules, is dependent upon the flow regime of the gas. If the mean free path of the gas is much greater than the diameter of the tube, the molecules strike the container walls much more than the hot wire and are thus completely in accommodation with the wall. Under such conditions, the energy loss is simply proportional to the pressure and the temperature difference

$$\dot{Q}_c = \alpha K'_c P(T_w - T_g) \tag{10}$$

since $T'_g \sim T_g$.

3. End Supports Loss

The heat loss through the end supports of the wire is essentially proportional to the area of the support, the average temperature difference of the support and wire, and the thickness of the support. If it is assumed that the temperature of the support is essentially that of the gas, then

$$\dot{Q}_e = K_e(T_w - T_g) \tag{11}$$

where K_e is a constant.

4. Electrical Energy Input

When the bridge is balanced, the power dissipated in R_w may be calculated immediately as

$$P = i^2 R_w = \frac{E^2}{R_w} \tag{12}$$

where i equals the current flowing through that arm of the bridge and E equals the voltage.

The energy balance equation thus becomes

$$\frac{E^2}{R_w} = 4K_r T_g^3 (T_w - T_g) + \alpha K_c' P (T_w - T_g) + K_e (T_w - T_g) \tag{13}$$

which, upon combining terms and generalizing, can be written as the following equation

$$E^2 = AP + B \tag{14}$$

provided the temperature difference, ΔT, is constant. If the voltage reading across R_w at zero pressure is denoted by E_0, a simple relationship,

$$E^2 - E_0^2 = AP \qquad (15)$$

exists between the voltage and the pressure of the system.

APPENDIX B

PIRANI GAUGE RESPONSE AND TEMPERATURE LAG

An analysis of whether or not the Pirani gauge will "follow" the change of pressure in the flow reservoir leads to the following considerations. If $\dot{W}_{in}$ is the electrical work done on the wire, $\dot{Q}_{out}$ is the heat flow out of the wire, and C_w is the heat capacity of the wire, then

$$\frac{dT}{dt} = \frac{1}{C_w}[\dot{W}_{in} - \dot{Q}_{out}] \tag{1}$$

where T is the wire temperature and t is the time. Upon substitution of the equations governing the operation of the hot wire manometer (see Appendix A), the following expression is obtained

$$\frac{dT}{dt} = \frac{1}{C_w}[aE^2 - b \cdot p \cdot \Delta T - c \cdot \Delta T] \tag{2}$$

where a, b, c, and ΔT are constants, E is the voltage across the Pirani gauge, and the accommodation coefficient, α, has been incorporated into the constant b. If the expression for ΔT is substituted into the equation above and the heat capacity of the wire is incorporated into the new constants A, B, and C as follows

$$\frac{dT}{dt} = [A-(BP+C)T+(BP+C)T_0] \tag{3}$$

one obtains finally

$$\frac{dT}{[(A+B'T_0)-B'T]} = dt \tag{4}$$

where $B' = BP + C$ for convenience. Integrating this differential equation for the case of constant pressure between an initial temperature, T_i, and some temperature, T, and between 0 and some time, t, yields

$$\begin{aligned} \int_{T_i}^{T} \frac{dT}{[(A+B'T_0)-B'T]} &= \int_0^t dt \\ &= -\frac{1}{B'} \ln[(A+B'T_0)-B'T]\Big|_{T_i}^{T} = t\Big|_0^t \end{aligned} \tag{5}$$

from which it follows that

$$-\frac{1}{B'} \ln \frac{(A+B'T_0) - B'T}{(A+B'T_0) - B'T_i} = t. \tag{6}$$

Rearranging this expression, and making the substitution for B', we obtain finally

$$\frac{(BP+C)(T-T_0) - A}{(BP+C)(T_i-T_0) - A} = e^{-(BP+C)t} \tag{7}$$

from which the response time of the gauge, τ, may be determined.

As t approaches infinity, the temperature of the gauge approaches its final temperature, T_f, where

$$(T_f - T_0) = \frac{A}{BP + C} . \tag{8}$$

Thus

$$\frac{(T_f - T)}{(T_f - T_i)} = e^{-(BP+C)t} = e^{-t/\tau} \tag{9}$$

where the relaxation time is given as a function of the pressure through the expression

$$\tau = \frac{1}{BP + C} . \tag{10}$$

Response Time During a Flow Measurement

A general solution to the equation giving the temperature variation of a hot wire manometer during a flow measurement can be obtained in the following way. Since the pressure during a flow measurement follows a first order rate expression, let the pressure vary exponentially with time such that

$$P = P_0 e^{-kt} \tag{11}$$

so that one obtains for the differential equation after making the appropriate substitutions, the expression

$$\frac{dT}{dt} = \frac{1}{C_w}\left[aE^2 - bP_0 e^{-kt}\Delta T - c\Delta T\right] \tag{12}$$

or, upon factoring and substituting for ΔT,

$$\frac{dT}{dt} = A - (T-T_0)(BP_0 e^{-kt}+C) \tag{13}$$

where k is the rate constant obtained from the flow experiments and A, B, and C are again constants to be determined. Since

$$T = T_0 + \frac{A - \frac{dT}{dt}}{(BP_0 e^{-kt}+C)} \tag{14}$$

it is apparent that

$$\lim_{\tau \to 0} T(t) = T_0 + \frac{A}{(BP_0 e^{-kt}+C)} = T_e. \tag{15}$$

Solving for the equilibrium temperature, T_e, one obtains the expression

$$T_e = T_0 + \frac{A}{(BP_0 e^{-kt}+C)}. \tag{16}$$

The derivative of the equilibrium temperature with respect to time is given by

$$\frac{dT_e}{dt} = \frac{kABP_0 e^{-kt}}{(BP_0 e^{-kt}+C)^2}. \tag{17}$$

Now consider the change of T with time (see Figure 27). The true temperature will lag the steady state temperature. If the lag is small, and it can be assumed that the slopes of the two curves are equal, then

$$\dot{T} = \dot{T}_e \tag{18}$$

and

$$A - BP_0e^{-kt}(T-T_0) - C(T-T_0) = \frac{kABP_0e^{-kt}}{(BP_0e^{-kt}+C)^2} . \tag{19}$$

Rearranging this expression and dividing by (T_e-T_0) we obtain

$$\frac{(T-T_0)}{(T_e-T_0)} = 1 - \frac{kBP}{(BP+C)^2} . \tag{20}$$

Substitution of the expression for τ yields

$$\frac{(T-T_0)}{(T_e-T_0)} = 1 - kBP\tau^2 . \tag{21}$$

It is clear that an experiment which yields the value of τ will also yield information concerning the temperature lag of the hot wire gauge.

Evaluation of Wire Temperature and Response Time

The resistance of the Pirani gauge is essentially an indication of its operating temperature. The resistance of the gauge can be computed from the voltage across the wire and the current through it

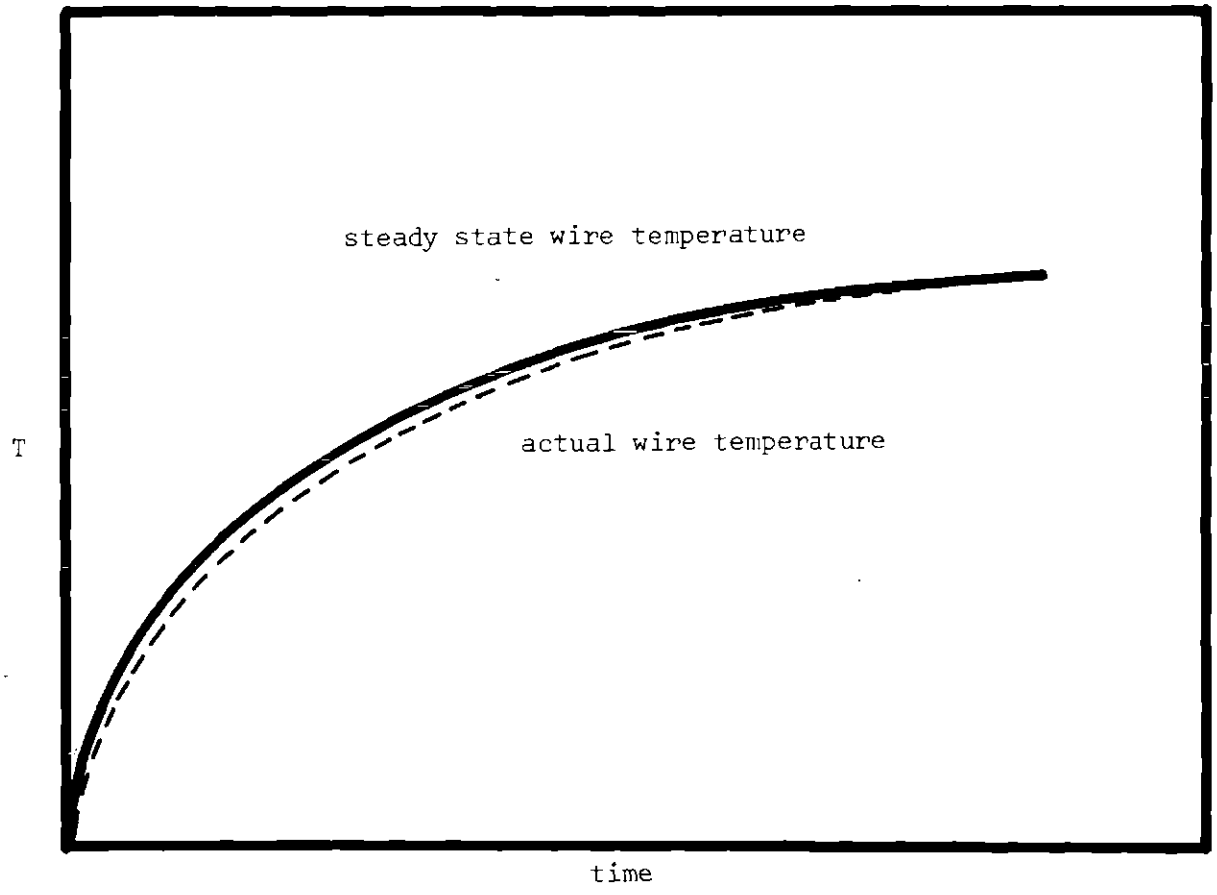

Figure 27. Lag of the Actual Wire Temperature from the Steady State Value

according to the expression

$$R_w = \frac{E}{i} = \frac{E}{E_0} \cdot R_0 \ . \tag{22}$$

In addition, the power dissipated by the bridge can be computed from a knowledge of the current and wire resistance by

$$\begin{aligned} P = i^2 R_w &= \left(\frac{E^0}{R^0}\right)^2 \cdot \left(\frac{E}{E^0}\right) \cdot R^0 \\ &= \frac{EE^0}{R^0} \ . \end{aligned} \tag{23}$$

If a plot of E/E^0 versus EE^0 is made and extrapolated to $(EE^0) = 0$, the resulting E/E^0 ratio is characteristic of the bath temperature, since when $EE^0 = 0$, there would be no power dissipation from the wire. If measurements are made at several temperatures, it is possible to evaluate the temperature dependence of the Pirani gauge.

Different values of E and E^0 were determined for various bridge current settings at temperatures of 25, 50, 70, and 90 degrees. In each case the bridge balance was adjusted, its setting recorded, and the galvanometer balanced before recording the values of E and E^0. Plots were then made and each set of readings extrapolated to zero power dissipation. The results are shown in Table 13. The value of the pressure in the system during these determinations was 4.216 microns, and changing the pressure to other values seemed to have little effect on the extrapolations.

Table 13. Results of Extrapolation to Zero Power Dissipation for Bath Temperature, T

T^0 K.	$(E/E^0)_{(EE^0=0)}$
298.15	0.828
323.15	0.906
343.15	0.972
363.15	1.034

The values of $(E/E^0)_{EE^0=0}$ were then plotted versus the absolute temperature to obtain the slope of the line. The results are shown in the plot in Figure 28. The slope of the line was constant over the temperature range and a least squares data fit of the numbers gave a slope of 0.31806×10^{-2} deg^{-1} with a coefficient of correlation of 0.9999.

The response time of the gauge and the temperature lag of the wire may be determined in the following way. One type of response is that of the gauge to a small change in pressure when the gauge is initially stabilized at some pressure within the range of interest. Suppose the system is initially at a pressure P_1 and a wire temperature T_1. If the pressure of the system changes to a new pressure P_2, then the temperature of the hot wire must change to T_2 where the time change interval is characterized by the response time, τ.

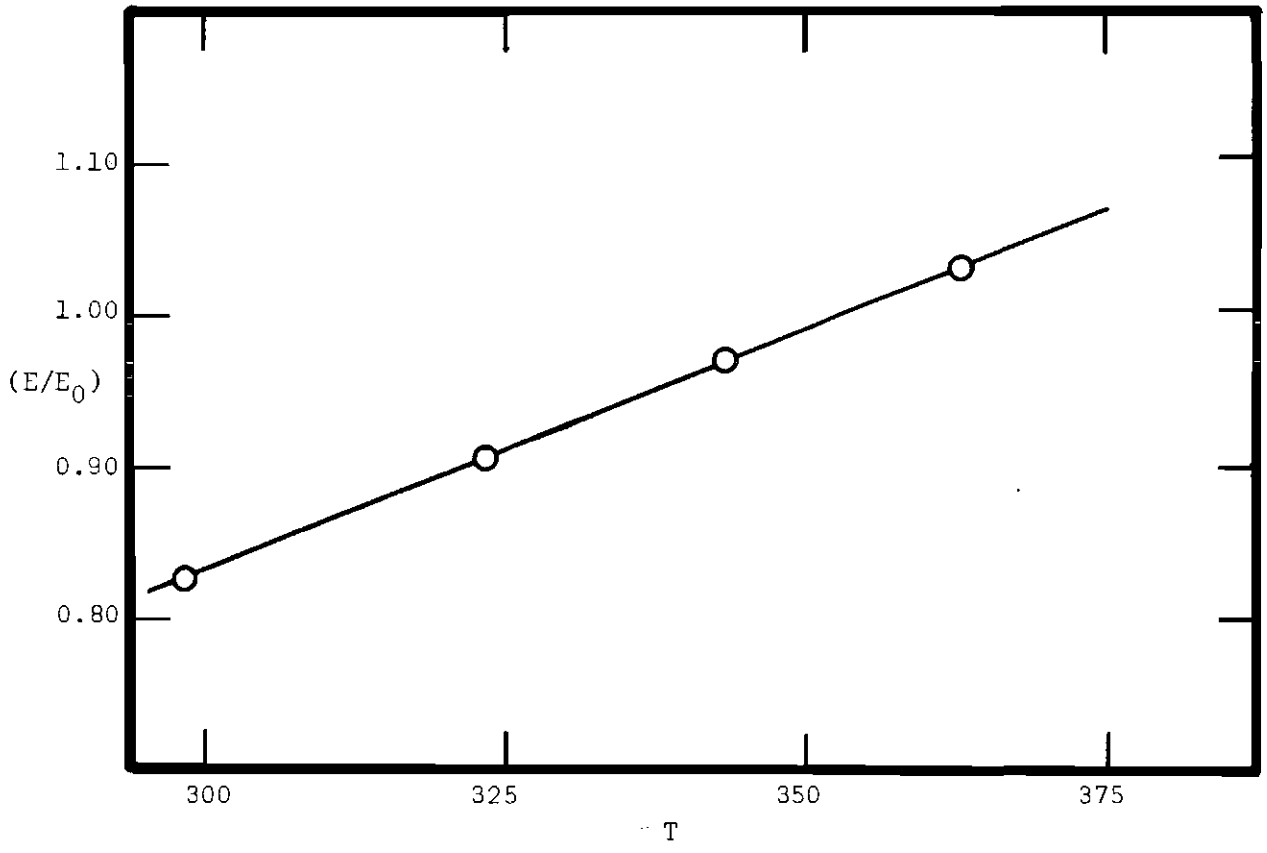

Figure 28. Plot of E/E^0 Versus Temperature

$$\begin{array}{ccccc} P_2 & & P_2 & & P_2 \\ T_1 & \longrightarrow & T_1 & \xrightarrow{\tau} & T_2 \\ \text{initial state} & & \text{intermediate state} & & \text{final state} \end{array}$$

A similar response would occur if the gauge tube is held at a representative pressure and the electrical heating power is changed by a small step function. Suppose that by making an adjustment in E_1, the power input to the bridge, we cause a temperature change in the system in the following manner:

$$\begin{array}{ccccc} P_2 & & P_2 & & P_2 \\ T_1 & \longrightarrow & T_1 & \xrightarrow{\tau} & T_2 \\ E_1 & & E_2 & & E_2 \\ \text{initial state} & & \text{intermediate state} & & \text{final state} \end{array}$$

If a value of the pressure is now selected, a measurement of the response time can be made by making a change in the input power and measuring the interval of time necessary for the galvanometer to deflect at mid-scale. Such measured response times would be related to the response time, τ, according to

$$\tau = \frac{t_{\frac{1}{2}}}{0.693} . \qquad (24)$$

The results of such an experiment are summarized in Table 14 where the response times are tabulated as a function of the pressure.

Table 14. Values of the Response Time, τ, for Different Pressures

Pressure	$\tau_{\frac{1}{2}}$	τ
0.0339	4.3	6.2
4.55	3.8	5.5
12.3	2.0	2.9
22.2	1.7	2.5

Now the basic equation for the change in temperature with time is given by

$$\frac{dT}{dt} = \frac{1}{C_w}\left[aE^2 - b \cdot P \cdot \Delta T - c \cdot \Delta T\right] \tag{25}$$

and at equilibrium, dT/dt can be set to zero with the following result

$$aE^2 = b \cdot P \cdot \Delta T + c \cdot \Delta T \tag{26}$$

where E is the voltage across the Pirani gauge, and the constant "a" can be calculated from the wire resistance. The constants b and c may be calculated from simple measurements of the pressure and voltage if such measurements are made for a bridge balance for which the value of

ΔT is known. The bridge was set so that ΔT was equal to 100°C. The resistance of the Pirani gauge was measured and found to be 90 ohms so that the constant a was calculated to be 2.66×10^{-3} cal $sec^{-1} ohm^{-1}$. A series of measurements of pressure versus voltage were then made to determine the constants in the Pirani gauge equation from a plot of E^2 versus P using the method of least squares. When evaluated in this manner, the constant b was found to be 7.76×10^{-8} cal $sec^{-1} \mu^{-1} deg^{-1}$ and the constant c was found to be 7.12×10^{-7} cal $sec^{-1} deg^{-1}$.

The heat capacity of the wire was evaluated from the response time data in Table 14 using least squares methods and was found to be 6.30×10^{-6} cal deg^{-1}. At an average pressure of 10 microns the response time would be expected to be about 2.7 seconds and the rate constant for, say, argon, would be about 3.0×10^{-4} sec^{-1}. The temperature lag of the hot wire from its equilibrium temperature can therefore be estimated:

$$\frac{(T-T_0)}{(T_e-T_0)} = 1 - kBP\tau^2 = 1 - (3.0\times10^{-4})(1.23\times10^{-2})(10)(2.7)^2$$

$$= 1 - 2.66 \times 10^{-4} = 0.9997.$$

It is apparent that under typical operating conditions there is no temperature lag of the wire.

REFERENCES

1. R. D. Present, *Kinetic Theory of Gases*, McGraw-Hill Book Company, New York, 1958.

2. A. Kundt and E. Warburg, *Ann. Phys. (Leipzig), 155*, 337 (1875).

3. Earle H. Kennard, *Kinetic Theory of Gases*, McGraw-Hill Book Company, New York, 1938.

4. James Clerk Maxwell, *Scientific Papers*, 1890, Ed. W. D. Niven, Cambridge University Press, Cambridge.

5. W. C. De Marcus, *AEC Research and Development Report K-1435*, Oak Ridge, Tennessee, 1959.

6. Osborne Reynolds, *Phil. Trans. Roy. Soc. London, Ser. A, 170*, 727 (1879).

7. Martin Knudsen, *Ann. Phys., 28*, 75 (1908).

8. Martin Knudsen, *The Kinetic Theory of Gases*, 3rd Ed., John Wiley and Sons, New York, 1950.

9. Farrington Daniels and Robert A. Alberty, *Physical Chemistry*, 3rd Ed., John Wiley and Sons, New York, 1966.

10. Martin Knudsen, *Ann. Phys., 31*, 205 (1910).

11. Martin Knudsen, *Ann. Phys., 85*, 797 (1909).

12. Martin Knudsen, *Ann. Phys., 28*, 999 (1909).

13. A. S. Berman and L. M. Lund, *Proc. Int. Conf. Peaceful Uses At. Energy, 2nd, 4*, 359 (1958).

14. T. Edmonds and J. P. Hobson, *Trans. Int. Vac. Congr. 3rd, 2*, 75 (1966).

15. J. P. Hobson, T. Edmonds, and R. Verreault, *Can. J. Phys., 41*, 983 (1963).

16. H. H. Podgurski and F. N. Davis, *J. Phys. Chem., 65*, 1343 (1961).

17. T. Edmonds and J. P. Hobson, *J. Vac. Sci. Technol., 2*, 182 (1965).

18. F. C. Hurlbut, *J. Appl. Phys., 28,* 844 (1957).

19. D. R. Miller and R. B. Subbarao, *J. Chem. Phys., 52,* 425 (1970).

20. S. Yamamoti and R. E. Stickney, *J. Chem. Phys., 53,* 1594 (1970).

21. P. Clausing, *Ann. Phys., 7,* 569 (1930).

22. P. Clausing, *Ann. Phys., 12,* 961 (1932).

23. P. Clausing, *Ann. Phys., 14,*]29 (1932).

24. P. Clausing, *Ann. Phys., 14,* 134 (1932).

25. W. C. De Marcus and E. H. Hopper, *J. Chem. Phys., 23,* 1344 (1955).

26. W. C. De Marcus, *U. S. Atomic Energy Comm. Oak Ridge Report K-1302, Part I,* 1956-1957.

27. W. C. De Marcus, *U. S. Atomic Energy Comm. Oak Ridge Report K-1302, Part II,* 1956-1957.

28. W. C. De Marcus, *U. S. Atomic Energy Comm. Oak Ridge Report K-1302, Part III,* 1956-1957.

29. W. C. De Marcus, *U. S. Atomic Energy Comm. Oak Ridge Report K-1302, Part IV,* 1956-1957.

30. W. C. De Marcus, *U. S. Atomic Energy Comm. Oak Ridge Report K-1302, Part V,* 1956-1957.

31. W. C. De Marcus, *U. S. Atomic Energy Comm. Oak Ridge Report K-1302, Part VI,* 1956-1957.

32. W. C. De Marcus, *Advances in Applied Mechanics, Supplement 1, Rarefied Gas Dynamics,* Ed. L. Talbot, Academic Press, New York, 1961.

33. E. D. Cashwell and C. J. Everett, *The Monte Carlo Method for Random Walk Problems,* Pergamon Press, New York, 1959.

34. A. H. Meyer, Ed., *Symposium on Monte Carlo Methods,* John Wiley and Sons, New York, 1954.

35. D. H. Davis, L. L. Levenson and N. Millerson, *Advances in Applied Mechanics, Supplement 1, Rarefied Gas Dynamics,* Ed. L. Talbot, Academic Press, New York, 1961.

36. Martin Knudsen, *Ann. Phys., 18,* 75 (1909).

37. Satoru Iuchi and Tatsuo Kanki, *J. Chem. Eng. Jap., 34,* 607 (1970).

38. C. Y. Liu, *Phys. of Fluids, 11,* 481 (1968).

39. G. M. Fryer, *Proc. Roy. Soc. London, Ser. A, 193,* 329 (1966).

40. D. S. Scott and F. A. L. Dullien, *A. I. Ch. E. Journal, 8,* 293 (1962).

41. J. H. Leck, *Pressure Measurement in Vacuum Systems,* The Institute of Physics, New York, 1957.

42. M. Pirani, *Deutsche Phys. Ges. Verk., 8,* 686 (1906).

43. R. B. Scott, *Temperature. Its Measurement and Control in Science and Industry,* American Institute of Physics, Reinhold, New York, 1941, p. 212.

44. J. O. Hirshfelder, C. F. Curtis, and R. B. Bird, *Molecular Theory of Gases and Liquids,* John Wiley and Sons, New York, 1954.

45. A. S. Berman, *J. Appl.Phys., 36,* 3356 (1965).

46. H. J. M. Hanley and W. A. Steele, *J. Phys. Chem., 68,* 3087 (1964).

47. H. J. M. Hanley, *J. Chem. Phys., 47,* 4271 (1967).

48. W. A. Steele and H. J. M. Hanley, *Trans. Faraday Soc., 67,* 3484 (1071).

49. E. A. Mason, R. B. Evans, III, and G. M. Watson, *J. Chem. Phys., 38,* 1808 (1963).

50. L. M. Lund and A. S. Berman, *J. Appl. Phys., 37,* 2489 (1966).

51. L. M. Lund and A. S. Berman, *J. Appl. Phys., 37,* 2496 (1966).

VITA

Ralph Lendon Buice, Jr. was born to Ralph Lendon and Sara Elizabeth (Edwards) Buice in Chattanooga, Tennessee, on February 14, 1942. He attended the McCallie School in Chattanooga where he received his secondary school education and from which he was graduated in 1960.

He received the degree of Bachelor of Arts in Chemistry from Vanderbilt University in Nashville, Tennessee, in 1964.

During the summers of 1964 and 1965 he worked in the Technical Laboratories of E. I. Du Pont in Chattanooga, in a research training program for students.

During his studies as a graduate student at the Georgia Institute of Technology he was a research assistant, a teaching assistant, and the recipient of a National Science Foundation Fellowship.

In June, 1972, he completed the requirements for the degree of Doctor of Philosophy in Chemistry under the supervision of Dr. G. A. Miller.